Summer 2014

Repeatability of medial olivocochlear efferent effects on transient-evoked otoacoustic emissions in normal-hearing adults

Ian Benjamin Mertes
University of Iowa

REPEATABILITY OF MEDIAL OLIVOCOCHLEAR EFFERENT EFFECTS ON TRANSIENT-EVOKED OTOACOUSTIC EMISSIONS IN NORMAL-HEARING ADULTS

by

Ian Benjamin Mertes

A thesis submitted in partial fulfillment
of the requirements for the Doctor of
Philosophy degree in Speech and Hearing Science
in the Graduate College of
The University of Iowa

August 2014

Thesis Supervisor: Associate Professor Shawn S. Goodman

Graduate College
The University of Iowa
Iowa City, Iowa

CERTIFICATE OF APPROVAL

_____

PH.D. THESIS

_____

This is to certify that the Ph.D. thesis of

Ian Benjamin Mertes

has been approved by the Examining Committee
for the thesis requirement for the Doctor of Philosophy
degree in Speech and Hearing Science at the August 2014 graduation.

Thesis Committee: _____
Shawn S. Goodman, Thesis Supervisor

_____
Paul J. Abbas

_____
Ruth A. Bentler

_____
Carolyn J. Brown

_____
Lenore A. Holte

To Tracy and William

ACKNOWLEDGMENTS

I would first like to thank all of those who helped to make this project possible. My mentor, Dr. Shawn Goodman, provided guidance, perspective, and support for me and this project throughout. I also thank my dissertation committee members for their insight and encouragement regarding this project. I thank my sources of financial support, which includes the University of Iowa Graduate College, the University of Iowa Executive Council of Graduate and Professional Students, and the University of Iowa Department of Communication Sciences and Disorders. I also thank the research subjects who generously volunteered their time to return to the lab for multiple visits.

Finally, I would like to thank my wonderful wife Tracy who has been my biggest supporter and has been patient and understanding throughout my graduate career and this project in particular.

ABSTRACT

The medial olivocochlear reflex (MOCR) is a brainstem-mediated reflex that reduces cochlear amplifier gain when elicited by sound. The MOCR may provide benefits such as protection from acoustic trauma and improved hearing in background noise. Measurement of MOCR effects may also have clinical applications. MOCR effects can be measured using transient-evoked otoacoustic emissions (TEOAEs), as amplitudes of TEOAEs are typically reduced during MOCR activation.

The primary purpose of the current study was to quantify the repeatability of MOCR effects on TEOAEs because high repeatability in a healthy population is a necessary (but not sufficient) component of a clinically-useful test. A secondary purpose was to assess the relationship between MOCR strength and speech perception in noise. Twenty-one normal hearing subjects ages 18-30 participated. TEOAEs were elicited using 35 dB SL clicks. The MOCR was elicited using contralateral acoustic stimulation (CAS) consisting of 35 dB SL broadband noise. Sixteen measurements were made across a 5-week period (4 visits × 4 measurements per visit). TEOAEs were bandpass filtered in 1/6-octaves from 1-2 kHz. An individualized time-frequency analysis was used to select the largest TEOAE envelope peak within a restricted time analysis window. Responses were characterized as the complex ratio of TEOAEs obtained with versus without CAS. The statistical significance of effects was assessed.

Results revealed generally high levels of stability across time, as assessed by the interquartile ranges of all results and as assessed by Cronbach's alpha. Four MOCR measurements appeared to be adequate to obtain a reliable baseline measurement. Individualized time-frequency analyses were also important for obtaining reliable measurements. However, several subjects showed stable baseline measurements but unusual patterns of variability at subsequent sessions. These changes did not appear to be the result of changes in auditory status, methodological issues, or equipment issues. No

significant relationship was found between MOCR strength and speech perception in noise. Results suggest that MOCR measurements are stable in most subjects when using careful measurement and analysis methods, but that further work is needed to better characterize changes in MOCR and to validate the current methodology in a larger number of subjects.

TABLE OF CONTENTS

LIST OF FIGURES

Figure

LIST OF ABBREVIATIONS

μs – microsecond

ABR – auditory brainstem response

ACh - acetylcholine

ANOVA – analysis of variance

CAS – contralateral acoustic stimulation

cc – cubic centimeter

CF – characteristic frequency

CM – cochlear microphonic

CN – cochlear nucleus

Coch – cochlea

CWN – contralateral white noise

daPa – decapascal

dB – decibel

dB HL – decibels hearing level

dB pSPL – decibels peak sound pressure level

dB SL – decibels sensation level

dB SPL – decibels sound pressure level

DPOAE – distortion-product otoacoustic emission

FFT – fast Fourier transform

HINT – Hearing in Noise Test

ICC – intraclass correlation coefficient

IHC – inner hair cell

IQR – interquartile range

K^+ – potassium

kHz – kilohertz

LSO – lateral superior olive

m – meter

MANOVA – multivariate analysis of variance

MEMR – middle-ear muscle reflex

mm – millimeter

mmho – millimho

MOC – medial olivocochlear

MOCR – medial olivocochlear reflex

mPa - millipascal

ms – millisecond

MSO – medial superior olive

mV – millivolt

Na^+ – sodium

OAE – otoacoustic emission

OHC – outer hair cell

PC – personal computer

rad - radian

RMS – root-mean-square

s – second

SDD – smallest detectable difference

SDT – speech detection threshold

SEM – standard error of measurement

SFOAE – stimulus frequency otoacoustic emission

SNR – signal-to-noise ratio

SOAE – spontaneous otoacoustic emission

SOC – superior olivary complex

SRT – speech recognition threshold

SSOAE – synchronous spontaneous otoacoustic emission

TEOAE – transient-evoked otoacoustic emission

LIST OF MATHEMATICAL SYMBOLS

A – Matrix of TEOAE waveforms without CAS

B – Matrix of TEOAE waveforms with CAS

n – Total number of samples in the time window

m – Number of recorded buffers

$\bar{a}$ – $n \times 1$ vectors of the mean of A across m buffers

$\bar{b}$ – $n \times 1$ vectors of the mean of B across m buffers

Δ – $n \times 1$ vectors of complex ratios obtained by point-wise division

F – Fourier matrix

j – Rows

k – Columns

i (superscript) – Imaginary operator $\sqrt{-1}$

δ – Ratio of discrete Fourier transforms, Δ, reduced to a single complex value

D – The set containing all elements of Δ from indices i_{f_L} and i_{f_H}

i_{f_L}– Index of the low cutoff frequency of the bandpass filter

i_{f_H} – Index of the high cutoff frequency of the bandpass filter

$|\delta|$ – Magnitude of the complex ratio δ

$\angle\delta$ – Phase angle of the complex ratio δ

$\hat{\delta}$ – Resampled complex ratio

K – Number of resampling iterations

S – Unscaled covariance matrix of $\hat{\delta}$ matrix

T – Matrix transpose operator

R – $m \times 2$ vector designating the elliptical region

v – Matrix of eigenvalues

λ – Matrix of eigenvectors

C – Circle defined by a $2 \times m$ matrix

θ – Row vector of m equally-spaced radian phase values from 0 to 2π

R_α – Elliptical tolerance region encompassing $100(1-\alpha)\%$ of $\hat{\delta}$

∇ – "nabla": Total quantity of change; Fourier transform of difference $\bar{a}-\bar{b}$ divided by Fourier transform of $\bar{a}$

ϱ – "turned delta": Mean of subset of elements in ∇ corresponding to range of frequencies

$\overleftarrow{R_\alpha}$ – Tolerance region expected to encompass $100(1-\alpha)\%$ of subsequent repeated measurements of δ

INTRODUCTION

This dissertation examined the repeatability of efferent effects on the cochlea. Specifically, the *medial olivocochlear reflex* (MOCR), which can alter the amplification of sound provided by the cochlea, was examined in this study. The primary purpose was to examine the repeatability of MOCR effects across time in individual subjects. Measurement of the MOCR has been proposed to have clinical utility, but the repeatability has not been definitively established. The results therefore have clinical implications as well as implications for better understanding the function of the MOCR and the cochlea.

The outer hair cells normally amplify sound-induced motion within the cochlea, a mechanism called the cochlear amplifier (Davis 1983). This improves the ability to detect soft sounds and to distinguish between closely-spaced frequencies (e.g., Brownell et al. 1985; Ruggero and Rich 1991; Dallos 1992). The medial olivocochlear (MOC) bundle, located in the brainstem, can reduce the sensitivity and frequency selectivity of the cochlea (e.g., Galambos 1956; Wiederhold and Kiang 1970; Mountain 1980; Gifford and Guinan 1983). This may serve to protect the cochlea from acoustic trauma, improve hearing in background noise, and aid in development of the auditory system (Guinan 1996).

In humans, MOCR effects are assessed primarily using otoacoustic emissions (OAEs), which are measurable sounds generated as a byproduct of the cochlear amplifier (Kemp 1978; Brownell 1990). OAEs are measured quickly and non-invasively by presenting sound and recording the response with a small microphone placed in the ear canal. Typically, OAE amplitudes are reduced when the MOCR is activated (e.g., Mountain 1980; Collet et al. 1990; Hood et al. 1996; Guinan et al. 2003), presumably because the MOCR reduces OHC motility and thus reduces OAE amplitudes.

Measurement of the MOCR may be clinically useful. However, basic factors regarding the MOCR remain unclear. One important factor is the repeatability of MOCR effects on OAEs across time. A clinically useful test must be highly repeatable in a control population. Several studies have investigated MOCR repeatability (Graham and Hazell 1994; Kumar et al. 2013; Mishra and Lutman 2013), but inconsistencies and weaknesses in the methodology limit the conclusions that can be drawn from these studies. These studies lacked control of confounding factors that could affect measurements of MOCR effects, such as activation of the middle-ear muscle reflex. Additionally, they did not assess the statistical significance of MOCR effects in individual subjects. Recent studies have demonstrated the importance of assessing statistical significance, as some individuals show changes in OAEs that are not significant and therefore may not be indicative of MOCR effects (Backus and Guinan 2007; Goodman et al. 2013).

Given the limitations of previous research, this study used methods to improve the accuracy of detecting MOCR effects in individual subjects. Short- and longer-term repeatability was examined with an eye toward the clinical feasibility of MOCR measurements.

The organization of this dissertation is as follows. Cochlear anatomy and mechanics are reviewed in Chapter I. Otoacoustic emissions are reviewed in Chapter II. The MOCR and assessment of MOCR effects in humans are reviewed in Chapter III. The methodology used in the current study is described in Chapter IV. The results are presented in Chapter V. Finally, the discussion is presented in Chapter VI.

CHAPTER I

COCHLEAR MECHANICS

1.1 Overview

The cochlea is the first part of the auditory pathway in which sound is amplified nonlinearly and analyzed in terms of its frequency content. The auditory efferent system exhibits its effects primarily by modifying the amplification of low-level sounds provided by the cochlea (Guinan 1996). Because this dissertation examines auditory efferent effects, this chapter will review the literature on the cochlea and its mechanics.

The human auditory system can encode sounds over a wide range of intensities (12 orders of magnitude) and frequencies (10 octaves). The major divisions of the auditory system amplify and/or convert sound into a different form of energy. These divisions include the outer ear, middle ear, inner ear, and the central auditory system.

The outer ear consists of the pinna and ear canal. It primarily collects sound and funnels it to the middle ear, while providing some amplification in the 2 – 3 kHz region due to ear canal resonance (Shaw and Teranishi 1968). The middle ear consists of the tympanic membrane and ossicles, a chain of three small bones. Vibration of the tympanic membrane in response to sound causes vibration of the ossicular chain. The middle ear serves as an impedance matching device between air (sound pressure waves) and fluid (the cochlear fluid). The middle ear provides approximately 32 dB of gain to the input in the 1 – 4 kHz range, mainly due to the area difference between the tympanic membrane and footplate of the stapes, the third ossicle (e.g., Møller 1963; Tonndorf and Khanna 1967).

The stapes footplate rocks back and forth into the oval window of the cochlea (inner ear), a fluid-filled cavity composed of three chambers separated by membranes. Pressure waves travel through the cochlear fluid, displacing the basilar membrane. The sensory cells are located on top of the basilar membrane. Displacement of the membrane

results in bending of the sensory cells. This opens ion channels on top of the sensory cells, allowing for ions to flow into the cells. This flow of ions causes depolarization, releasing excitatory neurotransmitters into the synapses on auditory nerve fibers.

The central auditory system begins with the auditory nerve, which encodes the frequency, intensity, and timing information about the input. This information is sent to the cochlear nucleus, which preserves and refines the information provided by the auditory nerve. The cochlear nucleus projects bilaterally to the superior olivary complex, where information about the timing and intensity differences between the ears is encoded. The auditory efferent structures are also located in the superior olivary complex, which will be discussed in Chapter III. The lateral lemniscus carries signals from the superior olivary complex and cochlear nucleus to the inferior colliculus, where processing of frequency and binaural input continues. The medial geniculate nucleus serves as a relay from the inferior colliculus to the auditory cortex. Processing of complex stimuli and perception of sound occurs in the cortex.

1.2 Cochlear Anatomy

Cochlear anatomy has been well-investigated throughout the 20th century and beyond and has been described thoroughly in the literature (e.g., reviewed in Lim 1986; Slepecky 1996; Raphael and Altschuler 2003, and many other secondary sources). The cochlea is a bony coiled labyrinth located in the temporal bone, with one located on each side. The cochlea coils with approximately three turns. The coiling occurs around the modiolus, which is the bony center of the cochlea that holds spiral ganglion cells of the auditory nerve. The lateral end of the cochlea contains the oval and round windows, which are membrane-covered openings. The stapes footplate rests in the oval window, which forms the connection between middle and inner ear.

The cochlea is divided into three chambers (scala), separated by two membranes (Fig. 1.1). The chambers are the scala vestibuli, media, and tympani. The scala vestibuli and scala media are separated by Reissner's membrane, and the scala media and scala

tympani are separated by the basilar membrane. The oval and round windows are located laterally to the scala vestibuli and scala tympani, respectively.

Each chamber is filled with fluid. The scala vestibuli and scala tympani each contain perilymph. Perilymph is rich in Na^+, and has a resting potential near 0 mV relative to the vascular system (Geisler 1998). The scala vestibuli and scala tympani are joined together at the end of the cochlea at a juncture called the helicotrema; therefore the two scalae share perilymph. The scala media is filled with endolymph, which is rich in K^+. Endolymph has a resting potential of approximately +80 mV. This potential is referred to as the endolymphatic potential and is provided by the stria vascularis, a vascular structure located on the outer portion of the scala media.

The basilar membrane runs the length of the cochlea. There is a change in stiffness and width as the membrane runs from the entrance of the cochlea (base) to the helicotrema (apex). This stiffness gradient will be important to consider in the discussion of cochlear mechanics in Chapter 1.3.

Resting on the basilar membrane is the organ of Corti, which contains the sensory cells called the outer hair cells (OHCs) and inner hair cells (IHCs). “Hair” refers to the tiny bundles called stereocilia which project from the top of the cells and resemble hairs. OHCs are cylindrical, number around 12,000, and are divided into three rows, with the outermost row being the tallest. IHCs are rounded, number around 3,000, and are contained in one row. The hair cells are innervated by afferent and efferent nerve fibers. Auditory nerve fibers belong to the afferent pathway. Approximately 95% of afferent fibers innervate IHCs, while the remaining portion innervates OHCs. The spiral ganglion cells of the auditory nerve travel from the modiolus and synapse at the base of the hair cells. Approximately 10 nerve fibers innervate a single IHC, whereas one nerve fiber can innervate six or more OHCs. Efferent fibers innervate both IHCs and OHCs, and will be described in more detail in Chapter III.

Both IHCs and OHCs are negatively charged, with resting potentials of approximately -40 and -70 mV, respectively. Because endolymph is positively charged while hair cells are negatively charged, there is a large electrical potential (approximately +120 to +150 mV) between the endolymph and the hair cells. The hair cells are held in place by numerous supporting cells. The stereocilia, but not the rest of the hair cells, extend through a layer called the reticular lamina. With this arrangement, the stereocilia are bathed in endolymph, while the rest of the hair cell is surrounded by perilymph. Above the stereocilia is the tectorial membrane, which runs approximately parallel and superior to the basilar membrane. The stereocilia of the OHCs (but not IHCs) are embedded in the tectorial membrane. The stereocilia of each row of OHCs are connected by filaments called tip links. Movement of the stereocilia adjusts the tension of the tip links, which opens or closes ion channels located in the stereocilia. Flow of ions into the stereocilia forms the basis of mechanoelectric transduction, described in the next section.

1.3 Cochlear Mechanics

1.3.1 Passive Mechanics

1.3.1.1 Traveling Wave

The primary role of the cochlea is to transduce the mechanical vibrations of the ossicles into a neural signal that is sent to the auditory nerve. One major component of this process is sound propagation along the basilar membrane. This propagation, referred to as a traveling wave, was described in detail by von Békésy (1960).

The basilar membrane runs the length of the cochlea, separating the scala media and scala vestibuli. The basilar membrane increases in width as it goes from base to apex, but has relatively constant mass throughout. The change in width results in a stiffness gradient, where it becomes progressively less stiff from base to apex. This stiffness gradient and constant mass also results in a resonance gradient. The place of resonance is where the effects of stiffness and mass are equal and opposite in phase. The base vibrates preferentially to high frequencies and the apex vibrates preferentially to low frequencies.

For example, if a high-frequency sinusoidal sound is introduced to the cochlea, the largest amplitude of vibration will occur in the base. This is called a *tonotopic* arrangement, meaning that the frequency of a sound is encoded by the place on the basilar membrane where the largest vibration occurs.

The traveling wave begins when the stapes footplate rocks back and forth into the oval window, causing a pressure wave to propagate through the cochlear fluid. There is a pressure differential between the scala vestibuli and scala tympani that causes the basilar membrane to be displaced. Due to the thinness of Reissner's membrane, which separates the scala vestibuli and scala media, there is virtually no pressure differential between these scalae and can be considered one unit for the purposes of cochlear fluid mechanics (Dallos 1996). Inward movement of the stapes footplate causes the basilar membrane to be displaced toward the scala tympani; conversely, outward movement causes displacement toward the scala vestibuli.

The wave that propagates along the basilar membrane is referred to as the traveling wave. The traveling wave propagates from base to apex until it reaches the resonant place determined by the frequency of the input. Prior to the resonant place, the impedance of the basilar membrane is high, which causes the wave to propagate. At the resonant place, impedance is low because the effects of mass and stiffness cancel. This results in a large amplitude of displacement, referred to as the peak. After the peak is reached, impedance becomes high again and causes the wave to dissipate. The basilar membrane is approximately scaling symmetric, meaning that the traveling wave takes approximately four wavelengths to reach the resonant place, regardless of frequency (Shera and Zweig 1991).

1.3.1.2 Mechanoelectrical Transduction

The cochlea transduces vibrations of the ossicles into neural signals. This process is termed *mechanoelectrical transduction*. Once a traveling wave has propagated along the basilar membrane, the next step is stimulation of the sensory hair cells.

Displacement of the basilar membrane causes the stereocilia of the hair cells to bend. Stereocilia of OHCs bend because they are embedded in the tectorial membrane, whereas the stereocilia of IHCs bend due to fluid flow during basilar membrane vibration. Upward movement of the basilar membrane bends stereocilia away from the modiolus. This stretches the tip links and causes the ion channels in the stereocilia to open. Conversely, downward movement bends stereocilia toward the modiolus. This in turn causes the tip links to relax, which closes the ion channels.

Recall that there is a voltage difference between the endolymph and the inside of the hair cell, where endolymph is positively charged and the hair cell is negatively charged at rest. When ion channels are opened, K^+ ions flow from the endolymph into the hair cells. This causes depolarization of the hair cells. In the IHCs, depolarization results in the release of neurotransmitter into the synapse with spiral ganglion fibers. Increased neurotransmitter release increases the probability of causing an action potential in the auditory nerve. Bending of the stereocilia away from the modiolus is therefore excitatory. Conversely, bending of the stereocilia toward the modiolus closes the ion channels, which will reduce the probability of an action potential, and is therefore inhibitory. Larger amplitudes of basilar membrane vibration, caused by higher intensity sounds, will cause larger displacement of stereocilia and more excitation, thus encoding the intensity. Because this process begins with mechanical vibration of the ossicles and ends with generation of electrical potentials, it is termed mechanoelectrical transduction.

The process of mechanoelectrical transduction is nonlinear (Fig. 1.2). As displacement of the stereocilia increases (either in the excitatory or inhibitory direction), progressively more ion channels open or close, changing the voltage of the hair cell. This change is called the receptor potential. However, there reaches a certain point where all the channels are opened or closed, so further displacement does not change the receptor potential (Russell et al. 1986). Additionally, displacement in the inhibitory direction reaches saturation sooner than for the excitatory direction, which is due to most ion

channels being closed at rest. This asymmetry in excitatory versus inhibitory changes in receptor potential is more pronounced for IHCs than OHCs. The nonlinearity in mechanoelectrical transduction forms the basis of the nonlinearity of the cochlea, discussed further in the following section.

1.3.2 Active Mechanics

1.3.2.1 Evidence for an Active Process

Although von Békésy (1960) described passive cochlear mechanics in great detail, the sensitivity and frequency resolution predicted from his findings grossly underestimated what was demonstrated from auditory nerve fiber recordings (e.g., Kiang et al. 1967; Evans 1972) and in human psychoacoustic experiments (e.g., Fletcher 1940; Steinberg et al. 1940). This discrepancy between basilar membrane responses and higher-order responses led some to posit that a "second filter" existed at the level of the auditory nerve, and this was believed to account for the observed sensitivity and frequency selectivity observed behaviorally (e.g., Duifhuis 1976; Hall 1977). However, multiple discoveries in the 1970s and early 1980s pointed to the OHCs as the source of the observed sensitivity and frequency selectivity. This was also combined with an understanding that the results of von Békésy (1960) were obtained in cadaver ears using high sound levels, rather than in living animals at lower sound levels. These discoveries led to the concept of a "cochlear amplifier" (Davis 1983), which is a mechanism that introduces energy (i.e., active) into the passive mechanics of the cochlea to overcome the viscous damping of the cochlear fluids, improving the sensitivity to low-level sounds and increasing the frequency resolving ability.

One of the earliest indications of an active process in cochlear mechanics came from measurements of basilar membrane motion in living animals. Measurements at a single location showed nonlinear growth, where responses to low levels grew nearly linearly and then grew compressively at higher levels (Rhode 1971; Sellick et al. 1982). This compressive nonlinearity was eliminated after death (Sellick et al. 1982) or when

OHCs were damaged due to ototoxicity or noise exposure (e.g. Patuzzi et al. 1984; Rugerro and Rich 1991). Cochlear injury or death resulted in basilar membrane responses that resembled those reported by von Békésy (1960). Basilar membrane responses obtained in live animals also strongly resembled those obtained from auditory nerve fibers (e.g., Robles et al. 1986), suggesting that the basilar membrane was the source of the sensitivity and frequency selectivity. The fact that basilar membrane motion was susceptible to damage strongly suggested that it was due to an active component, meaning that energy is introduced into the system to amplify the basilar membrane displacement provided by the passive mechanics (Robles and Ruggero 2001). Computational models involving an active component were able to simulate the observed responses (e.g., Neely and Kim 1983), further suggesting the presence of an active component to basilar membrane motion.

Evidence that the OHCs were the source of the cochlear amplifier also came from the finding that the cell bodies of OHCs could change their length in response to electrical stimulation, where depolarization caused length contractions (Brownell et al. 1985). This process was referred to as *electromotility*. Contraction of the OHCs could enhance the passive mechanics by reducing resistive forces that impede basilar membrane vibration, allowing it be displaced further (e.g., Neely 1993; de Boer 1996). The source of electromotility was later found to be a motor protein called prestin (Zheng et al. 2000). The cell wall of OHCs contains many prestin molecules, which can alter their shape with voltage changes and thus make OHCs motile. Mice engineered to lack prestin demonstrate poorer hearing thresholds and reduced OHC motility (Liberman et al. 2002; Wu et al. 2004), providing further evidence for the importance of electromotility itself and confirming prestin's role in electromotility.

The auditory efferent pathway involving the medial olivocochlear (MOC) bundle also provides indirect evidence for OHCs as the source of the cochlear amplifier. Nearly all MOC fibers synapse directly on the base of OHCs (Warr and Guinan 1979). When the

MOC bundle is stimulated, evoked responses from the cochlea and afferent auditory nerve fibers are reduced in amplitude and the frequency selectivity is broadened (e.g., Galambos 1956; Brown and Nuttall 1984; Collet al. 1990). Because MOC fibers synapse on OHCs, this implicates the OHCs as being responsible for frequency and intensity selectivity.

Finally, sounds can be measured in the sealed ear canal without the presence of external stimulation (e.g., Wilson 1980; Zurek 1980). These emitted sounds, called otoacoustic emissions, were evidence of an active process in the cochlea because spontaneous energy could not be emitted by a passive system. Otoacoustic emissions will be described in more detail in Chapter II.

1.3.2.2 Action of the Cochlear Amplifier

Given that the OHCs have been established as the source of cochlear amplification, the discussion will now turn to how cochlear amplification occurs. Recall that in the passive mechanics, the traveling wave peaks at its characteristic place on the basilar membrane based on the frequency of the input. When there is an active element, the peak of this wave is enhanced by becoming more localized and larger in amplitude (Fig. 1.3). A more localized peak results in stimulation of fewer auditory nerve fibers, resulting in encoding of more specific frequency information relative to a broader peak. An increase in the peak amplitude increases the sensitivity to low-level sounds. In the passive case, the amplitude may be insufficient to bend IHC stereocilia far enough to depolarize and release neurotransmitter. An increase in the peak amplitude bends the stereocilia farther, increasing the likelihood of neurotransmitter release and firing of an action potential.

In order to amplify basilar membrane motion, contraction of the OHCs must be in phase with basilar membrane motion to overcome resistive forces from the fluid in the cochlea (Neely and Kim 1986; Withnell et al. 2002). Cochlear models and physiologic data indicate that this occurs slightly basal to the traveling wave peak (e.g., Russell and

Nilsen 1997; Shera 2007; Ren et al. 2011). Cochlear amplification is also said to occur in a feedback loop (e.g., Patuzzi and Robertson 1988), where increased basilar membrane motion increases shearing of the OHCs, in turn increasing basilar membrane motion, etc. The presence of spontaneous emissions from the ear canal (e.g., Wilson 1980; Zurek 1980; Zwicker 1983) is evidence of this feedback process.

1.4. Summary

The cochlea is the first portion of the auditory system that analyzes a sound into its component frequencies. An active amplification source provides gain for low-level sounds and improves the frequency selectivity. Numerous studies have provided strong evidence that OHCs are the source of the cochlear amplifier. The next chapter will cover otoacoustic emissions, a byproduct of the cochlear amplifier that can be used to assess the function of OHCs and indirectly assess efferent effects.

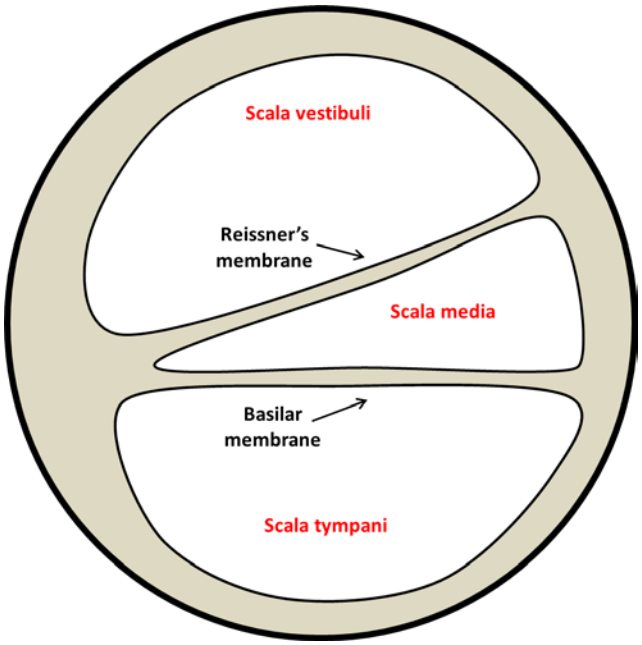

Figure 1.1. Schematic cross-section of the cochlea showing the three scalae and corresponding membranes.

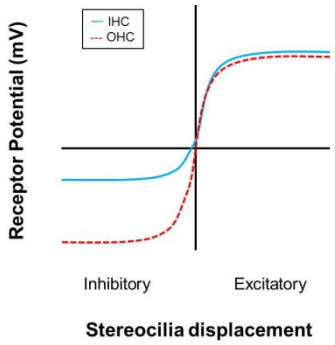

Figure 1.2. Hair cell receptor potential as a function of stereocilia displacement. Inner hair cell (IHC) response shown as solid blue line. Outer hair cell (OHC) response shown as dashed red line. Figure is based on Russell et al. (1986) and Pickles (2012).

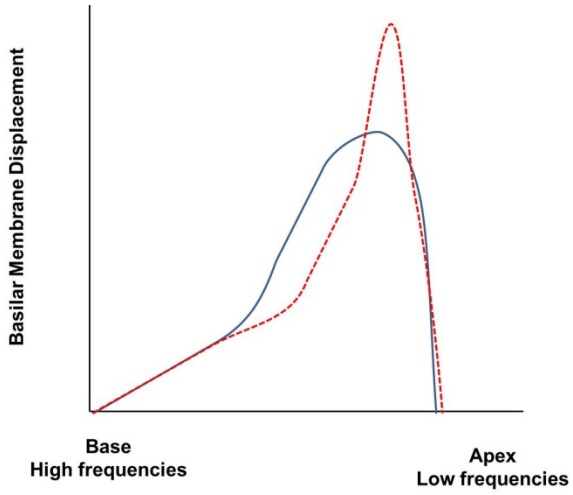

Figure 1.3. Schematic of a passive and active traveling wave along the basilar membrane. The passive and active traveling waves are shown by a solid blue line and dashed red line, respectively. Figure is based on Pickles (2012).

CHAPTER II

OTOACOUSTIC EMISSIONS

2.1 History and Overview

The auditory efferent system alters the gain of the cochlear amplifier. In humans, these effects are typically assessed using otoacoustic emissions, which are sounds generated as a byproduct of the cochlear amplifier (Kemp 1978; Brownell 1990). This chapter will review the literature on otoacoustic emissions, including their measurement, uses, and generation.

When the theory of an active cochlear mechanism was first proposed, it was hypothesized that the cochlea should emit some portion of sound back into the ear canal (Gold 1948). At that time, it was not technologically feasible to record very low-level sounds in the ear canal. It was not until 1978, when experimenters were examining the origin of hearing threshold microstructure, that evidence of sounds emitted by the cochlea was found.

Kemp (1978) presented click stimuli to normal hearing ears through earphones. The resulting responses were recorded with a small microphone sealed in the ear canal, and the responses were synchronously averaged to reduce physiologic noise. Normal hearing ears were found to have an oscillatory sound that persisted for up to tens of milliseconds after the stimulus stopped. The amplitude of the responses was approximately 50 dB lower than the eliciting stimulus. These responses were absent in a metal coupler and in ears with sensorineural hearing loss. This was the first known study to report the presence of *otoacoustic emissions* (OAEs), sounds generated by the cochlea.

This study also described other important aspects of OAEs elicited by clicks. This includes frequency dispersion, where the higher frequency portions of the response return earlier in time than the lower frequency portions due to differences in travel time to reach the characteristic place on the basilar membrane. The nonlinear growth of OAE

amplitudes was also described, where a 1 dB increase in stimulus level resulted in a fraction of a decibel increase in the OAE amplitude. In addition to click stimuli, measurable sounds could be obtained by recording in the ear canal without stimulation (spontaneous OAEs) or by presenting two pure tones (Kemp 1979). These results were replicated by Kemp and colleagues (e.g., Anderson and Kemp 1979; Kemp 1979; Kemp and Chum 1980), as well as by other groups (e.g., Wilson 1980; Kim 1980; Wit and Ritsma 1980; Johnsen and Elberling 1982; Zwicker 1983).

The cochlea and OHCs were suspected to be responsible for the generation of OAEs. OAEs could not be explained by stimulus artifact, because they were absent in couplers and ears with sensorineural hearing loss (Kemp 1978). They also could not be explained by middle ear responses due to the observed nonlinear growth (Kemp 1978). Other advances in cochlear mechanics were occurring around this time, such as the discovery of outer hair cell motility (Brownell et al. 1985) and basilar membrane motion measurements demonstrating compressive nonlinearity and sharp tuning (Sellick et al. 1982). The theory of the cochlea as an active amplifier of incoming sound was taking hold, with the OHCs being the presumed location of the amplifier (e.g., Davis 1983; Neely and Kim 1983).

The nonlinear amplitude growth of OAEs and their susceptibility to trauma and ototoxic agents strongly suggested that the OHCs are the source of OAEs. OAEs were found to be absent in ears with sensorineural hearing loss (e.g., Kemp 1978; Rutten 1980; Probst et al. 1987). Ototoxic agents such as furosemide and aspirin were found to reduce or eliminate OAEs (Andersen and Kemp 1979; Wilson and Evans 1983; Long and Tubis 1988). It is now generally accepted that the OHCs are the source of both the cochlear amplifier and otoacoustic emissions. The remainder of this chapter is dedicated to the measurement, analysis, and usage of OAEs as well as a discussion of how OAEs are generated in the cochlea.

2.2 Types of OAEs and Their Measurement

2.2.1 Measurement Paradigm

OAEs are measured in the ear canal using a probe microphone. The ear canal is sealed to attenuate background noise that could interfere with the measurement. The probe microphone assembly houses one or two loudspeakers to present stimuli. Because OAEs are typically small in amplitude (often 10 dB SPL or less) and there is physiologic noise present in the recordings, noise is reduced through filtering and synchronous averaging. Finally, recordings are analyzed in the time and/or frequency domain to determine the presence of OAEs and their amplitudes and phases. The choice of analysis domain depends in part on the type of OAE being measured, as discussed next.

2.2.2 Types of OAEs

Traditionally, OAEs have been categorized by the evoking stimulus. Transient-evoked (TE) OAEs are elicited with brief stimuli such as clicks or tone bursts. Distortion-product (DP) OAEs are elicited with two pure tones presented simultaneously. Stimulus-frequency (SF) OAEs are elicited with a single pure tone. Spontaneous (S) OAEs are not elicited by external stimuli, and are instead measured by recording from the ear canal for several minutes or more and analyzing the recording in the frequency domain. Each type of OAE has advantages and disadvantages in terms of information provided about cochlear function and in terms of measurement and analysis methods.

2.2.2.1 Transient-evoked (TE) OAEs

Transient stimuli contain a broader bandwidth relative to longer-duration stimuli such as pure tones. Therefore, TEOAEs have the advantage of stimulating a broad region of the cochlea at one time, potentially providing more information about OHC function in a shorter amount of time. Transient stimuli elicit TEOAEs similar in frequency to that of the stimulus, so there is considerable overlap between the two when analyzed in the frequency domain. The ability to distinguish between the stimulus and emission is achievable in the time domain due to the inherent time separation between the stimuli

reaching the cochlea and the resulting TEOAEs returning to the ear canal. There is often residual ringing of the stimulus in the ear canal, which can obscure portions of the TEOAE that return quickly (Goodman et al. 2009). Stimulus artifact can be reduced by nonlinear extraction techniques that take advantage of the linear growth of a stimulus and nonlinear growth of the emission (Kemp et al. 1990; Keefe 1998). Stimuli of different levels (and in some cases, opposite polarity) are presented. Recordings using the lower levels are summed, and the recording using the higher level is subtracted. The result is cancelation of the stimulus, while the nonlinear portion of the emission remains. Because stimulus artifact is largest within the first several milliseconds of the recording, most analyses zero-out the first several milliseconds of the recording and apply an additional onset ramp afterwards (e.g., Bray and Kemp 1987; Kemp et al. 1990). The disadvantage of eliminating the first several milliseconds is that it restricts the upper measurable frequency of TEOAEs to approximately 5 kHz because higher-frequency TEOAEs return to the ear canal sooner. Recent methods of nonlinear extraction allow for stimulus cancelation without eliminating the first several milliseconds of the recordings, allowing for measurement of TEOAEs up to 16 kHz (Goodman et al. 2009; Keefe et al. 2011).

2.2.2.2 Distortion-product (DP) OAEs

DPOAEs are measured in response to two sinusoids of different frequencies (f_1 and f_2, where f_2 is higher in frequency). Each sinusoid creates a traveling wave that reaches a different characteristic place on the basilar membrane. When the frequencies are spaced by a certain amount, there is a region of overlap between the two traveling waves. The nonlinearity of basilar membrane motion creates distortion at this overlap region, and one or more reverse traveling waves return to the ear canal. Due to the nonlinear nature of this process, the returning waves are different in frequency from that of the input sinusoids. The frequencies are mathematically related to the input frequencies. In humans, the largest distortion product has a frequency of $2f_1$-f_2 (e.g., Probst and Hauser 1990; Gorga et al. 1997). DPOAEs have the advantage of being

analyzed easily in the frequency domain because the DPOAE frequencies are different from those of the input stimuli. However, time domain analysis of DPOAEs is more difficult because the stimuli and DPOAEs overlap in time except at the emission onsets and offsets.

2.2.2.3 Stimulus frequency (SF) OAEs

SFOAEs are elicited by a single sinusoid, and are of the same frequency as the input. The advantage is that SFOAEs provide more narrowband information about cochlear function relative to TEOAEs or DPOAEs. However, they have the disadvantage of overlapping with the input both in terms of frequency and time. Therefore, SFOAEs are measured using nonlinear extraction techniques to isolate the SFOAE from the stimulus (e.g., Brass and Kemp 1986; Schairer et al. 2006).

2.2.2.4 Spontaneous (S) OAEs

SOAEs are measured without the use of external stimuli. They are measured by recording from the ear canal for several minutes or longer in order to reduce background noise. SOAEs are typically analyzed in the frequency domain because they are exhibited as single frequencies. SOAEs are most prevalent in the 1-2 kHz region, and are more common in women than men (e.g., Penner and Zhang 1997).

2.3 Clinical Usefulness of OAEs

OAEs have become a part of routine audiologic testing for several reasons. First, they are useful for identifying pathologies that affect OHCs because OAE generation is dependent primarily on OHC function (e.g., Kemp 1978; Probst et al. 1987; Collet et al. 1989; Harris 1990; Martin et al. 1990; Prieve et al. 1993; Gorga et al. 1997). Because most forms of cochlear hearing loss affect the OHCs (Patuzzi et al. 1989), it follows that a measure of OHC function will be useful in detecting the presence of cochlear hearing loss (however, they are not useful for identifying non-cochlear hearing loss, such as conductive, neural, or central). Second, measurement of OAEs is objective, meaning that it does not require a behavioral response to stimuli on the part of the subject; the only

stipulation is that the subject must remain relatively still and quiet during measurement. Third, OAE equipment is portable, affordable (approximately several thousand dollars), and can be operated by individuals with basic training.

TEOAEs and DPOAEs are currently the only types of OAEs measured in routine clinical settings. SFOAEs are not used likely due to the time and difficulty involved in measuring and analyzing the responses. SOAEs are typically not measurable in ears with hearing loss, so their presence is indicative of normal hearing. However, many normal-hearing ears also do not exhibit SOAEs (e.g., Penner and Zhang 1997), which limits their diagnostic usefulness. TEOAEs and DPOAEs are typically present in ears with normal and borderline-normal hearing, and are absent when there is sensorineural hearing loss that exceeds a mild degree (e.g., Collet et al. 1991; Prieve et al. 1993; Hurley and Musiek 1994; Gorga et al. 1997; Hussain et al. 1998). This has made OAEs particularly useful in screening for the presence of hearing loss, especially for newborns (e.g., Norton et al. 2000; Mehl and Thomson 2002). However, OAEs have been found to be relatively inaccurate predictors of specific audiometric thresholds (e.g., Collet et al. 1991; Sückfull et al. 1996; Wagner and Plinkert 1999). More sophisticated analyses, such as extrapolated input-output functions (Gorga et al. 2003), isolation of individual DPOAE sources (Johnson et al. 2007), and examination of short- and long-latency TEOAE components (Mertes and Goodman 2013) have improved predictions only modestly, suggesting that OAEs are useful in clinical settings primarily for screening for the presence of hearing loss.

2.4 Generation Mechanisms of OAEs

Although OAEs are typically referred to by the eliciting stimulus (e.g., TEOAE, DPOAE, etc.), much work has focused on categorizing OAEs based on the underlying generation mechanisms. It is generally accepted that there are two primary mechanisms of OAE generation: linear coherent reflection and nonlinear distortion (Shera and Guinan 1999).

2.4.1 Linear Coherent Reflection

According to the theory of linear coherent reflection (Zweig and Shera 1995; Shera and Guinan 2008), the basilar membrane contains randomly-distributed discontinuities along its length. These discontinuities may be due to differences in the organization of the OHCs along the basilar membrane (Lonsbury-Martin et al. 1988) or perhaps differences in the behavior of the cochlear amplifier across the basilar membrane (Shera 2004; Shera and Guinan 2008). When a forward-traveling wave encounters these discontinuities, a small portion of the wave will be reflected backward. Because these discontinuities are distributed across the basilar membrane, reflections are thought to occur throughout as the traveling wave proceeds forward. When the relative phases of the reflected waves are different, they can cancel each other by the time they reach the microphone in the ear canal. However, when the reflections are in phase (i.e., coherent), they will sum in amplitude and reach the ear canal as an OAE. Linear coherent reflection theory states that the phase is most coherent at the peak of the traveling wave (Zweig and Shera 1995). Therefore, OAEs generated by linear coherent reflection (also referred to as reflection-source emissions) will be dominated by the peak of the traveling wave. The theory predicts that the total delay between stimulus presentation and measurement of emission is approximately twice the amount of time it takes for the stimulus to reach the characteristic place on the basilar membrane (Zweig and Shera 1995; Shera and Guinan 1999).

Evidence for linear coherent reflection comes from analysis of SFOAE phase (Shera and Guinan 1999). When the stimulus frequency is increased, the phase accumulation also increases. Due to cochlear scaling symmetry, traveling waves of different frequencies undergo approximately the same phase rotations to reach their characteristic place. However, when the traveling wave encounters discontinuities on the basilar membrane, a portion of the wave will be reflected back. If two waves of different frequencies are each reflected back at the same basilar membrane location, the higher

frequency wave would undergo more phase rotations and thus would have increased phase accumulation. Linear coherent reflection adequately explains the pattern of results seen for SFOAEs.

2.4.2 Nonlinear Distortion

OAEs can also be generated by nonlinear distortion, and are often referred to as distortion-source emissions (Shera and Guinan 1999). The nonlinear mechanics of the cochlea introduce distortion in the traveling wave, which in turn creates waves that travel apically and basally. This basally-traveling wave returns to the ear canal and is measured as an OAE. The nonlinearity is likely due to factors such as the nonlinear change in OHC receptor potential with displacement of the hair bundle (e.g., Russell et al. 1986; see also Fig. 1.2). Distortion is created at a point of overlap between two traveling waves, mainly at the peak of the traveling waves (Shera 2004). Due to scaling symmetry, traveling waves take approximately the same number of cycles to reach their peak, regardless of frequency. The process of nonlinear distortion therefore "follows" the waves, and the resulting distortion-source emission has the same relative phase regardless of the frequency of the inputs (Shera and Guinan 1999). This is contrasted with reflection-source emissions, where phase of the emission varies depending on frequency of the input.

2.4.3 Generation Mechanisms of the Different OAE Types

OAEs are currently believed to be generated by one or both of the aforementioned mechanisms. When elicited using low to moderate stimulus levels, TEOAEs and SFOAEs are generated by linear coherent reflection (Shera and Guinan 1999; Kalluri and Shera 2007). SOAEs are also generated by linear coherent reflection (Shera and Guinan 1999). DPOAEs are generated by both mechanisms (Mauermann et al. 1999; Shera and Guinan 1999; Talmadge et al. 1999). The overlap between the two sinusoids creates distortion, which travels back to the ear canal as a distortion-source OAE. However, the distortion also causes a forward-traveling wave of frequency $2f_1$-f_2 that travels to its

characteristic place on the basilar membrane (apical to the two input frequencies), and then returns to the ear canal as a reflection-source OAE. The two sources can be separated experimentally using methods such as time-windowing (because there is a delay difference between the two components) or use of a suppressor tone to reduce the distortion-source emission (e.g., Kalluri and Shera 2001; Konrad-Martin et al. 2001; Johnson et al. 2007). When the components are examined in isolation, the distortion- and reflection-source phases change across frequency in the expected manner, i.e., reflection-source phase lag increases with increasing frequency and distortion-source phase lag is nearly zero across frequency (Shera and Guinan 1999; Shera 2004).

2.4.4 Unresolved Areas of Research

Although SFOAEs and TEOAEs are generally considered to be reflection-source emissions generated at the peak of the traveling wave, there is evidence to suggest that this may not always be the case. Yates and Withnell (1999) found that TEOAEs contained energy that was not present in their click stimuli, suggesting that nonlinear distortion may have contributed to the measured response. Others have found short-latency components to TEOAEs that grow in amplitude less compressively than long-latency components, suggesting different generation mechanisms, locations, or both (Goodman et al. 2009, 2011; Moleti et al. 2012, 2013). Additionally, there are short-latency components to SFOAEs that could suggest generation at a location more basal to the traveling wave peak (e.g., Siegel et al. 2005; Choi et al. 2008; Shera et al. 2008). The mechanisms of these different components are currently under investigation by different research groups, suggesting that classifying TEOAEs and SFOAEs as strictly reflection-source emissions may be an oversimplification.

2.5 Summary

OAEs are a byproduct of the cochlear amplifier. They have proven useful for indirectly assessing the function of OHCs and for detecting sensorineural hearing loss.

Two primary mechanisms of OAE generation have been generally supported by experimental evidence, but this is still an area of investigation.

In following chapter, the auditory efferent system will be described. The primary effect of the efferent system is to modify the gain provided by the cochlear amplifier. This modification results in changes in OAEs, and therefore OAEs are the primary way in auditory efferent effects are assessed in humans. The next chapter will build upon the concepts of the cochlear amplifier and OAEs that were discussed in Chapters I and II.

CHAPTER III

MEDIAL OLIVOCOCHLEAR EFFERENT SYSTEM

3.1 Overview

3.1.1 Anatomy of the Auditory Efferent System

The auditory efferent structures in the brainstem were first described by Rasmussen (1946). They arise from the superior olivary complex (SOC) and terminate in the cochlea and auditory nerve. The SOC is the first site on the ascending auditory pathway that receives bilateral auditory input. It is divided into the lateral and medial superior olive (LSO and MSO, respectively), which are important for the processing of interaural intensity and timing differences for localization (Masterton and Imig 1984).

Rasmussen (1946) described *crossed* and *uncrossed* efferent fibers, which refers to crossing the midline of the brainstem. It was later found that auditory efferent fibers originate from one of two structures, the lateral and medial olivocochlear (LOC and MOC) bundles (Warr and Guinan 1979).

There are several important differences between the LOC and MOC systems. LOC fibers synapse on the type I auditory nerve fibers that innervate inner hair cells (IHCs). MOC fibers synapse primarily on outer hair cells (OHCs), with a small number synapsing on type II auditory nerve fibers that innervate OHCs (Liberman 1980). Efferent innervation in animals is densest in the mid- and high-frequency regions of the cochlea (Robertson et al. 1987; Liberman et al. 1990). Both humans and animals have demonstrated more LOC fibers than MOC fibers (Arnesen 1984; Warr 1992). LOC and MOC fibers both exhibit bilateral projections to the cochleae; however, LOC fibers primarily innervate the ipsilateral periphery while MOC fibers primarily innervate the contralateral periphery (Warr 1992). LOC fibers are not myelinated and are relatively thin compared to the myelinated MOC fibers, which makes electrical stimulation of LOC fibers difficult to achieve in research settings and thus much of LOC efferent effects

remain unknown (Guinan 1996; Guinan 2011). Except when otherwise noted, the remainder of this dissertation will focus on efferent effects due to the MOC system.

There is evidence of higher-level descending pathways that terminate in the superior olivary complex, suggesting that efferent activity can be influenced by the cortex. Anatomical evidence has been found in animals, showing projections from the auditory cortex to the MOC bundle (Feliciano et al. 1995; Mulders and Robertson 2000) as well as from the inferior colliculus to the superior olive (Vetter et al. 1993). Indirect evidence for descending pathways in humans has been exhibited in human studies of cortical ablation (Khalfa et al. 2001), cortical stimulation (Perrot et al. 2006), asymmetry in efferent effects (Khalfa 1997; Morand-Villeneuve et al., 2005), and modification of efferent effects via attention (e.g., Puel et al. 1988; Froehlich et al. 1993a; de Boer and Thornton 2007) and auditory training (de Boer and Thornton 2008).

3.1.2 Physiology of the Auditory Efferent System

When stimulated, MOC fibers release neurotransmitters (primarily acetylcholine, ACh) into the synaptic cleft between MOC axons and OHC dendrites. ACh binds to receptors on OHCs, which allows calcium (Ca^{2+}) ions that in turn cause potassium (K^{+}) ions to flow out of the OHC (Sewell 2011). Because OHCs have a negative resting potential, while endolymph has a positive resting potential, release of K^{+} causes the OHC to hyperpolarize and results in a decreased endocochlear potential (Guinan 1996). This effect has a time course of approximately 100 ms, and is often termed the MOC "fast effect" (Guinan 2006). There is also a "slow effect" that has a time course of >20 s (Sridhar et al. 1995), and is believed to be due to increased stiffness in OHCs due to changes in prestin (Cooper and Guinan 2003; Guinan 2006). Both effects result in reduced amplification of basilar membrane motion by OHCs.

Efferent stimulation has been shown to reduce basilar membrane motion, with the most pronounced effects at the characteristic frequency (CF) place along the membrane and at low sound levels (Murugasu and Russell 1996; Dolan et al. 1997). Similar efferent

effects have been demonstrated for recordings from inner hair cells (Brown and Nuttall 1984) and from auditory nerve fibers (Galambos 1956; Wiederhold and Kiang 1970; Guinan and Gifford 1988), suggesting a common underlying mechanism. As discussed in Chapter II, evidence strongly indicates that the outer hair cells (OHCs) are the source of the cochlear amplifier, which has its strongest effects at the CF place on the basilar membrane and at low levels. MOC fibers synapse onto OHCs and can induce changes in the OHCs and therefore changes in the amplification of basilar membrane motion.

Measures of OHC function also show efferent effects, including the cochlear microphonic (CM) and otoacoustic emissions (OAEs). The cochlear microphonic is dependent on flow of current through OHCs (e.g., Dallos and Cheatham 1976). Efferent stimulation increases the amplitude of the cochlear microphonic (Fex 1959; Mountain et al. 1980) due to increased current flow through OHCs (Guinan 1996). OAEs typically are reduced in amplitude with efferent stimulation (e.g., Mountain 1980; Mott et al. 1989; Guinan et al. 2003). MOC stimulation can also cause phase leads and decreases in OAE latency, which is likely due to broadening of the traveling wave peak (Ryan et al. 1991; Giraud et al. 1996, 1997; Francis and Guinan 2010). As will be discussed later, OAEs are particularly useful for studying efferent effects in humans because they can be measured quickly and non-invasively.

The efferent structures can be activated by sound or by electrical stimulation. The pathway between the peripheral auditory system and the efferent structures are well-understood (e.g., Warr and Guinan 1979; Liberman 1980; Guinan 1996; de Venecia et al. 2005), and is shown as a block diagram in Fig. 3.1. Beginning with the periphery, sound stimulation begins at the cochlea and auditory nerve, travels to the cochlear nucleus, and reaches the LOC/MOC system, after which the efferent system projects back to the periphery. Sound activation of the efferent system occurs reflexively, and is therefore termed the medial olivocochlear reflex (MOCR). Because there are projections from the MOC bundle to both cochleae, sound presented in either ear can activate the reflex and

influence OHC function in both cochlea. When MOCR activation and the resulting effects are measured from the same ear (the *ipsilateral* reflex arc), the ipsilateral cochlear nucleus activates MOC fibers on the contralateral side, which then project back to the ipsilateral cochlea, and therefore involve *crossed* MOC fibers. Conversely, when the MOCR is activated in one ear and MOCR effects are assessed in the opposite ear (the *contralateral* reflex arc), the contralateral cochlear nucleus activates MOC fibers on the ipsilateral side, which then project to the ipsilateral cochlea, and therefore involve *uncrossed* MOC fibers. As reviewed in Guinan (2006), ipsilateral MOC effects are generally more pronounced than contralateral MOC effects in non-primate animals owing to the larger number of crossed MOC fibers, but ipsilateral and contralateral effects in humans appear to be more similar in strength, which may be due to a similar number of crossed and uncrossed fibers as seen in primates (Thompson and Thompson 1986).

3.2 Purposes of the Auditory Efferent System

3.2.1 Protection from Acoustic Trauma

Given that activation of the MOCR reduces the enhancement of basilar membrane motion provided by the cochlear amplifier, the question turns to the purpose of this reflex. One proposed purpose is that it serves as a protective mechanism from cochlear damage due to loud sounds. This notion has been supported by the results of animal work. Rajan (2000) measured noise-induced threshold shifts in cats before and after sectioning MOC fibers; threshold shifts were significantly larger after the efferents were sectioned. Similar results have been reported when using DPOAEs in the chinchilla (Zheng et al. 1997). Rats with stronger (i.e., more effective) MOCR, as assessed by the magnitude of reduction in DPOAEs with versus without MOCR activation, had less severe threshold shifts after being exposed to high-level (109 dB SPL) sound (Maison and Liberman 2000). The same relationship has also been found for mice exposed to less extreme sound levels (84 dB SPL) (Maison et al. 2013). Although the MOCR appears to provide protection, it has been argued that sound levels in nature are lower than the sound

levels used experimentally, suggesting that efferent effects did not evolve to prevent noise damage (Kirk and Smith 2003). Results from limited human studies have not shown a clear relationship between the MOCR and noise damage, as discussed later.

LOC efferents may also have a role in protection from noise damage. Darrow et al. (2007) lesioned the LOC bundle of one hemisphere in mice but did not damage the MOC bundle. DPOAEs and ABRs were measured before and after noise exposure in both ears. DPOAEs were the same in both ears, suggesting equal damage to OHCs on both side, but ABR thresholds were poorer in the ear that was the same side as the lesion. Given that LOC fibers terminate on auditory nerve fibers primarily on the same side, the authors argued that the LOC bundle reduces auditory nerve responses to noise and thus protects from noise damage at the level of the nerve. Further investigation into LOC efferent effects is warranted.

3.2.2 Improved Hearing in Background Noise

Another potential purpose of the MOCR is to improve detection of sounds in the presence of background noise. When the auditory nerve responds to steady-state noise, adaptation occurs, which means that other sounds will need to be increased in level in order to be detected. Activation of the MOCR reduces the response to the noise and thus the adaptation. The auditory system can then respond to other sounds, primarily transients. Winslow and Sachs (1987, 1988) measured auditory nerve firing rate as a function of tone pip level. Responses were measured with and without noise and with and without MOCR activation. In quiet, efferent activation raised the threshold of the response to the tone because of the reduction in cochlear amplification. However, in the presence of background noise, efferent activation increased the response to the tone when it was at high stimulus levels. Similar results have been found for compound action potential responses (Kawase and Liberman 1993) and auditory nerve fiber responses (Kawase et al. 1993) to tone pips in cats. The increased responses were eliminated when efferent fibers were cut. Although improvement in detection of sounds in noise has been

demonstrated in animals, mixed results in humans using speech recognition have been seen and will be discussed later.

3.2.3 Normal Auditory Development

It has been speculated that MOC fibers are necessary for proper development of outer hair cell function. Walsh et al. (1998) investigated the effect of sectioning efferent fibers in neonatal cats. The authors investigated hearing thresholds and tuning and included two control groups, one with no surgical intervention and one with a sham surgery. After birth, the group with sectioned efferent fibers was found to have poorer thresholds and broader tuning relative to the control groups. However, it was found that the outer hair cells were structurally intact in both groups, suggesting that the lack of efferent fibers was involved in development of outer hair cell function and/or microstructure. However, the results were not able to be replicated (Liberman et al. 2000), leaving the importance of the efferent system to auditory development an open question.

3.3. Assessing MOCR Effects Using OAEs

3.3.1 Rationale for Using OAEs

In humans, efferent effects are primarily studied via OAEs because they can be measured quickly and non-invasively. Efferent effects on OAEs are quantified by the change in OAEs obtained with and without the presence of an MOCR activator. Differences in OAE amplitude, phase, and/or latency are attributed to MOCR-induced changes in OHC properties. Efferent effects have been examined for all types of OAEs.

For reflection-source emissions, efferent effects nearly always result in a decrease in amplitude, as assessed by TEOAEs (e.g., Puel et al. 1988; Collet et al. 1990; Berlin et al. 1993; Hood et al. 1996; de Boer and Thornton 2008; Garinis et al. 2008; Goodman et al. 2013), SFOAEs (Souter 1995; Guinan et al. 2003; Backus and Guinan 2007; Francis and Guinan 2010; Boothalingam and Lineton 2012), and SOAEs (Mott et al. 1989; Harrison and Burns 1993; Zhao and Dhar 2010). In addition to amplitude decreases,

TEOAEs and SFOAEs have shown decreases in latency and phase leads with efferent stimulation (Ryan et al. 1991; Giraud et al. 1996; Francis and Guinan 2010). Because efferent activation broadens the traveling wave peak basally, it would be expected that OAEs reach the site of reflection sooner and would therefore return to the ear canal sooner than OAEs generated without efferent stimulation. However, others have found a lack of phase and latency changes in SFOAEs and TEOAEs (Souter 1995; Boothalingam and Lineton 2012), suggesting that the effect may be difficult to detect or is not present in all subjects.

Efferent effects on distortion-source OAEs (i.e., DPOAEs) have also been examined (e.g., Chéry-Croze et al. 1993; Williams and Brown 1997; Abdala et al. 1999; Büki et al. 2000; Deeter et al. 2009; Kumar et al. 2013). Although DPOAE amplitudes are often decreased with efferent stimulation, the amplitude can sometimes be increased. This is believed to be due a differential effect on the distortion- and reflection-source components (Müller et al. 2005; Sun 2008). In normal measurement conditions (i.e., without efferent stimulation), the two components can be out of phase and result in a cancelation when measured in the ear canal (Heitmann et al. 1998; Talmadge et al. 1999). When measured across frequencies with narrow resolution, there is a repeating pattern of dips and peaks in response magnitude, termed fine structure. If efferent stimulation disrupts the phase cancelation by affecting one component more than the other, the result can be an increase in measured amplitude. When the two components are separated experimentally, each shows a decrease (Henin et al. 2011). The differential effects can also be minimized by analyzing MOCR effects in the dips of the DPOAE fine structure (Wagner et al. 2007). However, these methods are not routinely used, especially in clinical settings, and can be time-consuming. Therefore, DPOAEs have been used less for studying efferent effects in humans compared to reflection-source OAEs, especially TEOAEs.

3.3.2 MOCR Strength

In this paper, the term "strength" in the context of the MOCR refers to the degree of change in amplitude and/or phase in OAEs with versus without MOCR activation, where "stronger" indicates a larger reduction in amplitude and/or a larger phase change in the presence of MOCR activation. One might presume that a stronger MOCR effect is desirable based on the studies that found stronger MOCR effects were associated with more protection from noise-induced hearing loss (Maison and Liberman 2000) and with improved speech-in-noise performance (e.g., Kumar and Vanaja 2004). However, as discussed in Chapter 3.2.2, other studies have not found this association. Regardless, descriptions of MOCR strength will be used throughout this paper because subjects show a range of MOCR effects, presumably due to variability in the functioning of the MOCR across subjects.

3.3.3 Factors Influencing MOCR Effects on OAEs

3.3.3.1 Ipsilateral, Contralateral, and Bilateral Activation

As discussed previously, the MOCR is a bilateral reflex, so sound presented in either ear can activate the reflex and influence OHC function in both ears. The strongest MOCR effects occur when the reflex is elicited bilaterally, with weaker effects occurring for ipsilateral and contralateral activation (Berlin et al. 1995; Lilaonitkul and Guinan 2009). Ipsilateral and contralateral activation appears to have similar effects, contrary to animal work which demonstrates stronger effects for ipsilateral stimulation (Guinan 2006). Most human studies use contralateral activation of the MOCR, which has the advantage of acoustically separating the MOCR and OAE activating stimuli. To avoid acoustic contamination in the ipsilateral and bilateral cases, a forward masking paradigm is required in which the activator is presented and then OAEs are elicited after the activator is terminated. However, ipsilateral sound can cause changes in the OAEs even when the efferent fibers are cut (Liberman et al. 1996) and cannot be disentangled from efferent effects (Guinan 2006). Given that the majority of human studies implemented

contralateral activation of the MOCR, the remainder of this review will focus on studies using a contralateral activation paradigm unless otherwise stated.

3.3.3.2 Stimulus Parameters

The MOCR can be activated by a variety of sounds, including pure tones, tone bursts, clicks, narrowband and broadband noise (Guinan et al. 2003). Efferent effects become stronger as the stimulus bandwidth increases due to increased number of efferent fibers stimulated (Norman and Thornton 1993; Maison et al. 2000; Velenovsky and Glattke 2002; Lilaonitkul & Guinan 2009). Therefore, broadband noise is typically used as the MOCR-eliciting stimulus. MOCR effects also become stronger as the level of the eliciting stimulus increases (Collet et al. 1990; Veuillet et al. 1991; Hood et al. 1996).

Although intense, broadband stimuli seem ideal for eliciting MOCR, elicitation of the middle-ear muscle reflex (MEMR) also increases as stimulus bandwidth and level increases (e.g., Popelka et al. 1974; Gorga et al. 1980; Margolis et al. 1980). Activation of MEMR increases the impedance of the middle ear primarily below 1 kHz (Møller 1962), reducing transmission of sound through the tympanic membrane in the forward and reverse direction. Activation of MEMR reduces OAE amplitudes (Whitehead et al. 1991), similar to MOCR activation. It can therefore be difficult to determine if decreases in OAE amplitudes were due to MEMR and/or MOCR. Methods have been proposed for disentangling these effects (e.g., Guinan et al. 2003), but it may be preferable to avoid MEMR elicitation. An additional confound is that OAE-eliciting stimuli, especially clicks, can also elicit the MEMR (Veuillet et al. 1991; Rawool 1995; Guinan et al. 2003) as well as MOCR activity. Partial activation of the MOCR by the OAE-eliciting stimuli themselves will reduce OAE amplitudes, making it more difficult to detect a change in OAE amplitudes due to an intended MOCR activator.

3.3.3.3 OAE Frequency Effects

MOCR effects in humans have typically been found to be most prominent on OAEs in the 1-2 kHz region (e.g., Collet et al. 1990; Hood et al. 1996; Goodman et al.

2013). Effects are weak or absent above 4 kHz, although this may be due to poor signal-to-noise ratios (SNRs) of higher-frequency emissions (Goodman et al. 2013). This pattern of frequency effects may be related to the density of efferent innervation (Robertson et al. 1987; Liberman et al. 1990). It may also be related to the middle ear transfer function, which is most efficient in the 1 – 4 kHz region (Møller 1963; Aibara et al. 2001). OAEs in this frequency region would be strongest and therefore changes would be most easily observable in this region.

3.3.3.4 Lateralization of MOCR

There is evidence of lateralization of the MOCR, suggesting a difference between the olivocochlear bundles on the left and right sides. MOCR effects tend to be stronger in right ears relative to left ears (Khalfa et al. 1997, 1998; Morlet et al. 1999). Administration of benzodiazepines, of which there are more receptors in the left hemisphere, reduced MOCR effects when measured in the right ear relative to the left ear (Morand-Villeneuve et al. 2005). These studies used contralateral MOCR activators, which primarily excites the uncrossed MOC fibers (Liberman et al. 1990; Guinan 1996). One study that included an ipsilateral MOCR activator, which excited crossed MOC fibers, found that MOCR effects were stronger in the left ear, suggesting that lateralization is different for crossed and uncrossed fibers (Philibert et al. 1998).

3.3.3.5 Attention Effects

The presence of descending pathways from the cortex to the brainstem suggests that the cortex can influence efferent activity. Efferent effects are reduced or absent in the presence of sleep (Froehlich et al. 1993b) and anesthesia (Boyev et al. 2002; Chambers et al. 2012). Auditory and visual attention tasks in animals and humans decrease the amplitude of evoked potentials and otoacoustic emissions relative to measurements made with no attention task (e.g., Bũno et al. 1966; Oatman 1976; Lukas 1980; Puel et al. 1988; Froehlich et al. 1993a; Giard et al. 1994; Ferber-Viat et al. 1995; Maison et al. 2001; de Boer and Thornton 2007; Delano et al. 2007; Harkrider and Bowers 2009).

It has been suggested that efferent activity will be strongest when it is advantageous to reduce sensitivity to auditory input (Guinan 2011). For example, an individual attending to visual stimuli in the presence of distracting acoustic stimuli may benefit from the MOCR, whereas an individual attending to soft acoustic stimuli would likely not benefit from the MOCR. This notion has been supported by studies that compared visual and auditory attention tasks, in which visual tasks were found to increase the amount of efferent activity more than auditory tasks (Lukas 1980; Froehlich et al. 1993a; de Boer and Thornton 2007; Delano et al. 2007). A reduction in auditory sensitivity may have been beneficial in order to attend to visual input. Additionally, auditory tasks that involved attending to stimuli in the ear in which OAEs were recorded from showed less efferent activity relative to attending to stimuli in the contralateral ear or no task (Ferber-Viat et al. 1995; Harkrider and Bowers 2009). In this type of task, reducing sensitivity in the contralateral ear would be expected to be beneficial, but not in the ipsilateral ear. The results of these studies on attention suggest that the cortex can modify efferent activity beyond what is achieved reflexively to aid in accomplishing a task.

3.3.3.6 Age Effects

Age appears to show the largest effect in older adults. MOCR effects in newborns are similar to those in young adults (Abdala et al. 2013). Others have found decreasing MOCR strength with increasing age in adults (Parthasarathy 2001; Kim et al. 2002; Jacobson et al. 2003; Keppler et al. 2010a). These differences remained after controlling for hearing thresholds. Interestingly, a study in a mouse model of presbycusis found that MOCR effects on DPOAEs dissipated before DPOAEs (Zhu et al. 2007), suggesting that loss of MOCR may predict the onset of hearing loss prior to more well-established measures of auditory function.

3.3.4 Potential Clinical Utility of MOCR Measurements

3.3.4.1 Predicting Susceptibility to Acoustic Trauma

Given the proposed purposes of the MOCR discussed earlier, measurement of MOCR effects in humans using OAEs may be clinically useful. Animal work has suggested that the strength of the MOCR may predict susceptibility to noise-induced hearing loss (Maison and Liberman 2000). Few studies have examined this in humans, and the results have been conflicting. Veuillet et al. (2001) studied 36 adults exposed to rifle blasts in a military setting. All subjects had a temporary threshold shift (TTS) of ≥20 dB at one or more frequencies. For thresholds at 6 and 8 kHz (but not other frequencies), there was a statistically significant correlation between MOCR-induced TEOAE amplitude reduction and threshold recovery measured 3 days after exposure, but not 30 days after exposure. Only 13-20% of the variance in threshold recovery was explained by MOCR effects at these frequencies, indicating a very small effect. The MOCR was elicited with 30 dB SPL noise, which is fairly low relative to other studies that present at 50-60 dB SPL (e.g., Hood et al. 1996; Guinan et al. 2003). Therefore, the authors likely did not elicit strong MOCR effects with this stimulus level. However, the results do suggest a role for predicting recovery from TTS at a limited range of frequency. It is possible that elicitation of stronger MOCR effects would result in better or more useful predictions.

Another study found no correlation between MOCR effects on DPOAEs and threshold recovery after exposure to impulse noise (Wagner et al. 2005). The study of Wagner et al. involved 83 ears exposed to rifle blasts while wearing earplugs. The authors found only 9 of 83 ears had a temporary threshold shift which did not exceed 15 dB, which likely resulted in limited statistical power to detect an effect of MOCR functioning. The MOCR was elicited with 60 dB SPL broadband noise, which was likely sufficient to elicit measurable efferent effects. The authors examined the $2f_1$-f_2 DPOAE but did not separate the components, which may have resulted in inconsistent efferent

effects across subjects. Due to ethical and practical reasons, human noise exposure studies have little experimental control over the noise parameters (noise level, duration of exposure, distance from noise source, noise exposure outside the research setting, etc.) and it is therefore difficult to compare results across studies. The usefulness of MOCR measurement to predict noise-induced hearing loss in humans remains an open question.

3.3.4.2 Assessing Benefit for Hearing in Background Noise

Animal work has found that auditory nerve responses to stimuli in noise can be increased in the presence of noise, likely due to efferent inhibition of the response to noise (e.g., Winslow and Sachs 1987; Kawase and Liberman 1993; Kawase et al. 1993). However, studies in humans have shown conflicting results. Kumar and Vanaja (2004) found that MOCR strength was positively correlated with performance on a speech-in-noise task in ten normal-hearing children. However, Wagner et al. (2008) and de Boer et al. (2012) found no significant correlation between MOCR strength and performance. Differences in the speech and noise stimuli and levels may partly explain the varying results, but the limited evidence suggests that the effect is not robust. More research in this area is warranted.

3.3.4.3 Assessment of Clinical Populations

Various clinical populations demonstrate difficulty hearing in the presence of normal hearing. Given that the MOC system may provide benefit for hearing in noise, some researchers have speculated that these populations may demonstrate reduced or absent MOCR function. MOCR effects on OAEs have been studied for various conditions, such as auditory processing disorder (Muchnik et al. 2004; Sanches and Carvallo 2006), learning disabilities (Garinis et al. 2008), specific language impairment (Clarke et al. 2006), dyslexia (Veuillet et al. 2007), and Asperger's syndrome (Kaf and Danesh 2013). These studies compared MOCR-induced changes in OAEs between the clinical population and a control group. Some of these studies have shown smaller changes in OAEs for the clinical group (Muchnik et al. 2004; Sanches and Carvallo

2006). Others have shown that the clinical group demonstrated more efferent activity in the left ear, whereas the control group demonstrated more activity in the right ear (Veuillet et al. 2007; Garinis et al. 2008; Kaf and Danesh 2013). These results may suggest that reduced or abnormal MOC functioning causes difficulty hearing in noise or is a symptom of a more central auditory problem. Although the results also suggest a clinical role for MOCR testing, analyses were performed on group data rather than on individuals which does not allow for an assessment of MOCR functioning in individuals. The issue of assessing individual effects will be discussed in Chapter 3.4.2.

Auditory neuropathy is a condition in which the auditory nerve cannot fire synchronously but OHC function is normal, and presents clinically as present OAEs, abnormal or absent ABR, and poor speech discrimination (Starr et al. 1996). Because the MEMR and MOCR pathways involve the auditory nerve, these reflexes are also abnormal or absent in patients with auditory neuropathy (Hood et al. 2003; Berlin et al. 2005). Diagnosis of auditory neuropathy requires ABR measurement (Berlin et al. 2003), which typically requires sedation in older infants and younger children. MOCR testing may find use as a screening tool and/or addition to the test battery because it can be measured non-invasively without the need for sedation.

3.3.4.4 Assessing Outcomes of Auditory Training

As discussed previously, anatomical studies show descending pathways from the cortex to the brainstem, which includes the MOC bundle. This could indicate that the cortex can modulate efferent activity. In humans, several sources of evidence suggest that auditory training can strengthen efferent effects, presumably through a cortically-mediated mechanism. Individuals with musical training have stronger effects than untrained individuals (Micheyl et al., 1997; Perrot et al., 1999). Additionally, de Boer and Thornton (2008) found a relationship between MOCR strengthening and improvement on phoneme discrimination after an auditory training task. Individuals with weak baseline MOCR effects improved their performance after the training, and also had increases in

MOCR strength after the task. However, it is unclear if MOCR strengthening resulted in improved performance, or if both were the result of a more central change. Veuillet et al. (2007) examined the effect of auditory training on MOCR effects in children with dyslexia. At baseline, dyslexic children showed asymmetry in MOCR effects, where larger effects were seen in left ears relative to right ears. An opposite pattern was seen in a control group. After training on a phoneme discrimination task, the dyslexic children showed MOCR ear effects that were more similar to the control group. These results suggest that auditory training can both strengthen the MOCR and reduce abnormalities in MOCR asymmetry. However, the mechanism for how this occurs is unclear and requires further study.

3.4 Limitations of Previous Research

3.4.1 Control of Confounds

3.4.1.1 Middle-ear Muscle Reflex

The MEMR is a brainstem-mediated effect that increases middle-ear impedance by stiffening the ossicular chain, which reduces transmission of frequencies primarily at 1 kHz and below (Møller 1962). Like the MOCR, the magnitude of MEMR effects are increased with increasing stimulus level and stimulus bandwidth (Liberman and Guinan 1998) and it can reduce OAE amplitudes (Whitehead et al. 1991; Guinan et al. 2003). Therefore, MEMR activation may be misinterpreted as MOCR effects.

Some studies reported using stimulus levels that did not activate MEMR as assessed with standard clinical immittance measurements (e.g., de Ceulaer et al. 2001; Muchnik et al. 2004; Clarke et al. 2006; de Boer and Thornton 2008; Mishra and Lutman 2013). However, it is possible that sub-clinical activation of MEMR could still occur (Feeney and Keefe 2001). A preferable method is to examine the presence of MEMR within the MOCR measurement. This method has been advocated by several studies (e.g., Guinan et al. 2003; Goodman and Keefe 2006; Guinan 2006; Goodman et al. 2013). The OAE-eliciting stimulus can be examined for amplitude and/or phase changes. MEMR

activation will affect transmission of the stimulus through the middle ear, whereas MOCR only affects the OAEs returning to the ear canal. Therefore, significant changes in the stimulus suggest that the MEMR was activated. Because few studies have assessed MEMR in this way, it is unknown the number of MOCR shifts that may have been due in part or in full to MEMR effects.

3.4.1.2 Slow Drift in OAE Amplitude

OAEs can exhibit slow drifts in amplitude when measured across time (Backus 2006; Goodman et al. 2013). This may be due to slippage of the probe in the ear canal, slight changes in middle ear pressure, or other factors. Slow drifts may be exhibited as increases or decreases in amplitude, may or may not be monotonic, and may involve changes of 1 dB or more across time (Goodman et al. 2013). When examining MOCR effects, slow drift may present as a change due to MOCR activation. Some studies have attempted to reduce the effect of drift by interleaving conditions, in which OAEs are measured with and without an MOCR activator in an alternating fashion (e.g., Guinan et al. 2003; Hood et al. 2003; Mishra and Lutman 2013). However, this does not fully alleviate the problem because a systematic trend in the drift will cause one condition to be different in amplitude from the other condition. Goodman et al. (2013) described a de-trending procedure in which a median filter (Little and Jones 2010) is fit to the amplitude data across time, and the trend line is then subtracted from the recorded waveforms. Qualitatively, this procedure removed the trends across time. In several subjects, de-trending changed the statistical significance of MOCR effects relative to no de-trending. However, in the majority of subjects, statistical significance was unaffected. Regardless, it is apparent that slow drifts need to be accounted for before one can assess whether or not a change in OAE amplitude was due to MOCR effects.

3.4.1.3 Subject's Attentional State

As discussed previously, the subject's attentional state can alter the MOCR effect. If measurements are taken within a brief time, such as a single visit, lack of attention

could reduce the ability to detect an MOCR effect. It may or may not affect any differences between measurements. A study of repeatability must take into account the subject's attentional state within and across visits. Ideally, attention would be controlled for by having the subject perform the same task each time and ensure similar performance. Other than studies that have specifically examined the role of attention, no known studies in humans have controlled for the subject's attentional state. This is a weakness of studies that have examined the repeatability of MOCR effects.

3.4.2 Lack of Examination of Effects in Individuals

Because MOCR effects on OAEs tend to be small (amplitude changes of often 1 dB or less), nearly all previous studies have assessed the statistical significance of these effects using group data only. Often, mean amplitudes obtained with and without an MOCR activator are compared using a parametric statistical test such as a *t*-test or analysis of variance (ANOVA) (e.g., Giraud et al. 1995; Maison et al. 2000; Hood et al. 2003; Muchnik et al. 2004; Clarke et al. 2006; Garinis et al. 2008). If the means are significantly different, typically lower in the presence of MOCR activation, this is interpreted as an MOCR-induced change in OAEs. However, most studies do not adequately control for the confounds discussed above, so it is usually not known how many differences were due to MOCR effects.

Additionally, few studies have reported individual data. In a clinical setting, it is usually of interest to determine whether or not there is a statistically significant effect in an individual. De Ceulaer et al. (2001) reported the distribution of MOCR effects measured in a group of 60 subjects. The authors were interested in obtaining normative data for clinical applications. MOCR effects were measured four times and the mean was calculated; however, the authors did not assess if the MOCR effects were significantly different from zero. This study did highlight the importance of examining individual effects for clinical purposes.

Two studies have specifically examined the statistical significance in individuals. Backus and Guinan (2007) and Goodman et al. (2013) used statistical resampling procedures to create a distribution of MOCR effects obtained from an individual's own recordings and then compared the observed difference in OAE amplitudes to this distribution. Observed differences that fell outside this distribution were deemed statistically significant. Backus and Guinan found that all subjects (25) had significant MOCR effects on SFOAEs at or around 1 kHz. Goodman et al. examined 16 subjects, and found that approximately 65-85% had significant effects from 1-3 kHz depending on the frequency, with fewer significant effects seen at 4 kHz and above. Both studies demonstrated the feasibility and importance of measuring statistical significance of MOCR shifts. Future studies should therefore incorporate an analysis of statistical significance at the level of the individual to more accurately identify true MOCR shifts.

3.5 Assessing Repeatability of MOCR Effects

3.5.1 Rationale

One important aspect of a clinically useful measurement is that it is highly repeatable across time in a control population (e.g., normal hearing young adults with no noise exposure and no ear/hearing pathology). If changes in a metric across repeated measurements are to be of clinical value (e.g., detecting improvement in MOCR due to auditory training, or a decrement in MOCR due to hearing loss), then a healthy control population should demonstrate low variability and high repeatability in the measurements across time. A change in a measurement due to a pathology or intervention must be larger than the variability seen in a control population; smaller variability in the control population means that smaller changes can be detected and that the measurement may be clinically useful. High repeatability is a necessary, but not sufficient, component of a clinically useful test. Other important factors include high sensitivity and high specificity, administration in a feasible amount of time, cost-efficiency, and provision of consistent

results across testers and locations. These other factors are beyond the scope of the current study.

3.5.2 Repeatability of OAEs

Studies in normal-hearing adults have shown that TEOAE and DPOAE amplitudes are generally stable within ±3 dB or better when measured across the short-term (hours to days) and longer-term (weeks to months) (Harris et al. 1991; Franklin et al. 1992; Engdahl et al. 1994; Marshall and Heller 1996; Wagner et al. 208; Keppler et al. 2010b). Several studies that measured TEOAEs and DPOAEs in the same ears found that TEOAEs had smaller standard deviations than DPOAEs when compared at the same frequencies (Lapsley Miller et al. 2004; Keppler et al. 2010b; but see Franklin et al. 1992). This may be due to the inherent averaging across frequency when analyzing TEOAEs (typically in ½-octave or 1-octave bands), which could be expected to be less variable than analysis of DPOAEs, which are analyzed at a single frequency. Historically, DPOAEs have been advantageous for measuring higher frequencies than TEOAEs, which cannot be reliably measured above 4-5 kHz using standard instrumentation. However, recent studies have demonstrated the ability of TEOAEs to measure frequencies up to 16 kHz with nonlinear extraction methods (Goodman et al. 2009; Keefe et al. 2011). TEOAEs have also been shown to more accurately predict hearing status in the 1-2 kHz range relative to DPOAEs (Gorga et al. 1993). In terms of assessing MOCR effects, TEOAEs may be preferable to DPOAEs because TEOAEs have smaller standard deviations and are more useful for assessing effects at 1-2 kHz, which is where MOCR effects on OAEs tend to be the most pronounced (Collet et al. 1990; Berlin et al. 1993).

3.5.3 Previous Research on Repeatability of MOCR Effects

Although efferent effects on OAEs in humans have been assessed for nearly 30 years, relatively few have investigated the repeatability of these effects across time. Typically, the test-retest reliability between two sessions has been examined (e.g., Berlin et al. 1993; Berlin et al. 1995; Sanches and Carvallo 2006; de Boer and Thornton 2008;

Mishra and Lutman 2013). This has often been assessed within a single session, but studies have examined the reliability for sessions spaced by several days (de Boer and Thornton 2008; Mishra and Lutman 2013). Generally, these studies have demonstrated high test-retest reliability using various metrics, such as the correlation between two measures of OAE amplitude change and a t-test comparing mean amplitude changes between two tests. However, Berlin et al. (1995) showed low correlations between two measurements when using a forward-masking paradigm in which the MOCR elicitor was presented prior to measuring TEOAEs. The lowest correlation was found when noise was presented contralaterally, suggesting that a contralateral forward-masking paradigm may not be clinically useful for measuring MOCR effects.

Only three studies to data have focused on the repeatability of MOCR effects on OAEs, with mixed results regarding how repeatable the effects were. These results may be due to differences in methodology (e.g., the type of OAE measured, number of measurements, spacing between measurements, stimulus levels, analysis (e.g., quantification of repeatability, analysis frequencies and bandwidth), and subject characteristics. These studies examined repeatability using various statistical tests and metrics, which will be briefly explained as they are introduced in this section and will be more fully explained in the Chap. IV (Methods).

3.5.3.1 Graham and Hazell (1994)

Graham and Hazell (1994) were the first to examine repeatability across more than two sessions. They examined MOCR effects on TEOAEs in 6 adults with normal hearing; five were between 22-26 years old and one was 67 years old. Eighteen total measurements were taken: six measurements at three visits, with each visit spaced by three weeks. TEOAEs were elicited with 65 dB SPL clicks and the MOCR was elicited with 30 dB SL contralateral white noise (CWN). MOCR was quantified as the amplitude difference between mean TEOAE waveforms obtained with and without CWN. Across all measurements, mean TEOAE shifts ranged from approximately 0.3 – 0.6 dB and the

standard deviations ranged from 0.10 – 0.25 dB, indicating small but repeatable effects over time. The authors used a multivariate analysis of variance (MANOVA) to examine effects of measurement and day on the mean MOC shift. No significant effect was found for either, suggesting that the mean MOC shift did not change across measurements or days.

Although these results appear to suggest that MOC shifts of TEOAEs are stable, there are limitations that restrict the conclusions that can be drawn from the data. The authors did not examine the statistical significance of MOC shifts in individuals or in the group. Individual data are reported, and some mean MOC shifts are close to 0 dB. It is likely that the 95% confidence intervals would include 0 in some instances, suggesting that the MOC shift was not significantly different from zero. Therefore, it is not known how many of the shifts reported were actually significant. Additionally, the SNRs of the TEOAEs were not reported, so it is not known how robust the emissions were. The relatively low click stimulus level (65 dB SPL) and small number of averages (300) could result in low SNRs, especially in the older subject, but these data were not reported. The study examined a relatively small number of subjects (six), with one subject being appreciably older than the others, likely limiting the generalizability of the findings to the general population. Confounds of MEMR, slow amplitude drifts, and attentional effects were not controlled for. The result of these limitations is that little is known about how stable MOCR-induced shifts of TEOAEs are, as the shifts in TEOAEs may be due to other confounding factors or may simply represent measurement variability across time.

3.5.3.2 Kumar et al. (2013)

More recently, Kumar et al. (2013) examined repeatability of MOC shifts using DPOAEs. Subjects were 24 normal hearing adult males ages 18-45 years. Ten measurements were taken across a two-week span: two measurements on the first day and one measurement taken on eight additional days. $2f_1$-f_2 DPOAEs (f_2/f_1=1.2, L1/L2=65/55 dB SPL) were measured from 1-8 kHz (spaced by 1 kHz) with and without

the presence of CWN presented at 40 dB SPL. Repeatability was examined statistically using multiple metrics, including repeated measures ANOVA, Cronbach's alpha and interclass correlation coefficient (ICC), standard error of measurement (SEM, in dB), and the smallest detectable difference (SDD, in dB). The repeated measures ANOVA examined whether the mean MOC shift varied depending on the test session. Cronbach's alpha (Cronbach 1951) and the ICC (Shrout and Fleiss 1979) are measures of reliability, where a value of 1.0 indicates perfect reliability between measurements. The SEM is the standard deviation of errors of measurement (i.e., how far the measured values are from the true value) and is proportional to the reliability measures. Finally, the SDD (also referred to as minimum detectable change or MDC) is the smallest difference between measurements that are considered statistically significant.

DPOAE amplitudes without CWN had SEMs ranging from 0.7 – 1.4 dB across sessions and frequencies, suggesting stable emissions and consistency with previous reports of DPOAE amplitude stability. However, poor repeatability was seen for MOC shifts. Within a single session without probe re-insertion, Cronbach's alpha values ranged from 0.2 to 0.7 and ICC values ranged from 0.1 to 0.6 (for both metrics, 1.0 indicates perfect reliability). SEMs, which were calculated using Cronbach's alpha and the standard deviation, were 1 dB or less. Given that these values were relatively low, this indicates that the standard deviations of measurements were small while the Cronbach's alpha was large. SDD values ranged from 1.7 to 2.7 dB, which are large relative to most previous reports of MOCR effects that often show changes of 1 dB or less.

When repeatability across multiple sessions was examined, increases in Cronbach's alpha (ranging from 0.5 to 0.8) but decrements in the ICC (ranging from 0.1 to 0.3) were found. The reason for the discrepancy in these measurements was not explained. SEMs were slightly larger (1.6 dB or less), and SDDs also increased (ranged from 1.6 to 4.3 dB). The authors concluded that the results were too variable within and across subjects for DPOAEs to be clinically useful for assessing MOCR effects.

There are multiple shortcomings to the study of Kumar et al. (2013), which will be described in the following five paragraphs. First, it is possible that subjects' DPOAE responses were too noisy to reliably measure an MOC effect. Although they did not report quantitative data, most subjects appeared to have DPOAE amplitude changes less than the smallest detectable change (see their Figs. 3 and 4). A recent study demonstrated that the smallest detectable change in OAEs decreases exponentially with increasing OAE SNR (Goodman et al. 2013). Kumar et al. (2013) reported that DPOAEs were required to have a >6 dB SNR to be considered present, but the authors did not report the measured SNRs. They reported that DPOAE measurements lasted 30 seconds per frequency, which may have resulted in relatively low SNRs. Even though DPOAEs were present, the change in DPOAE amplitude may have been noisy (i.e., randomly fluctuating) and would not be expected to be repeatable. Increased averaging time would improve the SNR and may reduce the smallest detectable difference.

Second, effects were measured at seven discrete frequencies across a three octave range. In a study of MOCR effects on SFOAEs near 1 kHz, Backus and Guinan (2007) averaged the effects at multiple frequencies in order to detect significant effects. Therefore, analysis at single frequencies may have further reduced the authors' ability to detect MOCR effects.

Third, the purported MOCR activator, which was broadband noise presented at 40 dB SPL, may have been too low in level to elicit MOCR effects in most subjects. Studies have demonstrated that increasing the MOCR activator level increases the magnitude of change in OAE amplitudes (e.g., Collet et al. 1990; Hood et al. 1996). Studies have recommended noise levels of 60 dB SPL (Guinan et al. 2003; Guinan 2006). Hood et al. (1996) found no MOCR effects on TEOAEs using 40 dB SPL broadband noise. Although bandwidth of the noise must be known in order to directly compare levels (and it is often not reported), it is possible that the level of the stimuli was too low to activate the MOCR

in most subjects, resulting in the low number of subjects exhibiting measurable MOCR effects.

Fourth, the authors did not control for MEMR, slow amplitude drifts across time, and attentional state of subjects. The authors acknowledged that lack of attentional control was a potential weakness of the study. Elicitation of MEMR may have been low given the low CWN level and because narrowband stimuli were used to elicit DPOAEs (Guinan et al. 2003). The presence of slow drift may have masked actual MOC shifts, which may have contributed to the low prevalence of significant shifts.

Finally, the authors examined the composite DPOAE rather than separating it into the distortion- and reflection-sources, which could explain why some subjects exhibited increases in DPOAE amplitude with efferent stimulation. DPOAE fine structure appears to be repeatable across time (Reuter and Hammershøi 2006), so this may not account for the variability in MOCR effects. However, the authors may have reduced the ability to detect MOCR changes in DPOAE amplitude by not analyzing the two components separately. Although Kumar et al. concluded that MOCR effects on DPOAEs are not repeatable, methodological issues appear to have limited their ability to detect such effects, and would therefore not be expected to be repeatable.

3.5.3.3 Mishra and Lutman (2013)

Mishra and Lutman (2013) also examined the repeatability of MOCR effects on OAEs but concluded that the effects were highly repeatable and may be clinically feasible. MOCR effects on TEOAEs were measured in 35 normal-hearing young adults. Two measurements were obtained per subject, with measurements separated by one to four days. TEOAEs were obtained at five levels ranging from 57-69 dB pSPL in 3 dB steps. The MOCR activator was CWN presented at 35 dB SL. The MOCR effect was quantified as the change in the overall TEOAE amplitude. Test-retest reliability was assessed using Bland-Altman plots (Bland and Altman 1999), Cronbach's alpha, and a repeated measures ANOVA.

TEOAE SNRs ranged from 6 to 17 dB, with a mean of 12 dB. Repeatability results revealed low variability and high reliability across the two sessions. When MOCR effects were expressed as the dB change in TEOAE amplitudes, Bland-Altman plots showed that effects changed by 0.03 – 0.07 dB across session for each stimulus level. Cronbach's alpha was 0.8 for four stimulus levels and 0.7 for one level. The ANOVA revealed no main effect of test session, indicating that the mean MOCR effect did not change between sessions. Essentially similar results occurred when MOCR effects were expressed as the percentage of change in TEOAE amplitude without CWN. The authors concluded that the effects were highly repeatable and have the potential for clinical applications.

This study had several methodological advantages over those of Kumar et al. (2013). Mishra and Lutman (2013) used TEOAEs rather than DPOAEs, which allows for averaging across multiple frequencies due to the broadband nature. Additionally, multiple components of TEOAEs are separated in time (Goodman et al. 2009) and should therefore not be subject to the phase cancellation effects that multiple DPOAE components are.

However, Mishra and Lutman (2013) also had several limitations that were not present in Kumar et al. (2013). Mishra and Lutman reported the measured SNRs but did not include SDDs. Therefore, it is not known if the shifts that were observed were statistically significant. Additionally, only two measurements were made on each subject. Although this allows for test-retest reliability to be calculated, the variance is inversely proportional to the number of data points (in this case, measurements). Two measurements will result in a larger variance than multiple measurements, and therefore there may not have been enough statistical power to detect a difference in mean MOC shift between the two measurements. Also, two measurements taken within five days do not give an indication of the repeatability over a longer time span. Finally, the authors only examined changes in overall TEOAE amplitude rather than within frequency bands.

Although averaging amplitude shifts across multiple frequencies increases the likelihood of detecting a change (Backus and Guinan 2007), it may also be useful to look in more narrowband frequency ranges, such as 1/3 or 1/2-octave bands. For example, a broadband analysis would likely be less sensitive to the effects of high-frequency hearing loss relative to examination in more narrow frequency bands.

3.5.4 Need for Further Research on Repeatability

In summary, repeatability of MOC shifts of OAEs has received little study. Two studies suggest that MOC shifts of TEOAE amplitudes are highly repeatable across time, while one study suggests that MOC shifts of DPOAE amplitudes are variable and thus not highly repeatable across time. However, all three studies had methodological flaws that either limited the ability to detect MOC shifts or to detect differences in MOC shifts across sessions. Therefore, further investigation of the repeatability of MOC effects is warranted.

3.6 Purpose of Current Study

The primary purpose of this study was to investigate the repeatability of MOCR effects on TEOAEs in individual subjects. A secondary purpose was to compare MOCR effects on short- and long-latency TEOAE components. The results have implications for basic and clinical applications of the MOCR, as well as understanding the use of OAEs for assessing the MOCR. Careful control of confounding factors was implemented to reduce variability introduced by factors other than the MOCR. Statistical significance of MOCR shifts was assessed in individuals in order to accurately assess changes in OAEs due to MOCR and not random variability or other factors.

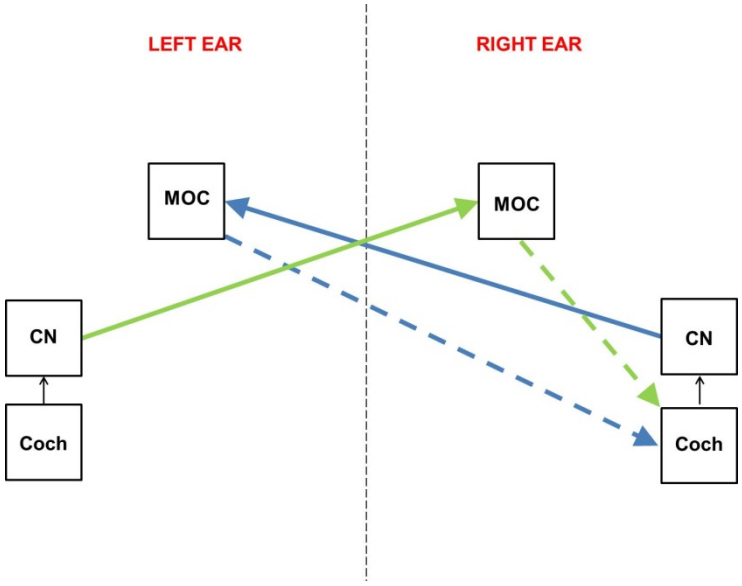

Figure 3.1. Block diagram of the MOCR pathway. This example shows the ipsilateral and contralateral MOCR pathways for the right ear. Solid arrows represent the afferent pathway. Dashed arrows represent the efferent pathway. Blue arrows represent the ipsilateral pathway, which involves crossed MOC fibers. Green arrows represent the contralateral pathway, which involves uncrossed MOC fibers. Small black arrows represent the auditory nerve. Vertical dashed line represents the middle of the brainstem. Coch=cochlea, CN=cochlear nucleus, MOC=medial olivocochlear bundle. Figure is based on Guinan (2006).

CHAPTER IV

METHODS

4.1 Subjects

Subjects were recruited from the University of Iowa campus and the surrounding community. Twenty-one normal-hearing adults (12 females, 9 males; mean age = 23 years, age range =18 – 29 years) participated. Inclusion criteria included the following in both ears: unremarkable otoscopic examination, tympanometric results within normal clinical limits (peak pressure: -100 – +50 daPa, static admittance: 0.3 – 2.5 mmho, ear canal volume: 0.7 – 2.5 cc), and behavioral pure-tone thresholds ≤15 dB HL (re: ANSI, 1996) from 0.25 – 8 kHz. Eligible subjects were also required to have a negative history of the following: known or suspected hearing loss, significant difficulty communicating in quiet and noisy environments, ear surgery besides pressure equalization tubes as a child, significant noise exposure without the use of hearing protection, tinnitus of a bothersome and/or constant nature, acute or chronic dizziness, and use of ototoxic medication. Finally, subjects were required to have normal or corrected-to-normal vision due to the visual attention task described below. Pure-tone behavioral thresholds and tympanometric measures were repeated at the beginning of each session to ensure subjects continued to meet the inclusion criteria. These measurements were stable in all subjects across sessions. Subjects were asked about their subjective hearing status and noise exposure at the beginning of each session. No subjects reported subjective changes in hearing or significant noise exposure between sessions. The research protocol was approved by the University of Iowa Institutional Review Board, and written informed consent was obtained from all subjects. Subjects received monetary compensation for their time.

4.2 Equipment

All screening and testing procedures took place in a double-walled sound-treated booth, with the subject seated comfortably in a recliner. Measurements of hearing function and speech perception testing (described below) were performed using standard clinical equipment. Presentation of stimuli and recording of responses was achieved using a personal computer (PC) running custom software written in MATLAB (The MathWorks, Inc.), the software utility Playrec (Humphrey 2008), and Windows Media Player (Microsoft). Auditory stimuli were presented using sound cards (LynxTwo, Lynx Studio Technology for clicks; onboard PC sound card for noise) routed to power amplifiers (GFA-5002, Adcom; HB7, Tucker-Davis Technologies) and variable attenuators (PA-5, Tucker-Davis Technologies; Hewlett-Packard), and connected to insert earphones (ER-2, Etymōtic Research). Ear canal pressure recordings in both ears were made using OAE probe microphone systems (ER-10B+, Etymōtic Research) connected to the 24-bit sound card (LynxTwo). Recordings were analyzed offline using custom software written in MATLAB.

4.3 Otoacoustic Emissions Testing

TEOAEs were measured with and without contralateral acoustic stimulation (CAS). The size of the change in TEOAEs measured with CAS, relative to TEOAEs measured without CAS, was taken as an indirect measure of the strength of MOCR. Stimuli consisted of clicks for eliciting TEOAEs, and broadband acoustic noise for activating the MOCR. Both stimuli were generated in MATLAB, using a sampling rate of 44.1 kHz. Clicks and noise had a nominal bandwidth of 1 – 10 kHz. Clicks had a duration of 1.2 ms and were presented at a rate of approximately 26/s. Using methods described by Goodman et al. (2009), click and noise stimuli were created to have an acoustically flat magnitude (±1.5 dB) from 1 – 10 kHz in a long, “reflection-less” tube. The long-tube method is insensitive to standing-wave effects that are present in

traditional *in-situ* dB SPL ear canal calibrations at higher frequencies (Stinson et al. 1982; Gilman and Dirks 1986).

Following the recommendations of Goodman et al. (2013), click and noise stimuli were presented at 35 dB SL (relative to the subjects' behavioral threshold for the stimuli). These levels were chosen to maximize activation of the MOCR without concurrently activating the MEMR. A direct check of the MEMR was also implemented, as described by Goodman et al. (2013), and none of the subjects showed evidence of MEMR activation at these stimulus levels.

At the first session, subjects' thresholds for the stimuli were determined. Stimuli were then presented at 35 dB SL, and the corresponding stimulus waveforms were measured in the ear canals using the ER-10B+ probe microphones. The waveforms were band-pass filtered from 1 – 4 kHz, and the RMS amplitude (dB SPL) of the filtered waveforms was calculated. This process was performed three times, and the mean SPL of the three samples was used as the target stimulus level for all test measurements. Prior to each set of TEOAE recordings, click and noise levels were calibrated in the ear canals to be within ±0.3 dB and ±1.0 dB, respectively, of the target values.

For the main experiment, TEOAEs were measured in subjects' right ears, and CAS was presented to left ears. This was done to improve the likelihood of detecting MOCR effects because right ears typically have larger TEOAEs amplitudes (e.g., Khalfa et al. 1997; Sininger and Cone-Wesson 2004; Keefe et al. 2008) as well as stronger MOCR effects (e.g., Khalfa et al. 1997; Morlet et al. 1999). In a subset of subjects, TEOAEs were also measured in the left ear and CAS was presented in the right ear in order to compare MOCR effects between ears.

Previous work has shown that OAE recordings tend to exhibit small drifts in amplitude over time, presumably due to middle ear static pressure fluctuations, probe movement, or other factors (Backus 2006; Goodman et al. 2013). In order to help avoid erroneously interpreting these drifts as evidence of MOCR, CAS was interleaved

throughout the recording process, switching on and off every 10 s. Whenever CAS was switched on or off, a delay of 500 ms was given to allow the MOCR to settle before beginning the TEOAE recordings (Backus and Guinan 2006). Each TEOAE *recording set* consisted of a total of K=2048 buffers recorded while CAS was turned on, and another 2048 buffers while CAS was turned off. In this paper, the term "*buffer*" refers to a recording of a single click stimulus presentation and the 38 ms immediately following, which contains the TEOAE. Total recording time for each recording set was approximately 2.6 min (4,096 buffers × 0.038 s per click stimulus). Interleaving by itself is sometimes still an insufficient control for slow drift artifact; therefore the recordings were de-trended prior to further analysis, as described by Goodman et al. (2013).

In addition to the TEOAE test condition described above, a control condition was recorded. The control condition was identical to the test condition, except that the electrical cable attached to the loudspeaker delivering CAS was unplugged, so that no acoustic noise was delivered to the ear canal. In this condition, it was expected that no significant differences would be seen between recordings made with and without CAS. The control condition was included as a check to ensure that TEOAE measurements of the MOCR represented true biological effects, rather than any unexpected artifacts.

4.4 Attention Task

Changes in attentional state and alertness can modulate the MOCR (e.g., Froehlich et al. 1993a, 1993b; Maison et al. 2001), and this could increase intra- and inter-session variability. To ensure that subjects remained alert during TEOAE recording and to help maintain a consistent attentional state, subjects participated in a visual attention task based on methods described by Meric and Collet (1992). A visual, rather than auditory, attention task was chosen because stronger MOCR effects have been shown to occur during a visual task (Froehlich et al. 1990; de Boer and Thornton 2007; Delano et al. 2007). While TEOAEs were being recording, subjects watched a computer screen with a black background, upon which a white box periodically appeared. The

white box encompassed the entire screen and remained present until subjects pressed the spacebar on a keyboard. Inter-stimulus intervals were randomly chosen each time and ranged from 300 – 4000 ms (Meric and Collet 1992). Subjects were instructed to press the spacebar as soon as they saw the box, but to do so quietly. The cables attached to the OAE probe were situated away from the subjects' bodies to minimize recorded noise from muscle movement associated with this task. The response time (ms) for each presentation was recorded and plotted on the screen so that the subjects and the researcher administering the testing could monitor performance on the task.

4.5 Speech Perception Testing

One purported purpose of the MOCR is to improve hearing in background noise. It is thought that stronger MOCR provides more unmasking from background noise (Kawase and Liberman 1993; Kawase et al. 1993). Increased unmasking would improve the SNR at the level of the auditory system and should therefore allow subjects to correctly detect or recognize the speech material at lower SNRs, relative to no unmasking. Several studies have attempted to show a relationship between the MOCR and speech perception ability; however, these efforts have yielded conflicting results (e.g., Kumar and Vanaja 2004; Wagner et al. 2008; de Boer et al. 2012; Mishra and Lutman 2014).

To help further elucidate the relationship between MOCR strength and perception, subjects were given three tests of speech perception in noise. The tests consisted of speech detection thresholds (SDTs), speech recognition thresholds (SRTs), and the Hearing in Noise Test (HINT; Nilsson et al. 1994). The purpose of using three tests was to assess whether the MOCR is associated with different levels of speech processing: detection of single words, discrimination of single words, and discrimination of sentences.

Performance was quantified as the SNR at which materials could either be correctly detected (SDTs) or repeated back verbally (SRTs and HINT). SDT and SRT

materials consisted of recorded spondees. HINT materials consisted of recorded sentences. For all measures, the speech material was varied adaptively in 2-dB steps and the noise was played at a fixed level. For the SDT and SRT, testing was stopped after reaching the lowest intensity level at which subjects could correctly detect or repeat back at least 50% of the materials at a given intensity level. For the HINT, testing was stopped after 17 sentences were presented, and the presentation levels of each sentence were averaged. This average value was subtracted from the level of the noise to provide an SNR that approximated 50% correct performance.

Each test was administered in two noise conditions. In the *ipsilateral* condition, speech and broadband noise were presented to the right ear. In the *bilateral* condition, speech and broadband noise were presented to the right ear and CAS was presented to the left ear. The CAS was the same as described previously for the MOCR measurements. The noise was uncorrelated between the two ears to avoid invoking central unmasking effects (Giraud et al. 1997). The ipsilateral noise was presented at 35 dB SL for the SDT and SRT, whereas the ipsilateral noise was presented at 65 dB SPL for the HINT as per the test's instructions. For all three tests, CAS was presented at 35 dB SL.

It was hypothesized that MOCR strength, as assessed by TEOAEs, would be significantly correlated with speech in noise performance. It was further hypothesized that performance would be improved if noise is presented bilaterally compared to ipsilaterally because bilateral presentation would activate more MOC fibers and thus produce more unmasking.

4.6 Testing Schedule

Each subject came to the lab for four sessions. Each session lasted between 1 – 2 hours. The first three sessions occurred within a 7-day period. The fourth session occurred four weeks after the third session.

Behavioral thresholds for the clicks and noise were obtained at the first session, as described previously. Speech perception testing was also administered during the first

session. At the beginning of each session, the subject's hearing was screened. During each session, five TEOAE recording sets were measured: four in the test condition and one in the control condition. After each recording set, subjects were given a 2-minute break, and the OAE probes were removed from the ear canals and re-inserted prior to the next recording set. Care was taken to place the probe in the same location in the ear canal each time. After each probe insertion, an *in-situ* calibration was performed to account for any small variations in probe placement and to ensure consistency of stimulus levels.

Measurements made within a session were used to establish within-session variability. Measurements made across the first three sessions were used to evaluate short-term repeatability. Measurements made on the fourth session were used to establish longer-term repeatability.

4.7 MOCR Analysis

4.7.1 TEOAE Time-Frequency Analysis Windows

The remainder of this chapter will describe how the TEOAE recordings were analyzed. Both magnitude and phase changes arising from the presence of CAS were examined. Hereafter in this paper, matrices of windowed TEOAE waveforms obtained without CAS (i.e., recorded with silence in the contralateral ear) are referred to by the variable *A*, while matrices of obtained with CAS (i.e., recorded with acoustic noise present) are referred to by the variable *B*. The *A* and *B* matrices were obtained by de-interleaving the buffers of a recording set, placing each buffer into the appropriate matrix, depending on whether CAS was present during the recording or not. A time vector was created for the waveform recordings, with the peak of the recorded stimulus set to time zero. The amplitudes of the first 2 ms of the recording (the portion containing the stimulus) were set to zero, and a raised-cosine onset ramp was applied to the following 2.5 ms. A similar offset ramp was applied to the last 2.5 ms of each recording buffer.

After eliminating the stimulus from the recordings, analysis time windows must be chosen. Recent work with TEOAEs has emphasized the distributed nature of TEOAEs

in both time and frequency (Goodman et al. 2011; Moleti et al. 2012; Moleti et al. 2013). In particular, TEOAE waveforms are characterized by peaks of energy localized in time and frequency. These localized peaks appear to be fairly consistent within a given subject, but are highly variable across subjects (e.g., Goodman et al. 2011). Given that high SNRs are needed to detect small MOCR-induced changes in emissions (Goodman et al. 2013), it seems reasonable that analyses should focus on localized energy peaks where SNR is the greatest. Recent work with TEOAEs has emphasized that they are composed of multiple components generated at different cochlear locations and having different delays and growth rates (e.g., Goodman et al. 2011; Moleti et al. 2012). Further, components generated more basally are expected to have less dependence on OHC function, and by extension show smaller effect of MOCR. If TEOAE analysis windows include multiple components, unanticipated interactions may easily occur, making the results difficult to interpret. Additionally, multiple components may result in localized regions of destructive waveform interference, which may be overly sensitive to very small changes.

As far as we are aware, all previous estimates of MOCR using TEOAEs have used fixed frequencies and fixed time windows when analyzing TEOAEs. In light of the distributed nature of TEOAEs, it seems warranted to use an individualized approach that focuses on stable, localized energy peaks. To this end, a relatively broad analysis frequency band from 1 – 2 kHz, and a corresponding analysis time window were chosen. The analysis frequency band was chosen based on previous work showing that this band contains the strongest MOCR effects (e.g., Hood et al. 1996; Goodman et al. 2013). Seven overlapping, 1/6-octave bandpass filters were created using a Hann window-based design method. Filter order decreased as center frequency and bandwidth increased. The filter center frequencies spanned 1 – 2 kHz, and the filter orders ranged from 4096 at 1 kHz to 2048 at 2 kHz. The recordings in the *A* and *B* matrices were filtered by each of

the seven filters, and the group delays of the filters were subtracted from filtered waveforms to ensure correct temporal alignment after filtering.

The analysis time window extended from 6.0 – 12.2 ms, relative to the peak of the stimulus waveform. These times were chosen based on confidence intervals for the expected SFOAE latencies in humans reported by Shera et al. (2002; see also Goodman et al. 2013, Eq. 1). The group delay of the 5% confidence interval associated with a 2 kHz SFOAE defined the start of the analysis window, and the group delay of the 95% confidence interval for a 1 kHz SFOAE defined the end of the analysis window. These times were chosen under the assumption that TEOAEs and SFOAEs are generated by linear coherent reflection (Shera and Guinan 1999; Kalluri and Shera 2007) and should therefore have similar latencies. Previous work with TEOAEs suggests that this assumption was warranted and that the chosen time windows contain what has been referred to as the "long-latency" TEOAE component (Goodman et al. 2011; Moleti et al. 2012).

A stable, localized energy peak was chosen individually for each subject (Fig. 4.1). The peaks were chosen in the following way. The mean of the waveforms in each filtered *A* matrix was computed. Complex analytic waveforms were then created, with the real parts being the mean waveforms and the imaginary parts being the Hilbert transforms of the mean waveforms. The filtered waveform envelopes were computed as the absolute value of the analytic waveforms. Each subject had seven filtered waveform envelopes, and each of these was examined for viable energy peaks within the 6.0 – 12.2 ms time window. At each frequency, a peak was considered viable for analysis if it monotonically decreased on each side of the peak to an amplitude reduction of at least 3 dB (the half-power point). Peaks that contained non-monotonicities in this region were suspect for containing multiple overlapping components, and were therefore not given further consideration for analysis.

After each filtered waveform envelope was analyzed in this way, a list of the viable energy peaks was made, and the peak with the largest amplitude (i.e., the best SNR) was chosen. Given the filter center frequency of the chosen energy peak, a related analysis time window was also assigned. The window included 9 full periods of the stimulus center frequency, 4.5 periods occurring before and after the peak location. The TEOAEs waveforms that were analyzed for each subject could therefore be described by three parameters: center frequency (f_c), the start of the analysis time window (t_1), and the end of the analysis time window (t_2). An example of the envelopes and time windows is shown in Fig. 4.1. Once the values f_c, t_1, t_2 were chosen for a given subject, these values were applied to all of the buffers in the *A* and *B* matrices of that subject: all of the buffers were filtered with the filter having a center frequency f_c, and all buffers were truncated so that they included only the time samples between t_1 and t_2, inclusive. Analysis of the time- and frequency-windowed TEOAEs then proceeded as described in the following sections.

4.7.2 Calculation of MOCR-induced Changes in TEOAEs

Recall that the matrices of windowed TEOAE waveforms obtained without CAS are referred to by the variable *A*, while matrices of obtained with CAS are referred to by the variable *B*. Both *A* and *B* matrices were of size $n \times m$, where n is the total number of samples in the time window (dependent on filter center frequency, f_c) and m is the number of recorded buffers ($m = 2048$, prior to artifact rejection). The number of samples in the matrices was zero-padded to $n = 1024$ for every subject, to ensure consistency in the analysis across subjects. First, the mean across buffers was computed as:

$$\bar{a} = A\mathbf{1}(1/m)\,, \qquad \text{Eq. 4.1}$$

$$\bar{b} = B\mathbf{1}(1/m)\,, \qquad \text{Eq. 4.2}$$

where $\bar{a}$ and $\bar{b}$ are $n \times 1$ vectors of the mean across m buffers, and **1** is a $m \times 1$ vector of ones. The change in means due to the addition of CAS was assessed by computing the ratio of $\bar{b}$ to $\bar{a}$ in the frequency domain,

$$\Delta = F\bar{b}/F\bar{a}\,, \qquad \text{Eq. 4.3}$$

where Δ is a $n \times 1$ vector of complex ratios obtained by point-wise division, and F is the $n \times n$ Fourier matrix having elements $f_{kj} = \omega^{jk}$, $\omega = e^{-2\pi i/n}$ (*j* and *k* designate rows and columns, and *i* is the imaginary operator, $\sqrt{-1}$). The ratio of discrete Fourier transforms, Δ, was reduced to a single complex value, δ, by taking the mean of the subset of elements in Δ corresponding to the passband frequencies of the filter that was applied to A and B.

$$\delta = \frac{1}{N}\sum D\,, \qquad \text{Eq. 4.4}$$

$$D = \left\{D \in \Delta : i_{f_L} \leq D \leq i_{f_H}\right\},$$

where *D* is the set containing all elements of Δ with indices *i* which are greater than or equal to the index of the low cutoff frequency of the band-pass filter (i_{f_L}) and less than or equal to the index of the high cutoff frequency (i_{f_H}) of the band-pass filter, the set *D* containing *N* elements. The magnitude of the complex ratio,

$$|\delta| = \sqrt{\mathrm{Re}(\delta)^2 + \mathrm{Im}(\delta)^2}\,, \qquad \text{Eq 4.5}$$

quantifies the amplitude of $\bar{b}$ relative to the amplitude of $\bar{a}$. The phase angle of the ratio,

$$\angle\delta = \tan^{-1}(\mathrm{Im}(\delta)/\mathrm{Re}(\delta))\,, \qquad \text{Eq. 4.6}$$

quantifies the phase of $\bar{b}$ minus the phase of $\bar{a}$ (expressed in radians).

When plotted on the unit circle with real values on the x-axis and imaginary values on the y-axis, δ provides a clear visual interpretation of how the presence of CAS

changes both emission magnitude and phase: if δ falls on the unit circle ($|\delta| = 1$), the addition of CAS did not change the emission magnitude. In contrast, if δ falls inside the unit circle ($|\delta| < 1$), the addition of CAS caused a reduction in emission magnitude, while if δ falls outside the unit circle ($|\delta| > 1$), the addition of CAS caused an increase in emission magnitude. In terms of phase angle, if δ falls directly on the x-axis ($\angle\delta = 0$), the addition of CAS did not cause a phase change in the emission. If δ falls above the x-axis ($\pi/2 > \angle\delta > 0$) in quadrant I, the addition of CAS caused a phase lead. If δ falls below the x-axis ($-\pi/2 < \angle\delta < 0$) in quadrant IV, the addition of CAS caused a phase lag. Based on previously published work, it was expected that the activation of the MOCR would result in a reduction of emission magnitude and a lead in emission phase, so that δ would most often be seen inside the unit circle in quadrant I. Examples of possible values of δ in relation to the unit circle and their associated waveforms are shown in Fig. 4.2.

4.7.3 Simultaneous Tolerance Regions and Statistical Significance

Since the ratio δ will almost never be exactly 1 (meaning there is precisely no difference as a result of the presence of CAS) it is desirable to determine what values of δ represent a statistically significant change. While it is possible to compute statistical intervals for this purpose on magnitude and phase separately, in cases like MOCR activation where both kinds of shifts are expected, it is preferable to compute a statistical interval that simultaneously includes both magnitude and phase. A simultaneous interval is potentially more sensitive than two independent intervals because it allows identification of shifts that may not be significant in terms of magnitude alone or phase alone, but are significant when the two are considered together.

In order to construct simultaneous intervals, the distribution of the sampling mean of δ must be estimated. A bootstrapping procedure for accomplishing this using magnitude only was described by Goodman et al (2013). This same operation can be performed on complex values, such as δ. A statistical resampling with replacement

(bootstrap) algorithm (Efron and Tibshirani, 1993) was implemented using custom software written in MATLAB and is described below.

Recall that the ratio δ was obtained from a pair of matrices, A and B, each of size *n* samples by *m* buffers. The null hypothesis was that there was no difference between the populations from which the matrices were sampled, and under this hypothesis all the buffers were pooled into a single $n \times 2m$ matrix. The distribution of ratios from this pooled matrix was estimated by randomly selecting (with replacement) two independently resampled matrices, each of size $n \times m$ and calculating the resulting complex ratio, $\hat{\delta}$. This process was iterated *K*=10000 times. On each iteration, the complex ratio of each resampled pair of matrices was calculated using the procedure described in the previous section: Each resampled matrix was averaged (Eqs. 4.1 and 4.2), and the resulting mean vectors were Fourier transformed and divided, yielding a vector of complex ratios (Eq. 4.3). The vector was reduced to a single complex number, $\hat{\delta}_k$, where *k* indicates the value on the k^{th} of *K* iterations.

The distribution of $\hat{\delta}$ showed the expected differences from sampling under the null hypothesis that there was no difference between the populations from which the matrices A and B were sampled. This distribution can be used to calculate a statistical tolerance region. While the distribution can be found empirically by sorting the set of resampled ratios, a computationally faster method can be used if the distribution of $\hat{\delta}$ is approximately bivariate normal, as was the case with the present data set.

Tolerance regions were computed as follows. First, the (complex) mean of the vector $\hat{\delta}$ was calculated, and $\hat{\delta}$ was centered about the origin on the complex plane by subtracting the mean. Next, for computational purposes, $\hat{\delta}$ was changed from a $K \times 1$ complex vector into a $K \times 2$ matrix of real values, by placing the real and imaginary parts of $\hat{\delta}$ in the first and second columns, respectively. The covariance matrix (unscaled) of the $\hat{\delta}$ matrix was then obtained by

$$S = cov(\hat{\delta}) = \frac{1}{K-1}\hat{\delta}^{T}\hat{\delta} \ , \qquad \text{Eq. 4.7}$$

where the superscript uppercase *T* indicates the matrix transpose operator. The covariance matrix *S* is a 2×2 matrix, with the diagonal elements being the variances of the real and imaginary parts and the off-diagonal elements being the covariance between the real and imaginary parts. The eigenvalues and eigenvectors of the covariance matrix *S* were computed and subsequently used to find the major and minor axes of an ellipse describing the bivariate distribution of the elements in $\hat{\delta}$:

$$R = \left(\sqrt{\upsilon}\lambda C\right)^{T} \ , \qquad \text{Eq. 4.8}$$

where R is an $m \times 2$ vector designating the elliptical region, υ is the matrix of eigenvalues, and λ is the matrix of eigenvectors. The variable C designates a circle defined by a $2 \times m$ matrix, where each element in the first row is defined by $\cos(\theta_j)$ and each element in the second row is defined by $\sin(\theta_j)$, θ a row vector of *m* equally-spaced radian phase values from 0 to 2π. Here, the choice of the number of columns, *m*, is somewhat arbitrary and is not critical, so long as it is relatively large, so as to allow reasonable estimation of the ellipse magnitude at any arbitrary phase value. In the present study, the value of *m* was 2000.

Finally, the elliptical region *R* was scaled to yield a tolerance region encompassing $100(1-\alpha)\%$ of the complex ratio values in $\hat{\delta}$. For a standard, bivariate normal vector, the squares of the major and minor axes can be estimated by the chi-squared distribution on 2 degrees of freedom (Chew 1966). A scaling factor was therefore found using the inverse chi-square distribution, with degrees of freedom $1-\alpha$ and 2. *R* was then multiplied by the scaling factor, yielding

$$R_{\alpha} = R\sqrt{\mathrm{Inv}\chi^{2}(1-\alpha, 2)} \ , \qquad \text{Eq. 4.9}$$

where R_α is the elliptical tolerance region encompassing $100(1-\alpha)\%$ of the complex ratio values in $\hat{\delta}$. In the present study, α was set to 0.05. The centering operation described towards the beginning of this section was undone (the original mean of the vector $\hat{\delta}$ was added to R_α), and R_α was changed from a $m \times 2$ matrix back into a $m \times 1$ complex vector.

The resampled tolerance region, R_α, defines which values of δ represent a statistically significant change: δ must fall outside of the ellipse described by R_α in order to be significant. This is most easily calculated by shifting both R_α and δ to the origin (by subtracting 1), and determining whether the magnitude of δ exceeds the magnitude of R_α at the phase angle of δ. If $|\delta| > |R_\alpha(\angle\delta)|$, then δ represents a statistically significant change at the α significance level, and the null hypothesis is rejected. In the context of the present study, a significant result for δ was cautiously interpreted to mean that the presence of CAS changed the measured TEOAE, presumably as a result of MOCR activation. As will be shown later, this interpretation appeared warranted in many, but not all cases. Significant changes could be due to change in magnitude, change in phase, or both. When δ and R_α are plotted together on the unit circle, the relative contribution of magnitude and phase changes can be examined, as shown in Fig. 4.3.

4.7.4 Total Quantity of Change

A common way of expressing change in emissions is to subtract the waveforms, compute the Fourier transform of the difference, and then express the magnitude of this result relative to the magnitude of the Fourier transform of the emission obtained without CAS. This value represents the "total quantity" of change, including both magnitude and phase. Here we use the nabla symbol (∇) to designate this quantity:

$$\nabla = \frac{\left|F\left(\bar{a}-\bar{b}\right)\right|}{|F\bar{a}|} \,. \qquad \text{Eq. 4.10}$$

(As a side note, the use of nabla in this work bears some similarities to its use in ship building, where it is commonly used to designate volume displacement, or the total

volume of water displaced by the ship. In the present context, nabla represents the total "displacement" of one emission from another). Similar to Δ, ∇ can be reduced to a single (though non-complex) value by taking the mean of the subset of elements in ∇ corresponding to a range of frequencies. Here, we define ϱ (turned delta) relative to the pass-band frequencies of the filter that was applied to A and B as:

$$\varrho = \frac{1}{N}\sum D\,, \qquad \text{Eq 4.11}$$

$$D = \left\{D \in \nabla : i_{f_L} \leq \mathrm{D} \leq i_{f_H}\right\},$$

where D is the set containing all elements of ∇ with indices i which are greater than or equal to the index of the low cutoff frequency of the band-pass filter (i_{f_L}) and less than or equal to the index of the high cutoff frequency (i_{f_H}) of the band-pass filter, the set D containing N elements.

The value ϱ represents the "total quantity" of change or "total displacement", including both magnitude and phase, as a single, relative value. There is a close mathematical relationship between δ and ϱ:

$$\varrho = |\delta - 1|\,. \qquad \text{Eq. 4.12}$$

The geometric interpretation of this relationship can be easily visualized by plotting δ on the unit circle as a vector centered at the origin (Fig. 4.4). A second vector is also drawn, pointing from the point (1,0) to the location of δ (see Fig. 4.4). The quantity ϱ is the magnitude of this second vector. Both δ and ϱ refer to the same point on the unit circle, but they point from different locations. Note that ϱ can be calculated from δ, but the reverse is not true. If ϱ is computed directly (via Eqs. 4.10 and 4.11), information about the direction of change, including whether magnitude increased or decreased and whether relative phase was a lead or lag, is irretrievably lost. It may therefore be preferable to first compute δ and then proceed to ϱ via Eq. 4.12.

Although all information about the direction of change is lost, the value ϱ can still be a very useful quantity. In particular, it may often be useful to have the total quantity of change expressed as a real (non-complex) scalar, making it easier to use in statistical calculations, for example, in making correlations with speech perception or susceptibility to noise-induced hearing loss. The statistical significance of ϱ can be found using the resampled tolerance region, R_α, just as it was used to determine the significance of δ.

4.7.5 Expected Variability

The elliptical tolerance region, R_α, is related to the SNR of the emissions. Specifically, the tolerance region represents the pooled variance of the emissions recorded with and without CAS. Within a single recording set (recall that a recording set consisted of *K*=2048 buffers recorded while CAS was turned on, interleaved with another 2048 while CAS was turned off), the variance (and covariance) of the buffers in the set are described by eigenvectors and eigenvalues, which are then scaled to yield the tolerance region (Eqs. 4.7 – 4.9). The tolerance region is therefore expected to account for all of the sources of variability that are present within that particular recording set. Figure 4.5 shows values of R_α obtained over a range of typical emission SNR values. In cases where the presence of CAS decreases the emission magnitude (the expected result), the SNR of the emission measured with CAS will decrease. Therefore, the area of R_α will increase slightly. However, because the change in emissions caused by MOCR activation is relatively small (e.g. a 1 – 2 dB change in an emission having a 30 dB SNR), the overall size of the tolerance region still gives a fairly good indication of the SNR of the emission measured without CAS. The size of R_α should be interpreted carefully, because larger areas may be associated with higher noise levels in the recordings, lower emission levels, and/or larger effects of MOCR activation. Nevertheless, smaller areas of R_α are desirable and allow detection of smaller MOCR effects.

The tolerance region R_α accounts for all of the variability within a particular recording set. Such sources of variability include physiologic noise (e.g. respiratory,

vascular, and muscular), environmental noise, and internal electrical noise associated with the measuring equipment. Movement or slippage of the probe in the subject's ear canal increases variability in the recording. Variability in the peripheral auditory system itself also contributes to the tolerance region. Examples include changes in middle-ear pressure and impedance during the recording session, and changes in centrally-mediated attentional control of the MOCR. All of the factors mentioned contribute to the total variability; however, it can generally be expected that the majority of the variability arises from physiologic noise and movement of the probe in the ear canal.

Because the tolerance region accounts for all of the variability within a particular recording set, it is also related to the expected variability of δ across repeated measures for a given subject: If there are no unexpected changes in any of the sources of variability discussed in the previous paragraph, nearly all subsequently repeated measurements of δ (specifically, $>100(1-\alpha)\%$) would be expected to fall within a region having the area of R_α, but shifted so as to be centered around μ_δ, the population mean of δ (Fig. 4.6). The value of μ_δ is unknown, but can be estimated from one or more measured samples of δ. We therefore define

$$\overleftarrow{R_\alpha} = \left(\frac{1}{n}\sum_{i=1}^{n} R_{\alpha_i}\right) + \left(\frac{1}{n}\sum_{i=1}^{n} \delta_i\right), \qquad \text{Eq. 4.13}$$

where $\overleftarrow{R_\alpha}$ is the tolerance region expected to encompass $100(1-\alpha)\%$ of subsequent repeated measurements of δ. By the law of large numbers, a sample mean converges to the population mean as the sample size increases; therefore, $\overleftarrow{R_\alpha}$ becomes a more accurate estimate of the true distribution of δ as *n*, the number of estimates of δ increases.

An important question then becomes how many estimates of δ are needed to obtain a reasonable estimate of $\overleftarrow{R_\alpha}$. While a large *n* is desirable, there are practical time and attentional constraints involved in taking repeated baseline measures from human subjects. Figure 4.7 shows the performance of $\overleftarrow{R_\alpha}$ as a function of *n*, the number of baseline measurements, using a computer simulation. The simulation was based on 1000

independently generated values of δ and their associated tolerance intervals, R_α. For each number of baseline measurements (1, 2, 4, or 8), 1000 iterations were computed. On each iteration, the desired number of baseline measures was taken by random sampling from the 1000 values of δ. From these randomly chosen baseline measures, $\overleftarrow{R_\alpha}$ was computed, and the percent of the remaining 1000 values of δ falling inside of $\overleftarrow{R_\alpha}$ was computed. Based on this simulation, it appears that adequate accuracy can be obtained using $n = 4$ baseline measurements of δ. When this is done, $\overleftarrow{R_\alpha}$ encompasses 95% of repeated measures of δ, 95% of the time. Equivalently, $\overleftarrow{R_\alpha}$ encompasses a total of 98% of repeated measures of δ.

When testing human subjects, it can be assumed that subsequent repeated measurements of δ falling outside of the region $\overleftarrow{R_\alpha}$, when $\overleftarrow{R_\alpha}$ is computed using 4 baseline measures, are associated with a significant change in one or more of the sources of variability discussed above. While one of the ultimate goals is to identify significant changes in the strength MOCR in individuals, it should not be automatically assumed that any subsequent measurements of δ falling outside of the region $\overleftarrow{R_\alpha}$ are due to changes in MOCR. This cannot be known, or even reasonably implied, until the other sources of variability are ruled out as significant contributors. This issue will be dealt with further in subsequent sections of this thesis.

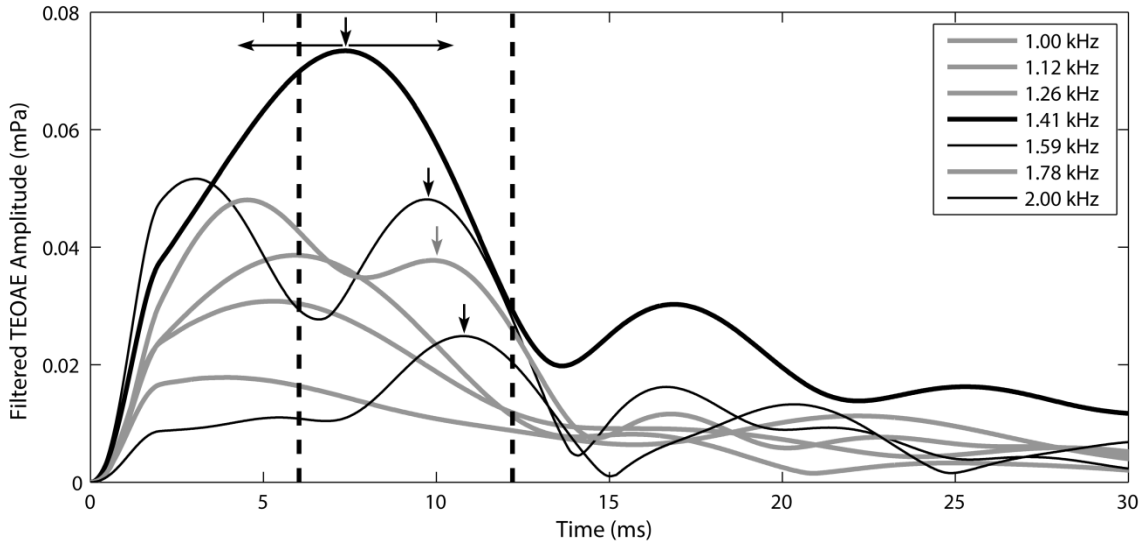

Figure 4.1. Example of choosing a stable, localized energy peak for one subject. Each tracing is the envelope of the mean TEOAE waveform filtered at a different center frequency between 1 and 2 kHz. The time window within which a peak must occur is shown by vertical dashed lines. Viable peaks are indicated by short downward-pointing arrows and black envelopes. Non-viable envelopes are shown by gray envelopes. One of the non-viable envelopes had a peak within the analysis window (gray downward-pointing arrow), but the others did not. Of the viable peaks, the one with the largest amplitude was chosen. In this example, the chosen peak was the peak obtained with the filter centered at 1.41 kHz (shown as the envelope with the thicker black line). The horizontal arrows show the extent of the time window associated with this filter center frequency (9 total cycles of 1.41 kHz).

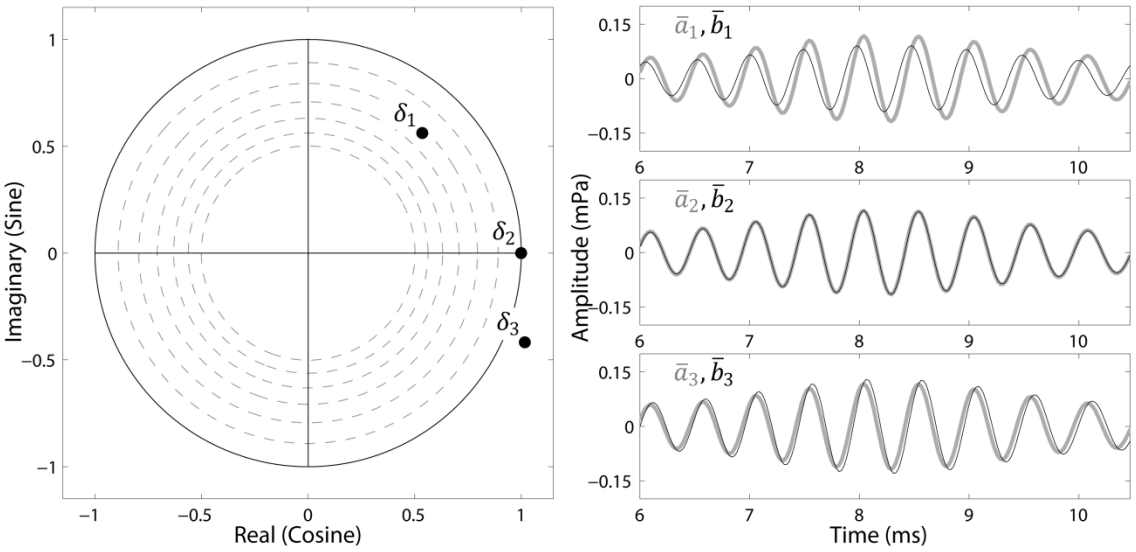

Figure 4.2. Three examples of the complex ratio, δ. Left panel shows results plotted relative to the unit circle. Right panel shows the associated waveforms that produced the complex ratios. The gray dashed lines inside the unit circle designate magnitude reductions in steps of 1 dB. In the right panels, the thicker gray waveforms, $\bar{a}$, represent mean filtered TEOAEs without CAS, while the thin black waveforms, $\bar{b}$, represent mean filtered TEOAEs with CAS (see Eqs. 4.1 and 4.2). The first example ($\bar{a}_1$, $\bar{b}_1$, δ_1) shows a hypothetical case where the presence of CAS resulted in a TEOAE magnitude reduction of 2 dB and a phase lead of $\pi/4$ radians. The second example ($\bar{a}_2$, $\bar{b}_2$, δ_2) shows a hypothetical case where the presence of CAS resulted in no change in either TEOAE magnitude or phase. The third example ($\bar{a}_3$, $\bar{b}_3$, δ_3) shows a hypothetical case where the presence of CAS resulted in a TEOAE magnitude increase of 1 dB and a phase lag of $\pi/8$ radians.

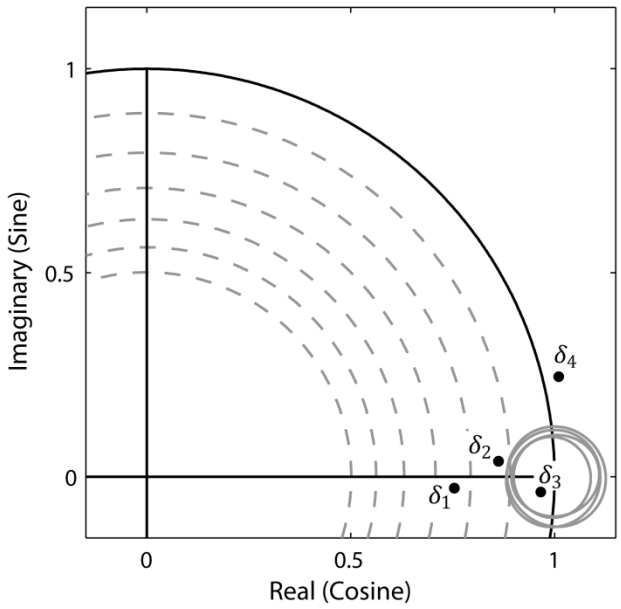

Figure 4.3. Four examples of the complex ratio, δ, and their associated tolerance regions, R_α. Tolerance regions are plotted as gray ellipses centered around (1,0) on the unit circle. Each measurement of δ has its own associated tolerance interval. For sake of visual clarity, the specific ellipse associated with each value of δ is not indicated in this figure; however, the significance of each δ was determined by its own tolerance region. Values of δ that fall outside of their associated tolerance region ($\delta_1, \delta_2, \delta_4$) represent a statistically significant change. Values of δ that fall inside their associated tolerance region (δ_3) do not represent a statistically significant change.

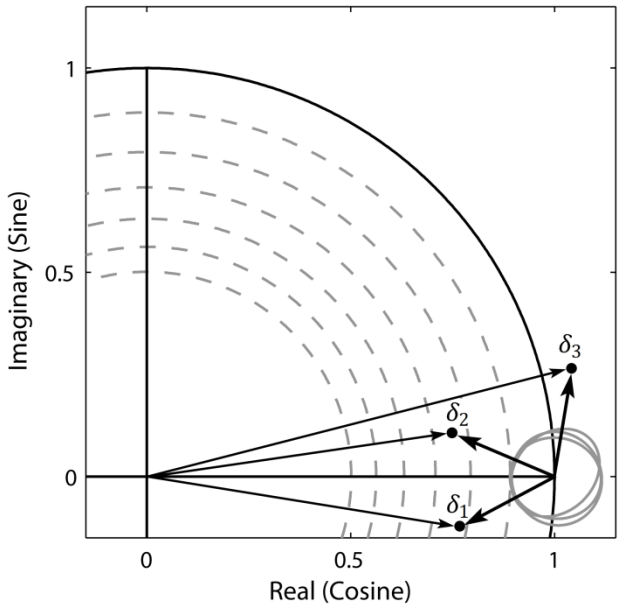

Figure 4.4. Three examples illustrating the geometric relationship between the complex ratio, δ, and the total displacement, ϱ. Tolerance regions are plotted as gray ellipses centered around (1,0) on the unit circle. Each measurement of δ can be considered a vector pointing from the origin (thinner black arrows). A second vector can also be drawn, pointing from the point (1,0) to the location of δ (thicker black arrows). The quantity ϱ is the magnitude of this second vector. The set of examples shown here represent very different emission changes (phase leads (δ_2, δ_3) vs. lags (δ_1); magnitude increases (δ_3) vs. decreases (δ_1, δ_2). However, these particular examples all have identical values of ϱ. Note that because the same tolerance region, R_α, is used to determine the significance of both δ and ϱ, both values will be significant, or both values will be non-significant. In this set of examples, all the values are significant.

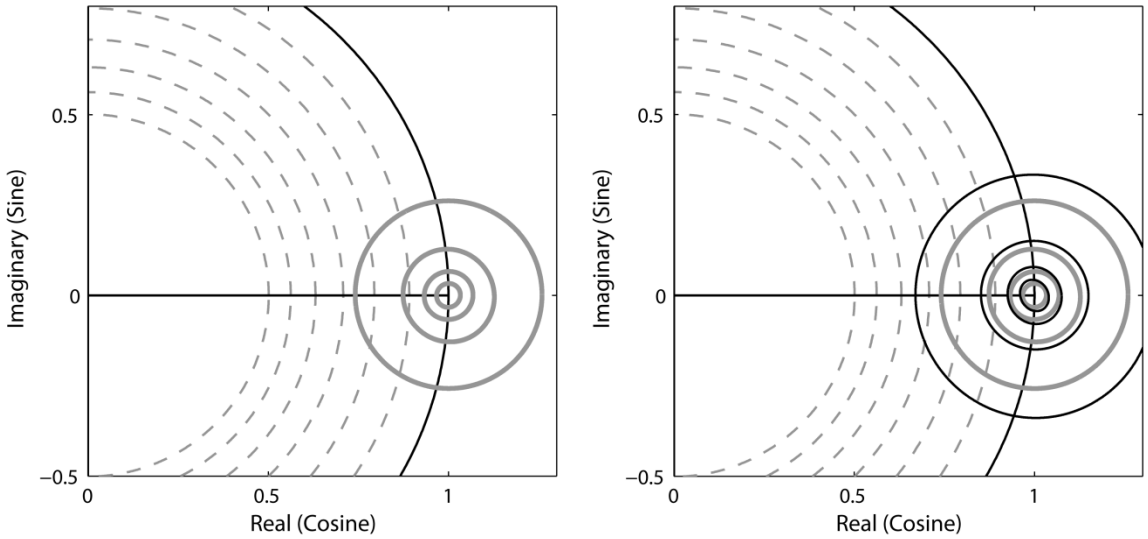

Figure 4.5. Relationship between the tolerance region and emission signal-to-noise ratio. Left panel: Four tolerance regions are shown by concentric gray ellipses centered around (1,0). From largest diameter to smallest, the ellipses are associated with TEOAE SNRs of 18, 24, 30, and 36 dB, respectively. These examples show the expected areas when there is no difference between the emissions recorded with CAS and without CAS, that is, when $\delta = 1$. In this case, the pooled variance is the same as the variances obtained with and without CAS. Right panel: The four tolerance regions from the left panel are re-plotted (gray ellipses), along with the slightly larger tolerance regions (black ellipses) that are obtained when δ has a value of $(0.712 + 0.321i)$, corresponding to a magnitude reduction of 2 dB and a phase lead of $1/16^{th}$ of a cycle. This represents a typical change due to MOCR activation.

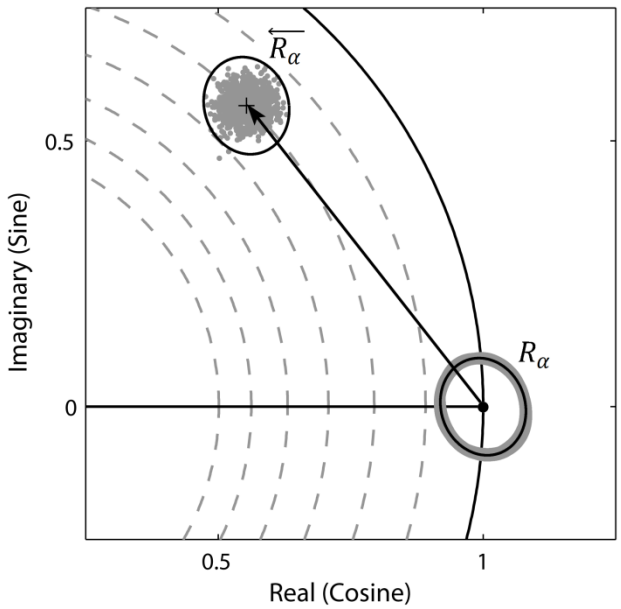

Figure 4.6. Relationship between the tolerance region R_α and the shifted tolerance region, $\overleftarrow{R_\alpha}$. Data for this figure were generated by a computer simulation using 1000 independent estimates. The 1000 tolerance regions are shown by gray ellipses centered around (1,0). Because they overlap so closely, they appear as a single thick gray ellipse. The mean of the 1000 ellipses is shown as a thinner black ellipse. The 1000 computed values of δ are shown as gray dots clustered in the upper left of the figure. The mean value of delta is shown as a black plus (+) symbol. When the mean value of R_α is shifted by the mean value of delta (shown by the black arrow; see Eq. 4.13), it encompasses $> 100(1-\alpha)\%$ of the repeated measurements of δ.

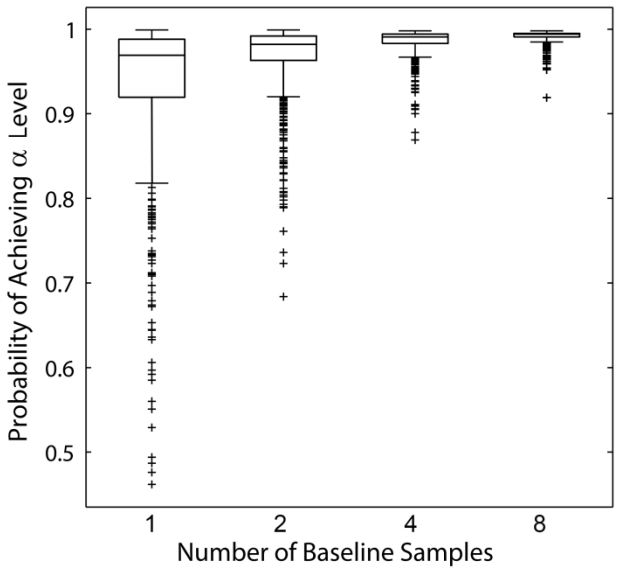

Figure 4.7. Relationship between the number of baseline samples used to estimate $\overleftarrow{R_\alpha}$ and the percentage of subsequently measured values of δ encompassed by that estimate. Data for this figure were generated by a computer simulation, and show that the estimate improves as the number of baseline samples increases. Based on this simulation, sufficient accuracy is achieved using 4 baseline samples.

CHAPTER V

RESULTS

5.1 Individual Data

Because the current study focused primarily on MOCR effects in individual subjects, results from selected individuals will be presented first to highlight important issues regarding TEOAE-based measurements of the MOCR. These issues have implications for both research-based and clinically-based assessments of MOCR.

The figure format for these case examples is the same, except when otherwise noted, in order to facilitate comparisons across subjects. TEOAE envelopes are plotted on the top panels and complex ratios are plotted on the bottom panels. To improve visual clarity, only envelopes obtained in the test condition (with versus without CAS) are plotted, but complex ratios obtained in the test and control conditions (CAS unplugged) are shown. All results are grouped according to the session in which they were obtained in order to demonstrate any similarities or differences within and across sessions. From hereafter, the term *baseline* will refer to results obtained at the first session, and *subsequent* will refer to results obtained at sessions 2, 3, and/or 4.

5.1.1 Low Intra- and Inter-session Variability

Figure 5.1 shows an example of a subject with low intra- and inter-session variability. This subject showed the expected effects in the time and frequency domain, in both the test and control conditions. In this example, the envelopes appeared stable within and across sessions, both in terms of their amplitudes and their overall morphology. Envelopes obtained with CAS (solid black tracings) were always slightly smaller in amplitude and exhibited a phase lead relative to envelopes obtained without CAS (solid blue tracings), as expected when the MOCR was activated. This subject also demonstrated one envelope peak within the time analysis window (shown as vertical dashed lines). TEOAE noise floor envelopes obtained with and without CAS (dotted

black and blue lines, respectively) were very low for all measurements, indicating sufficiently high SNRs.

The corresponding δ values are shown in the bottom panel. Results were also grouped according to session. δ values obtained in the baseline condition (filled black circles) demonstrated a magnitude decrease of approximately 1 dB and a phase lead of between 0.125 – 0.25 rad. δ values obtained at subsequent sessions were similar, although some inter-session variability is evident. Tolerance regions are plotted as thin gray ellipses. The tolerance regions (R_α) were similar within and across sessions, indicating that the SNR of the responses did not change appreciably within or across sessions. All complex ratios in the test condition fell outside their respective tolerance region, indicating that the effects seen were statistically significant ($p < 0.05$).

The shifted tolerance region ($\overleftarrow{R_\alpha}$) is shown as a thick blue ellipse encircling the baseline values of δ. In this example, all of the baseline δ values fell within $\overleftarrow{R_\alpha}$, indicating a very stable baseline. δ values obtained at subsequent sessions fell within or very near $\overleftarrow{R_\alpha}$, indicating low inter-session variability overall.

Finally, the δ values obtained in the control condition are plotted as × markers. It was expected that these values would fall close to (1,0) and would be non-significant (i.e., fall inside the respective R_α) because TEOAEs should not change significantly within a measurement if the MOCR is not activated. This subject demonstrated the expected results for the control condition.

5.1.2 High Intra- and Inter-Session Variability

In most cases, subjects demonstrated low intra- and inter-session repeatability and MOCR effects in the expected direction (i.e., a magnitude decrease and phase lead). However, several subjects demonstrated high intra- and inter-session variability for unclear reasons. Two of these subjects are shown in Fig. 5.2. The baseline δ values were stable because they fell within $\overleftarrow{R_\alpha}$. Additionally, R_α values appeared stable within and across sessions.

The subject in the left panels showed a decreasing MOCR effect across sessions. This can be seen by contrasting the envelopes and δ values in sessions 1 and 4. By session 4, the envelopes with and without CAS were similar in amplitude, indicating no change in TEOAE amplitude with CAS, and the δ values were mostly non-significant. The trajectory of δ values from sessions 1 to 4 are demonstrated by the red arrow in the bottom left panel. Additionally, the complex ratios at sessions 2 and 3 demonstrated high intra-session variability. Results were not improved when analyzing other frequencies (not shown). The reason for the observed decrement in MOCR strength is unclear. Potential reasons will be discussed further in the Discussion chapter.

The subject in the right panels demonstrated low intra-session variability at baseline but high intra-session variability at subsequent sessions. Interestingly, increasing phase leads were seen between the first and fourth measurement within a session. This is highlighted by the red arrows in the bottom right panel, indicating that phase leads increased within a session. δ values at subsequent sessions fell outside $\overleftarrow{R_\alpha}$, indicating high intra-session variability. Results for this subject also did not improve when analyzing other frequencies for unclear reasons.

The results in these subjects suggest that although baseline measurements can have low variability, there may be higher variability at subsequent sessions. One must examine all confounding factors in order to determine if an apparent change in results across sessions is truly due to a change in MOCR or to some other factor.

5.1.3 Importance of Obtaining Stable Baseline Measurements

Initially, a frequency was chosen for analysis if it resulted in the largest peak within the specified time window. There were originally no selection criteria regarding the stability of the baseline MOCR measurements (i.e., whether or not baseline δ values fell within $\overleftarrow{R_\alpha}$) and regarding the location of the mean baseline value of δ (i.e., whether there was a magnitude increase versus decreases and a phase lead versus lag). When only

using peak amplitude as the selection criteria, subjects with high intra-session variability at baseline also demonstrated high inter-session variability.

The importance of baseline stability is demonstrated in Fig. 5.3. The left panels show results in one subject for a frequency that had the largest peak amplitude but high baseline variability. Peak amplitudes of the envelopes appeared variable at baseline, and two of the four baseline δ values fell outside of $\overleftarrow{R_{\alpha}}$. Results at subsequent sessions were even more variable. Envelopes at subsequent sessions demonstrated two peaks within the analysis window, whereas only one peak was demonstrated at baseline. These double peaks were also unstable in terms of their amplitude and time locations. The result was increased intra-session variability relative to baseline, as well as high inter-session variability. Although the appearance of two envelope peaks at subsequent sessions was unexpected and could not be predicted from the baseline measurements, the high baseline variability suggested that the responses at this frequency were unstable and may not be adequate for assessing effects over time.

The right panels of Fig. 5.3 shows the results in the same subject after implementing additional inclusion criteria regarding baseline stability and location of the mean baseline value of δ. A different frequency was selected because the frequency analyzed in the left panels no longer met the criteria. Although the TEOAE amplitude was lower at this new frequency (compare the results in the top panels), baseline stability was sufficient and the mean baseline δ value fell within $\overleftarrow{R_{\alpha}}$. The resulting intra- and inter-session variability was appreciably improved using the current inclusion criteria.

A more pronounced example is shown for a different subject in Fig. 5.4. The left panels show the results obtained when selecting a frequency only based on the largest peak amplitude. Envelopes exhibited a large, broad peak. Two of the four baseline δ values fell well outside $\overleftarrow{R_{\alpha}}$, and exhibited magnitude increases as well as phase leads and lags. These results were not likely due to MOCR effects because large magnitude increases are not expected with MOCR activation. Results from subsequent sessions

revealed similarly large intra-session variability and large magnitude increases. The results were analyzed at a different frequency that met the baseline stability criteria and are shown in the right panels of Fig. 5.4. Similarly to the example shown above in Fig. 5.3, the baseline stability was adequate, and all subsequent measurements revealed low intra-session variability.

These two examples highlight the importance of obtaining stable baseline measurements in order to reliably assess MOCR changes across time. In these cases, high baseline variability at one frequency was not found at other frequencies. Therefore, careful selection of one or more frequencies with stable baseline measurements is important.

5.1.4 MOCR Strength and TEOAE Amplitude

Recent studies have demonstrated a range of MOCR strength across normal-hearing individuals (Backus and Guinan 2007; Goodman et al. 2013). It is possible that larger TEOAE amplitudes are associated with larger MOCR changes, which was found to be the case for SFOAEs (Backus and Guinan 2007). However, this did not appear to be the case in the current study.

Figure 5.5 shows two subjects with relatively low TEOAE amplitudes (relative to other subjects). Within each subject, envelope amplitudes and R_α values appeared similar within and across sessions, suggesting stable TEOAE amplitudes and SNRs. The left panels show results for a subject with weak or absent MOCR effects. Only five of the 16 measurements in the test condition were statistically significant. In contrast, the right panels show a different subject with similar TEOAE amplitudes but strong MOCR effects. All δ values were statistically significant, and all but two values fell within $\overleftarrow{R_\alpha}$, indicating low intra- and inter-session variability. These results indicate that weak TEOAE amplitudes alone do not preclude the measurement of MOCR effects.

5.1.5 Effect of Synchronous Spontaneous OAEs

TEOAEs typically follow an expected pattern of latency due to the round-trip travel time between an external stimulus reaching the cochlea and the resulting TEOAE returning back to the ear canal. However, normal-hearing ears can often exhibit TEOAEs that persist in time for much longer than what is expected. These emissions are referred to as synchronous spontaneous (SS) OAEs, and are believed to be due to spontaneous OAEs that become entrained to an external stimulus (Prieve and Falter 1995). The presence of SSOAEs may complicate measurements of TEOAE phase and latency because accurate assessments are dependent on the time-locked relationship between stimulus presentation and resulting TEOAE.

It was of interest to examine the effects of SSOAEs in the current study because changes in TEOAE phase were analyzed. Figure 5.6 shows results for a subject with apparent SSOAEs (left panels) and a subject with either weak or absent SSOAEs (right panels). SSOAEs were evidenced by the persistent energy in the TEOAE envelope after 15 ms (highlighted by red arrows in the top left panel), which was well later than the expected TEOAE latency (Tognola et al. 1997; Shera et al. 2002).

Despite differences in SSOAEs, both subjects demonstrated qualitatively similar MOCR effects, including low intra- and inter-session variability and magnitude decreases of approximately 2 dB. These results suggest that the presence of SSOAEs may not impact the measurement of MOCR effects, which is promising given that the prevalence of SSOAEs in normal-hearing individuals may be as high as 70% (Sisto et al. 2001).

5.2 Group Data

5.2.1 Statistical Significance of MOCR Effects

As described in Chap. 4.7.3, an MOCR effect was statistically significant when the δ value fell outside the ellipse described by R_{α}. The significance of all MOCR shifts was computed. The prevalence of significant effects in the test condition were as follows: 14 subjects (66.6%) had significant effects at all 16 measurements, 5 subjects (23.8%)

had significant effects from 12 – 15 measurements, 1 subject (4.8%) had significant effects at 9 measurements, and 1 subject (4.8%) had significant effects at 5 measurements. The subject with 5 significant effects is shown in Fig. 5.5 (left panel) and had weak TEOAEs, potentially explaining the lack of significant effects. These results appeared consistent with those reported by Goodman et al. (2013), who found the majority of subjects had significant MOCR effects at frequencies from 2 kHz and below.

5.2.2 Distribution of ϱ

As discussed in the previous chapter, ϱ describes the total change in TEOAEs because it incorporates changes in both magnitude and phase into a single value. It was important to also examine changes in magnitude ($|\delta|$) and changes in phase ($\angle\delta$) individually, because ϱ does not indicate the amount of change in either magnitude or phase alone.

Distributions of ϱ, $|\delta|$, and $\angle\delta$ are shown for each subject as box and whisker plots in Fig. 5.7. Each box plot represents the distribution of values obtained across all 16 measurements in the test condition. Boxes represent the first and third quartiles. Thick red lines represent the median. Red pluses represent outliers, which were any values falling outside 1.5 × the interquartile range (IQR). Whiskers represent the smallest and largest values that were not outliers.

The top panel of Fig. 5.7 shows the distribution of values for ϱ expressed as a percentage. Larger values correspond to a strong MOCR effect. For these plots, subjects were sorted according to their median ϱ value. This was done to allow for a visual examination of the distribution of MOCR strength across subjects. Across all 336 values of ϱ (16 measurement sets × 21 subjects), the range was 0.74 – 62.64%, with a median of 18.43%. For individual subjects, median values ranged from 4.98 – 52.69%. This indicated considerable variability between subjects in terms of MOCR strength, which is consistent with previous reports (e.g., Backus and Guinan 2007; Goodman et al. 2013).

The IQR (i.e., the height of the box) is an indication of variability, where a smaller IQR indicates lower variability. IQRs for ϱ across individual subjects ranged from 1.99 – 21.98%, with a median of 4.26%. The largest IQR was from the subject shown in the left panel of Fig. 5.2 (and corresponding to subject 10 in Fig. 5.7), who demonstrated decreasing MOCR strength across sessions. Excluding this subject, the largest IQR was 11.46%. These results suggest that a large majority of subjects had low variability in ϱ across all measurements.

Differences in ϱ between the left and right ears were assessed in a subset of 10 subjects. One set of four measurements in the test condition was made in the left ears of these subjects, and the mean ϱ value taken across these measurements was compared to the mean ϱ value obtained in the right ear at the same session. When computed across subjects, there were no significant differences in mean ϱ between ears, as assessed using a *t*-test ($p > 0.05$). An approximately equal number of subjects showed higher ϱ values in the right ear as those who showed higher ϱ in the left ear, with some differences as large as 10%. An optimized measurement protocol could test both ears or select the ear with the largest ϱ value, but optimization was beyond the scope of the current study.

5.2.3 Distribution of $|\delta|$

The middle panel of Fig. 5.7 shows the distribution of $|\delta|$ values expressed in dB. Negative values indicate a magnitude decrease (the expected result), while positive values indicate a magnitude increase. Larger negative values correspond to a stronger MOCR effect. Across all 336 values of $|\delta|$, the range was -4.13 – +1.07 dB, with a median of -0.94 dB. Of these values, 95.8% (322/336) were in the expected negative direction. For individual subjects, median values ranged from -2.94 – -0.30 dB. This result is consistent with the distribution of ϱ values.

IQRs for $|\delta|$ across individual subjects ranged from 0.19 – 1.59 dB, with a median of 0.46 dB. As with the IQR for ϱ, subject 10 had the largest IQR for $|\delta|$.

Excluding this subject, the largest IQR was 0.91 dB. These data indicated that magnitude changes were stable across measurements in nearly all subjects.

5.2.4 Distribution of $\angle\delta$

The bottom panel of Fig. 5.7 shows the distribution of $\angle\delta$ expressed in radians. Positive values indicate a phase lead (the expected result), while negative values indicate a phase lag. Larger positive values correspond to a stronger MOCR effect. Across all 336 values of $\angle\delta$, the range was -0.17 – +0.66 rad, with a median of 0.13. Of these values, 94.3% (317/336) were in the expected positive direction.

IQRs for $\angle\delta$ across individual subjects ranged from 0.02 – 0.35 rad, with a median of 0.05 rad. Subject 10 had the largest IQR for $\angle\delta$. Excluding this subject, the largest IQR was 0.13 rad. These data indicated that phase is also generally stable across measurements.

5.2.5 Relationship Between $|\delta|$ and $\angle\delta$

Because the MOCR reduces cochlear amplifier gain, changes in both magnitude and phase occur. It could be expected that larger decreases in magnitude are associated with larger phase leads. Decreasing cochlear amplifier gain would reduce basilar membrane displacement and reduce the slowing of the traveling wave as it reaches its characteristic place. This would have the effect of decreasing TEOAE magnitude and introducing a phase lead.

It was of interest to examine the relationship between $\angle\delta$ and $|\delta|$ to determine if the two metrics provide unique or redundant information about the MOCR. If they are highly correlated, they may provide redundant information and it may therefore be useful to only analyze one metric. The relationship between $\angle\delta$ and $|\delta|$ was examined using a linear regression analysis, with $\angle\delta$ as the dependent variable and $|\delta|$ as the independent variable. Results are shown in Figure 5.8. An outlier was present (represented as an × marker), so a linear fit to the data was computed with (dotted line) and without the outlier included (solid line). In both cases, the slope of the regression line was not statistically

significant (with outlier: $\beta = -0.32, r = 0.21, p = 0.37$; without outlier: $\beta = -0.38, r = 0.38, p = 0.10$). These results indicated that there was not a significant linear relationship between $|\delta|$ and $\angle\delta$, suggesting each parameter provides complementary, rather than redundant, information regarding MOCR-induced changes in TEOAEs.

5.2.6 Quantification of Repeatability

It was of interest to quantify the repeatability of MOCR changes across time by also using a metric that has been reported by previous studies. Cronbach's alpha is one such metric. It is an index of the reliability of data as assessed by different items (Cronbach 1951). It is typically used as a measure of inter-rater reliability, where the items are the different raters that each assess a given construct. In this study, the items were considered the different measurement sets. Cronbach's alpha (α_C) was calculated as:

$$\alpha_C = \frac{k\bar{c}}{\bar{v}+(k-1)\bar{c}}, \qquad \text{Eq. 5.1}$$

where k is the number of test items, $\bar{c}$ is the mean correlation between all items, and $\bar{v}$ is the mean variance of all items. The possible values of α_C range from 0 to 1, where 1 indicates perfect reliability. Cronbach's alpha increases with increases in *k*, increases in $\bar{c}$, and decreases in $\bar{v}$. An α_C of 0.7 has been considered the minimum acceptable level for a test (e.g., Kline 1999; George and Mallery 2003), although some sources have recommended an α_C of ≥0.9 for a clinical test (e.g., Bland and Altman 1997).

It was expected that α_C would be between 0.7 – 0.8 at a minimum, based on results reported recently by Mishra and Lutman (2013). α_C for ϱ values was first computed across all 16 measurements. The result was a very high value of 0.99. Although this suggests high repeatability across subjects, the value may have been inflated due to a large number of items (16) included in the calculation. α_C increases with the number of test items, and the values reported by Mishra and Lutman (2013) were computed using two items (test-retest). In order to more directly compare to their results,

α_C was computed using two items. Using the first measurement at session 1 as the reference, α_C was computed between the reference and each subsequent measurement (e.g., measurements 1 and 2, measurements 1 and 3, up to measurements 1 and 16). The goal was to quantify how repeatability changes with increasing time from the baseline measurement. The result is shown in Fig. 5.9. As expected, there was a trend of decreasing α_C with increasing amounts of time. However, even with the longest possible time between measurements (measurements 1 and 16), α_C was still acceptably high at 0.85. This value exceeds the values reported by Mishra and Lutman (2013), which may suggest that the current analysis methods yielded more reliable results.

5.3 MOCR and Speech Perception in Noise

Performance on speech perception in noise was assessed using three tests (SDT, SRT, and HINT) in two conditions (ipsilateral and bilateral noise). It was hypothesized that stronger MOCR effects would be correlated with better performance (ability to correctly perform at poorer SNRs). It was further hypothesized that performance would be improved in the bilateral condition relative to the ipsilateral noise condition due to presumably increased MOCR activation in the bilateral condition, and that MOCR strength would be correlated with the improvement seen between conditions. These hypotheses were based on the findings of previous studies (Kumar and Vanaja 2004; Mishra and Lutman 2014; but see Wagner et al. 2008).

Correlations of MOCR strength (ϱ) with SDTs and SRTs could not be validly performed because there was a very limited, discrete range of performance. SDTs ranged from -10 – -6 dB in 2-dB steps. SRTs ranged from -6 – -2 dB, also in 2-dB steps. Visual inspection revealed no apparent relationship between ϱ and performance. Additionally, there was no significant difference between performance in the ipsilateral versus bilateral noise conditions, as assessed using a paired *t*-test ($p > 0.05$). It appeared that SDTs and SRTs did not produce enough variability in performance to meaningfully correlate with MOCR strength.

However, correlations between ϱ and performance on the HINT were able to be examined because the HINT yielded scores in tenths of a dB, which provided more variability across subjects. Linear regression analyses were performed using the mean ϱ value across 16 measurements as the independent variable and performance on the speech test as the dependent variable. In the ipsilateral and bilateral conditions, performance was the SNR (dB) that resulted in 50% correct performance. In the bilateral-ipsilateral condition, the results from the ipsilateral condition were subtracted from the bilateral condition to yield a difference score (dB), where positive values indicated that performance was better in the ipsilateral condition.

Results of the regression analyses for each condition are shown in Fig. 5.10. There was one subject whose mean ϱ value was 53.62%, which was considered an outlier. This subject is shown as an × marker. Linear fits to the data were computed with and without the presence of the outlier to determine the effect of this outlier. In the ipsilateral condition, there was a trend of improved performance (i.e., lower SNR) with increasing ϱ value. However, the slopes of the linear fits with and without the outlier were non-significant ($p > 0.05$). In the bilateral condition, performance tended to decrease with increasing ϱ value. The fit was statistically significant when including the outlier ($r = 0.55, p < 0.01$), but was not significant when the fit was computed without the outlier ($r = 0.23, p = 0.23$). In the bilateral-ipsilateral condition, performance in the ipsilateral condition tended to be better relative to the bilateral condition with increasing ϱ value. The fit was statistically significant when including the outlier ($r = 0.60, p < 0.01$), but only approached significance when the fit was computed without the outlier ($r = 0.41, p = 0.07$). Correlations between HINT performance and $|\delta|$ (change in magnitude) and $\angle\delta$ (change in phase) were explored but were found to be non-significant for all three conditions.

The correlations between MOCR strength and speech perception in noise were inconsistent with our hypotheses. There was a trend toward poorer performance in

bilateral noise as the MOCR strength increased. This result is also inconsistent with some previous reports (e.g., Giraud et al. 1997; Kumar and Vanaja 2004), who found that stronger MOCR was associated with better speech perception in noise ability, and that performance was improved in the presence of bilateral noise as compared to ipsilateral noise. However, the current results are consistent with recent studies that found that stronger MOCR was associated with poorer speech in noise performance (de Boer et al. 2012) and poorer masked thresholds (Garinis et al. 2011). The reason for why stronger MOCR may be associated with poorer ability to hear in background noise is unclear, but will be addressed in Chap. VI (Discussion).

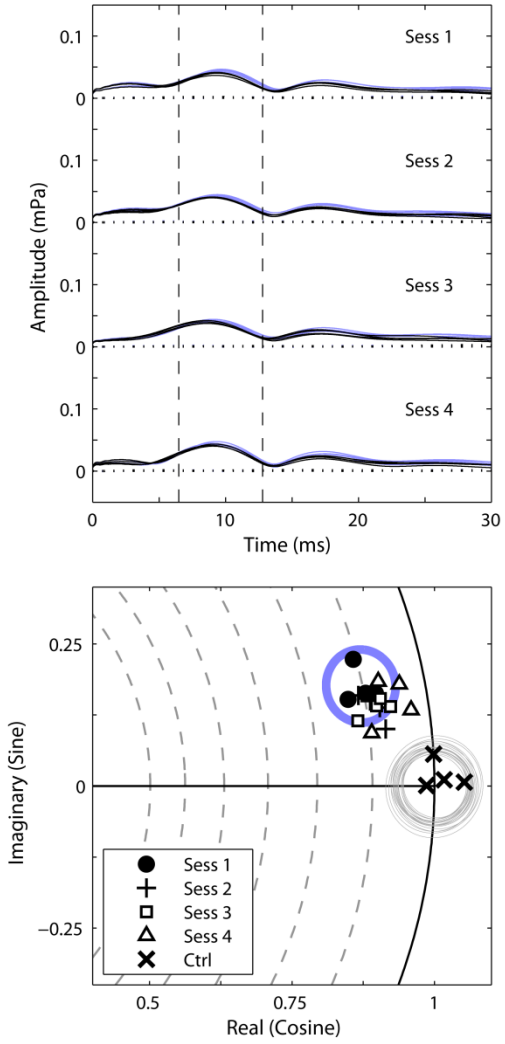

Figure 5.1. Low intra- and inter-session variability. Results are shown for Subject 11 (see Fig. 5.7). Top panel: Mean TEOAE envelopes without CAS (solid blue tracings) and with CAS (solid black tracings) are shown for each measurement, grouped according to session. Dotted horizontal lines represent the noise floors obtained without CAS (blue) and with CAS (black). Vertical dashed lines indicate the time analysis window used for this subject. Bottom panel: Frequency domain analysis of the envelopes shown in the top panels, plotted relative to the unit circle. Complex ratios (δ) are shown as markers, with the marker style indicating the session from which the value was obtained. Tolerance regions (R_α) for each measurement are shown as gray ellipses. The shifted tolerance region ($\overleftarrow{R_\alpha}$) is shown as a thick blue ellipse. Results from the control condition (CAS unplugged) are shown as × markers.

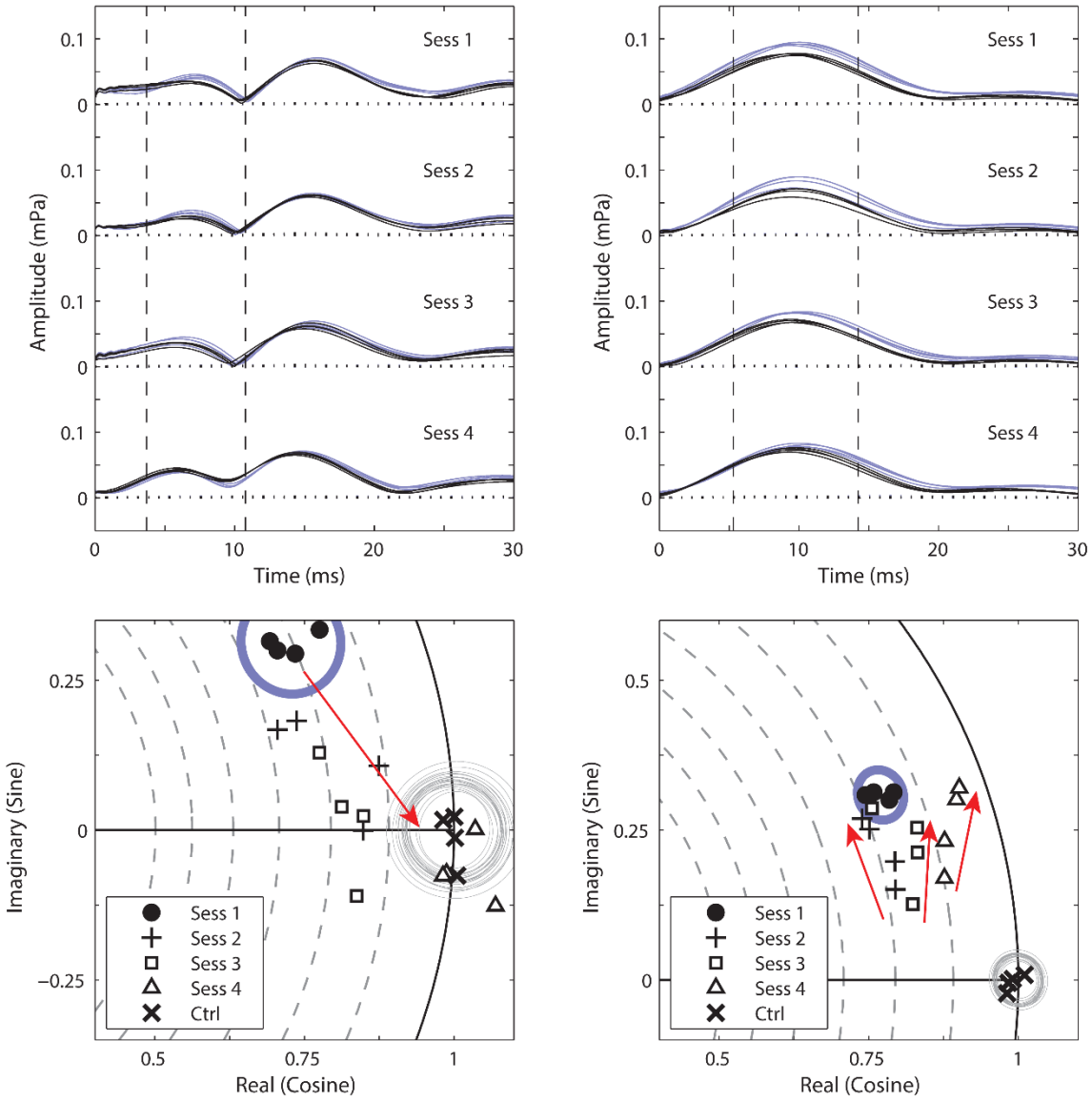

Figure 5.2. High intra- and inter-session variability. Results for subjects 10 and 03 (see Fig. 5.7) are shown in the left and right panels, respectively. In both cases, these subjects demonstrated sufficiently stable baseline δ values and R_α. Left panels: This subject demonstrated high intra-session variability at subsequent sessions, with a trend toward non-significant changes by session 4 (highlighted by the red arrow). Right panels: This subject demonstrated increasing phase leads within a session, highlighted by the red arrows. Note that the y-axis was shifted in the bottom right panel to make all ratios visible.

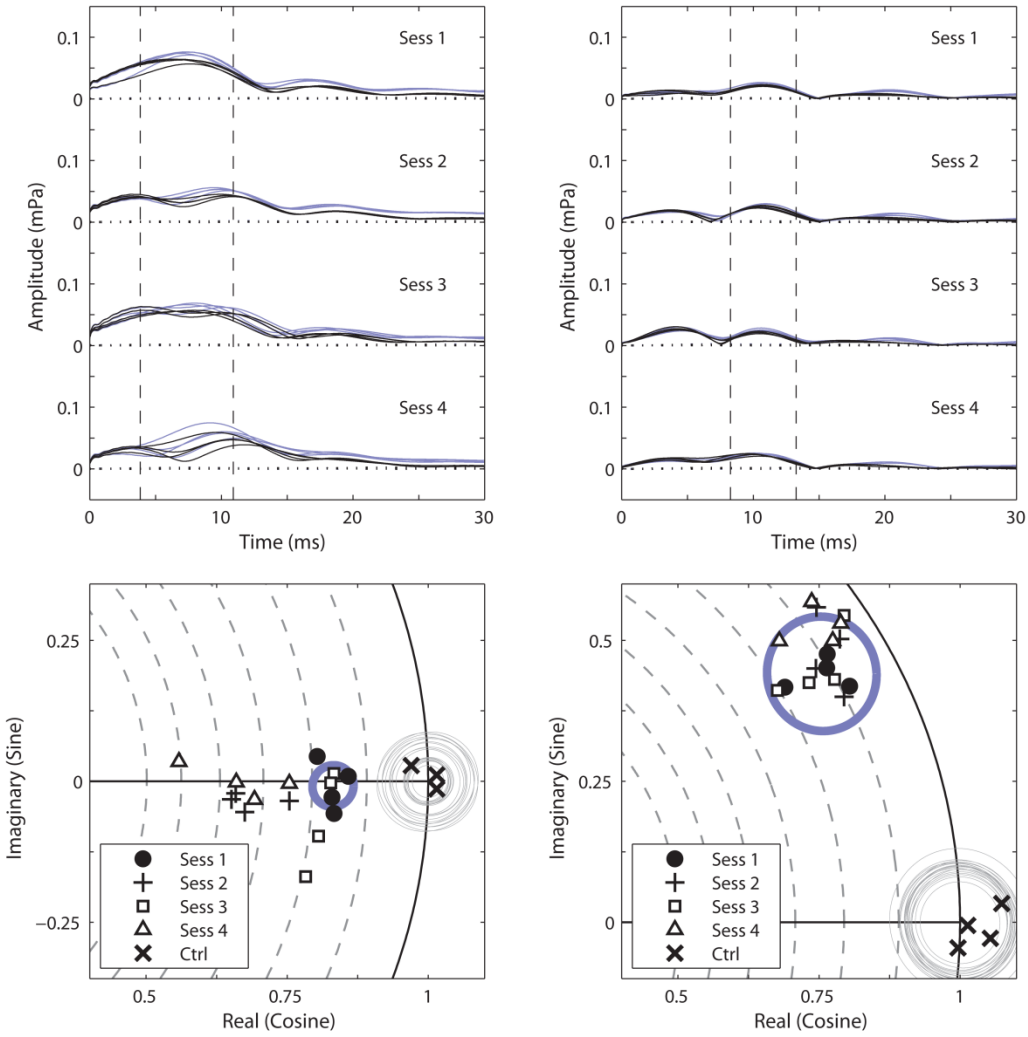

Figure 5.3. The effect of baseline stability on intra- and inter-session variability. Results are shown for subject 01 (see Fig. 5.7). Left panels: Results are shown for responses obtained at the frequency containing the largest peak (1.41 kHz), without consideration of baseline variability. Right panels: Results are shown for responses obtained at a different frequency (2 kHz) that met baseline variability requirements. Although this frequency did not contain the largest peak, the baseline results were stable and in the expected direction. Note the difference in y-axes between the bottom panels.

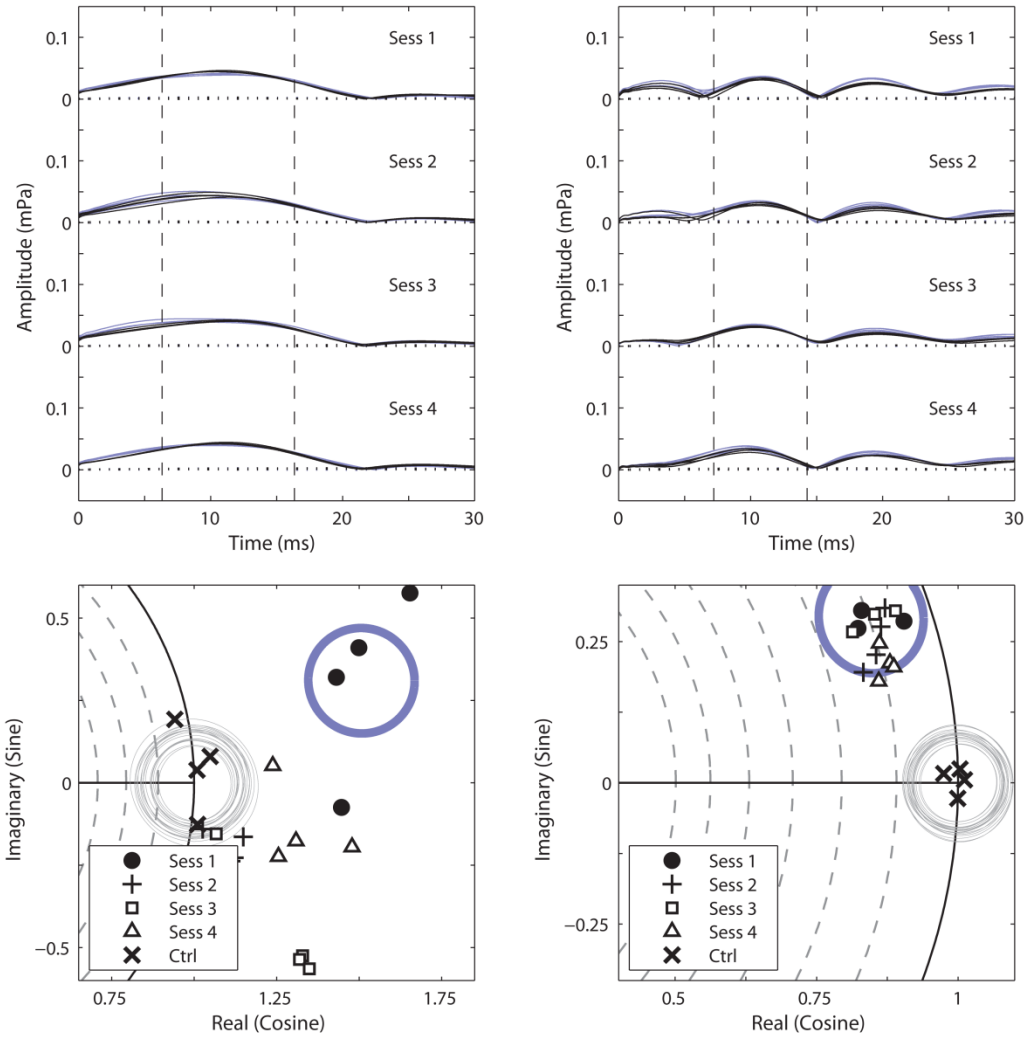

Figure 5.4. The effect of baseline stability on intra- and inter-session variability. Results are shown for subject 04 (see Fig. 5.7). Left panels: Results are shown for responses obtained at the frequency containing the largest peak (1 kHz) without consideration of baseline variability. Right panels: Results are shown for responses obtained at a different frequency (1.41 kHz) that met baseline variability requirements. Although this frequency did not contain the largest peak, the baseline results were stable and in the expected direction. Note the difference in x- and y-axes between the bottom panels.

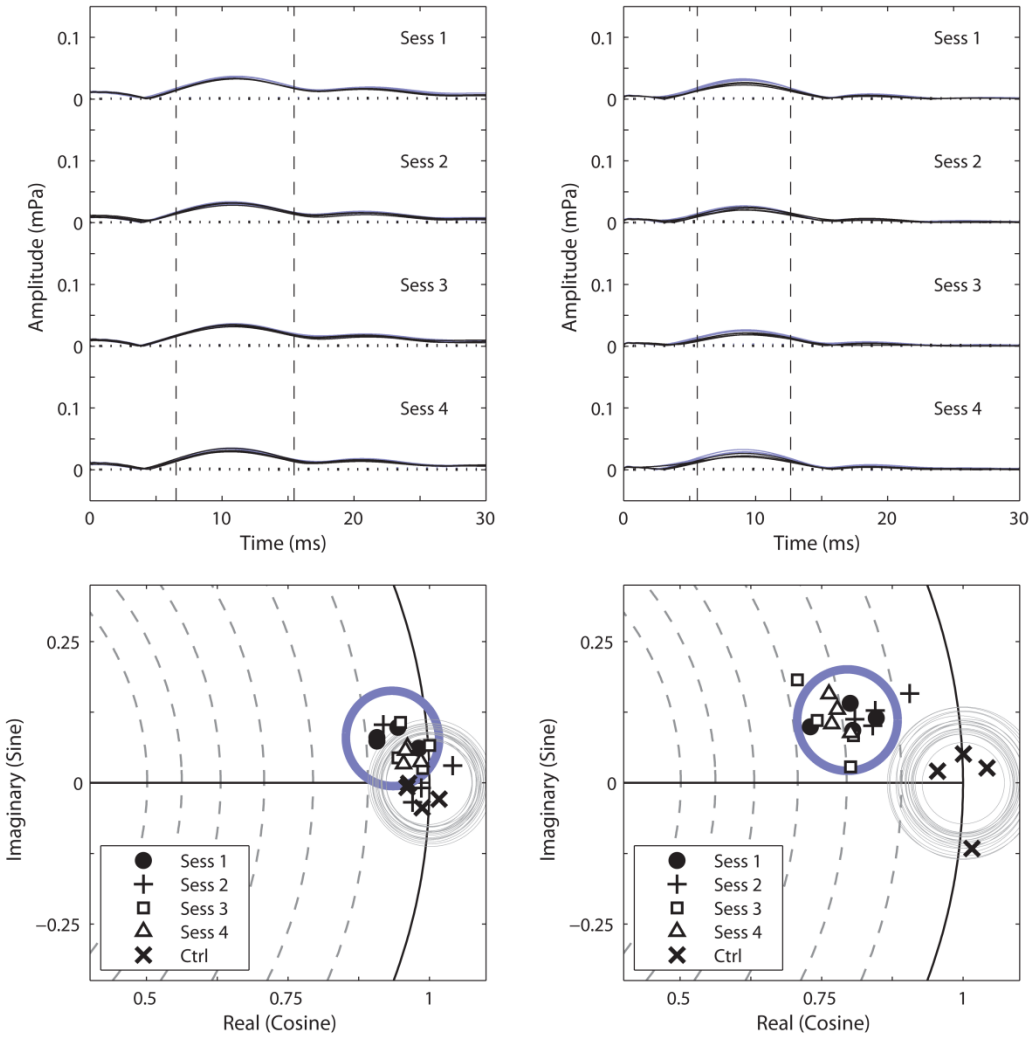

Figure 5.5. Weaker and stronger MOCR effects, both in the presence of low-amplitude TEOAEs. Results for subjects 09 and 20 (see Fig. 5.7) are shown in the left and right panels, respectively. Left panels: This subject demonstrated mostly non-significant MOCR effects. Right panels: This subject demonstrated magnitude changes of approximately 2 dB and clear phase leads, despite having weak amplitude TEOAEs.

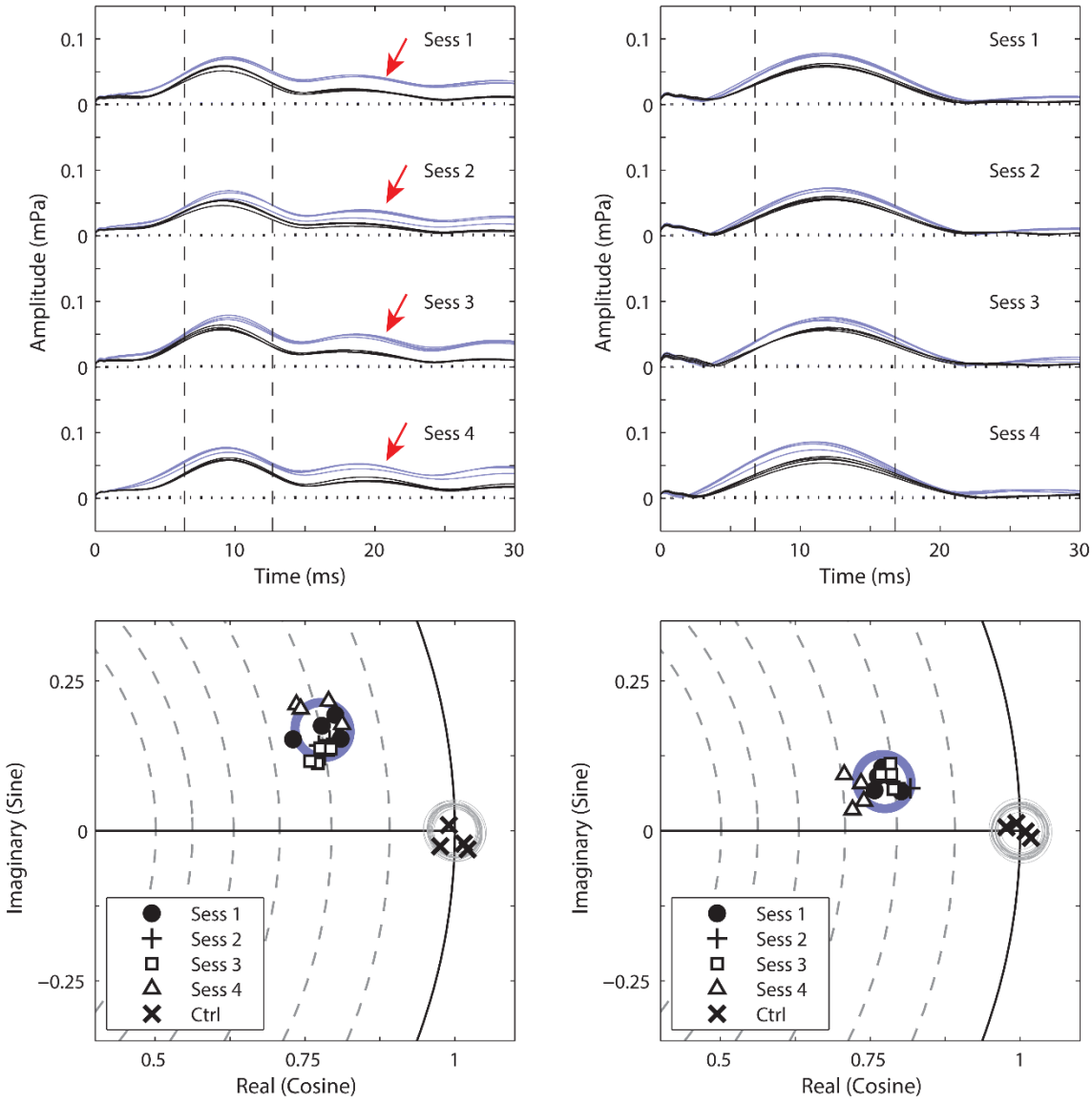

Figure 5.6. MOCR in a subject with SSOAEs (left panels) and in a subject without SSOAEs (right panels). Results for subjects 09 and 08 (see Fig. 5.7) are shown in the left and right panels, respectively. SSOAEs were evidenced by the persistent TEOAE energy in the envelope, highlighted by the red arrows in the top left panel. The subject in the right panel did not demonstrate apparent TEOAE energy outside of the analysis window. Both subjects showed similar magnitude changes (~2 dB) and similar intra- and inter-session repeatability.

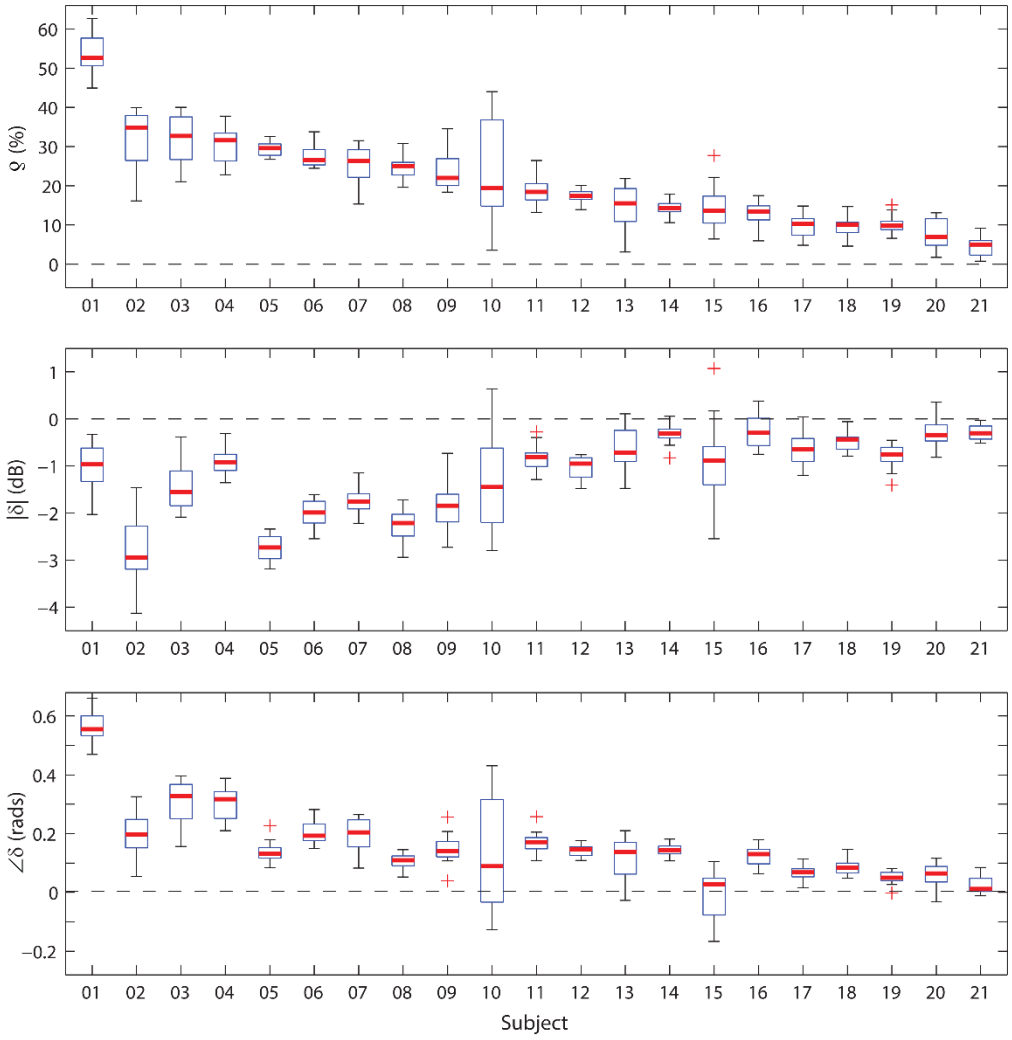

Figure 5.7. Distributions of mean MOCR effects using three metrics: ϱ (top panel), $|\delta|$ (middle panel), and $\angle\delta$ (bottom panel). Results are shown as box and whisker plots. Boxes represent the first and third quartiles, thick red lines represent the medians, whiskers represent the largest and smallest values that are not outliers, and red pluses represent outliers. Outliers were defined as values exceeding 1.5 times the interquartile range. Subjects are sorted according to their median ϱ value. Subject number corresponds to the same subject in each panel. Dashed horizontal lines represent where values fall if there were no change in TEOAEs.

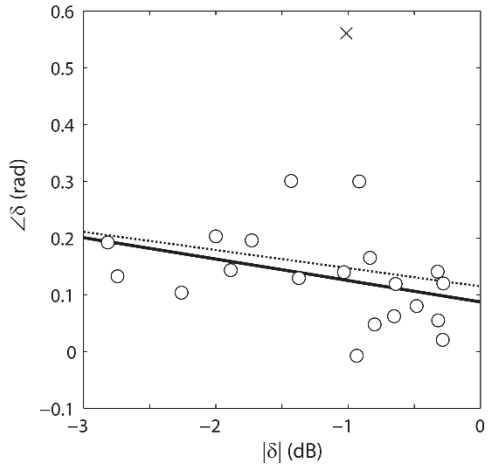

Figure 5.8. Correlation between $|\delta|$ and $\angle\delta$. Unfilled circles represent mean values for individual subjects, computed across 16 measurements. The × marker represents an outlier. The dotted line is a linear fit to all data, while the solid line is a linear fit to the data with the outlier excluded. The slope of each fit was not significantly different from zero ($p > 0.05$).

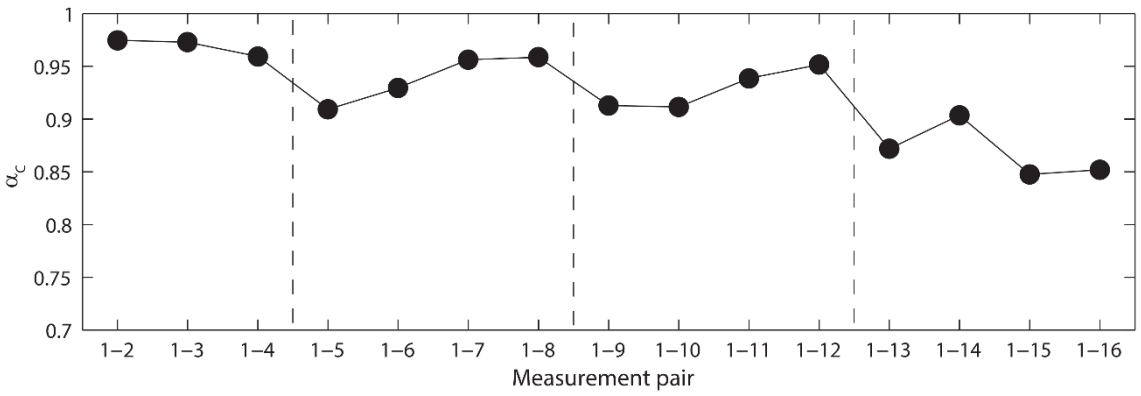

Figure 5.9. Cronbach's alpha (α_C) computed between the baseline measurement and all other individual measurements. Filled circles represent the α_C value using data from all subjects. Vertical dashed lines are used to visually separate the four sessions.

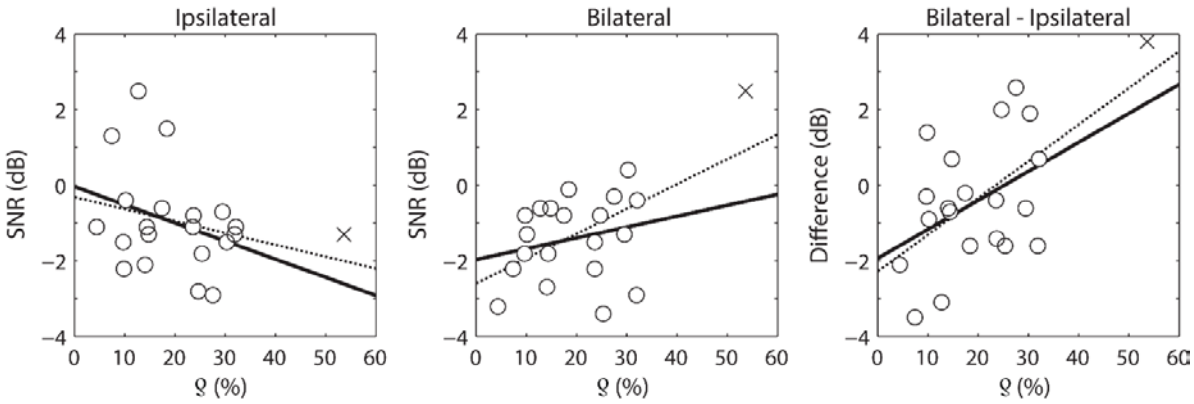

Figure 5.10. Relationship between HINT performance and ϱ. Left panel and middle panels show performance in the ipsilateral and bilateral noise conditions, respectively. Right panel shows the difference in performance between bilateral and ipsilateral conditions (bilateral – ipsilateral), where positive values indicate that performance was better in the ipsilateral condition. Unfilled circles represent values for individual subjects. The × marker indicates an outlier. Lines represent linear fits to the data. Dashed line is the fit that includes the outlier. Solid line is the fit to the data, excluding the outlier. In the ipsilateral condition, the slopes of both fits were not significant ($p > 0.05$). In the bilateral condition, the slope of the fit that included the outlier was significant ($r = 0.55, p < 0.01$); the slope of the fit that excluded the outlier was not significant ($p > 0.05$). In the difference condition, the slope of the fit that included the outlier was significant ($r = 0.60, p < 0.01$); the slope of the fit that excluded the outlier approached significance ($r = 0.41, p = 0.07$).

CHAPTER VI

DISCUSSION

6.1 Purposes of the Current Study

6.1.1 Repeatability of the MOCR

The primary purpose of the current study was to assess the intra- and inter-session variability in MOCR-induced changes in TEOAEs in individual subjects and in group data. Variability of the MOCR across time was of interest because numerous authors have speculated that OAE-based measurements of MOCR may have clinical applications. These potential applications include predicting susceptibility to noise-induced hearing loss (e.g., Maison and Liberman 2000; Wolpert et al. 2014), providing a physiologic explanation for difficulties hearing in noise (e.g., Tokgoz-Yilmaz et al. 2013), objectively assessing benefit from auditory training (de Boer and Thornton 2008), detecting subclinical changes in cochlear function prior to presbycusis (e.g., Zhu et al. 2007), and assisting in the diagnosis of auditory neuropathy (Hood et al. 2003).

For any of these applications, but especially for ones that involve serial measurements, a careful examination of the variability of the measurements across time is crucial to determine the potential clinical utility. Highly variable responses within a control population may preclude the ability to reliably interpret the responses. Additionally, if one is assessing changes in MOCR over time (e.g., to detect incipient presbycusis or to monitor changes due to auditory training), one must be able to assess the inherent variability of the measurements. Knowledge of the inherent variability allows one to determine if a new measurement represents a true change in MOCR, or if it falls within the inherent variability and therefore cannot be known if it represents a true change. Additionally, confounding sources of variability (i.e., variability that is unrelated to cochlear and olivocochlear function) must be controlled for in order to correctly interpret a measurement. Finally, one must be able to assess the variability of

measurements *in an individual subject*, as opposed to the variability in a group of subjects. Although analyses of group data lends well to parametric statistical methods such as a *t*-test, clinical applications are focused on an individual subject. Therefore, one must be able to assess the baseline MOCR functioning and its variability to be able to compare results across time.

To our knowledge, no previous study has incorporated all of the factors described above. The repeatability of MOCR effects on OAEs has been reported for group data (Graham and Hazell 1994; Kumar et al. 2013; Mishra and Lutman 2013). However, these studies either did not report or did not emphasize individual results, especially in terms of the intra- and inter-session reliability and the detection of statistically significant effects in individuals. Two studies have reported methods for detecting significant MOCR effects in individuals as well as careful control of confounding factors such as MEMR activation (Backus and Guinan 2007; Goodman et al. 2013), but the variability of the responses across time was not assessed.

The current study built upon previous studies to assess the variability of MOCR-induced changes in TEOAEs using careful recording and analysis methods. The MOCR could be reliably evoked and measured across time in nearly all subjects, although there were some exceptions. The results will be discussed in terms of MOCR behavior exhibited by individuals and by the group, issues in the measurement and analysis of MOCR, and recommendations for future studies and potential clinical implementation of MOCR testing.

6.1.2 MOCR and Speech Perception in Noise

A secondary purpose of the current study was to determine the relationship between MOCR strength and speech perception in noise. This issue has been examined previously, with some studies finding that MOCR strength is associated with better performance (e.g., Giraud et al. 1997; Kumar and Vanaja 2004; Mishra and Lutman 2014), poorer performance (de Boer et al. 2012), or no measurable association (Wagner

et al. 2008). Potential explanations for the differences seen across studies include differences in OAE stimuli (e.g., TEOAEs versus DPOAEs), differences in MOCR-evoking stimulus levels, differences in assessment of speech in noise performance (e.g., recognition of single words versus sentences), and differences in the characteristics of the subjects.

The current study examined the relationship between MOCR strength and speech perception in noise using methods to reliably evoke and measure the MOCR. Additionally, three levels of speech perception (detection, single word recognition, and sentence recognition) were assessed to see which, if any, levels are associated with MOCR strength. Most previous studies only examined one level of speech perception. It was hypothesized that stronger MOCR would be associated with better performance. However, results were contrary to the hypothesis. The potential reasons for these results will be discussed, as well as recommendations for future explorations of the relationship between the MOCR and speech perception in noise.

6.2 Important Factors in Assessment of MOCR

6.2.1 Ensuring Validity of Measured MOCR Responses

Because the MOCR was quantified as a change in TEOAE magnitude and phase, it was crucial to establish that the change was due to the MOCR and not to some other factor. Potential confounds include the MEMR, slow drifts in TEOAE amplitudes, changes in attention, and non-significant changes in TEOAEs. MEMR was assessed using methods described by Goodman et al. (2013) and was found to not be elicited in any subject. Slow drifts in TEOAE amplitude were controlled for by de-trending the recorded waveforms (Goodman et al. 2013). Changes in attention were controlled for by having all subjects perform a visual attention task during every measurement. Finally, statistical significance was assessed using statistical tolerance regions, as discussed in the Methods chapter. Implementation of these methods increased our confidence that the observed changes in TEOAEs were due to the MOCR. Control of confounds is important

for both research-based and clinically-based measurement of the MOCR. The controls implemented in the current study could feasibly be adapted into a clinical protocol.

6.2.2 Individualized Analysis of Magnitude and Phase

The current study implemented an individualized time-frequency analysis of TEOAE responses, as opposed to the more conventional analysis that uses a fixed time and/or fixed frequency analysis. This individualized analysis was necessary because the distributed nature of TEOAEs renders it difficult to use fixed analysis parameters that encompass a localized peak in all subjects. The optimal frequency and time window to use on an individual subject could not be known *a priori*, but selection of these parameters could easily be implemented into an automated algorithm.

Traditional assessment of MOCR function using OAEs has focused primarily on amplitude/magnitude changes (e.g., Veuillet et al. 1991; Hood et al. 1996; Clarke et al. 2006). However, the current results showed that phase changes were also present and could be assessed in combination with magnitude changes. Additionally, Fig. 5.8 demonstrated that changes in magnitude and phase were not linearly related, so they may not simply provide redundant information, but rather may provide complementary information that could improve detection and quantification of MOCR effects relative to amplitude/magnitude changes alone. Therefore, it is recommended magnitude and phase changes be measured simultaneously.

6.2.3 Establishing a Reliable Baseline

In order to assess MOCR effects on OAEs across time, it is important to establish a baseline that is reliable. An unreliable baseline may render it difficult or impossible to determine whether subsequent measurements represent a true change in MOCR functioning, or whether the measurement falls within the baseline variability. As discussed in Chap. 4.7.5 and shown in Fig. 4.7, simulations revealed that four measurements within a session resulted in tolerance regions that included approximately 95% of the data, 95% of the time. This suggests that a minimum of four measurements

should be taken at the baseline, which may be feasible in a clinical setting. Additional measurements at baseline would improve the reliability, but would come at the cost of increasing the test time.

In addition to making four measurements, obtaining a reliable baseline measurement required analyzing a specific portion of the recorded response. As discussed in Chap. 4.7.1, single energy peaks within the 6.0 – 12.2 ms time window were analyzed for MOCR effects. Initially, the bandpass filtered response (out of seven filter center frequencies) that had the largest peak amplitude was selected for analysis, under the assumption that this response would be most reliable because it had the largest SNR. However, it was found that this response was not necessarily the most reliable, as demonstrated in the left panel of Fig. 5.3. After selecting a different bandpass filtered response (albeit one with a lower peak amplitude and thus lower SNR), the reliability was much improved (Fig. 5.3, right panel). An advantage of TEOAEs over DPOAEs and SFOAEs is that the response contains a broad range of frequency elicited essentially at once, whereas DPOAEs and SFOAEs involve measurements made at single, discrete frequencies. Therefore, the TEOAE response can be elicited relatively quickly and responses at different frequencies can be analyzed post-hoc to potentially optimize MOCR measurement.

6.3 Implications of Individual Results

As illustrated in Chap. 5.1, a variety of responses were exhibited by individual subjects. A majority of subjects showed results similar to that shown in Fig. 5.1, i.e., a consistent magnitude change and phase lead within and across sessions. This result was encouraging because it was anticipated that MOCR-induced changes in TEOAEs would exhibit low variability when controlling for other sources of variability (e.g., changes in attention, changes in auditory function, etc.).

However, despite the efforts to minimize sources of variability, there were exceptions to this well-behaved pattern of repeatability. This was demonstrated in Fig.

5.2. One subject showed a progressive change from well-behaved MOCR effects at baseline to essentially no measurable MOCR effect at the fourth session. Such a progressive decline was unexpected, given that the subject had no measurable changes in hearing or middle ear status, no reported noise exposure between sessions, and there were no indications of calibration or equipment errors. Responses at other frequencies did not meet the criteria for baseline stability, so it could not be determined if a similar change across time was exhibited at other frequencies. If similar effects were exhibited at other frequencies and/or in the left ear, this could be taken as evidence of a potential change in cochlear and/or olivocochlear functioning. These data were not available for this subject, so it would be premature to attribute the observed changes to a decrement in MOCR based on results at a single frequency.

A different subject also showed changes both within and across sessions, despite having a stable baseline (Fig. 5.2, right panel). In this case, the change was exhibited as an increasing phase lead within a session. This pattern was seen at sessions 2 – 4, which may have been coincidental, but could have also represented a systematic change within a given session. There was also a trend of smaller magnitude decreases across time. As with the subject shown in the left panel, it was unclear as to why this change was seen across time, and also why it was not exhibited at the baseline. Interestingly, the fourth measurement in sessions 2 and 3 fell in or near the baseline R_{α}. These changes within a session lend further support to the notion that multiple measurements should be taken at a session to give a more complete picture of the MOCR effect, rather than simply making one measurement. These two examples also highlight that further work is needed to better determine when a significant change in MOCR has been observed, as opposed to another source of variability that is confounding the interpretation.

It was found that in some cases, reliable MOCR effects could be measured in the presence of weak TEOAE amplitudes. This was demonstrated in Figure 5.5. A subject with weak amplitude TEOAEs would have a lower SNR relative to a subject with larger

amplitude TEOAEs. Goodman et al. (2013) found that as the size of the MOCR effect decreased, a larger corresponding TEOAE SNR was required to reliably detect the change. Although the subject in the left panel had mostly non-significant MOCR effects, the subject in the right panel demonstrated large and reliable MOCR effects. This finding indicates that weak amplitude TEOAEs by themselves do not preclude measurement of the MOCR. However, it may prove to be more difficult to measure them, given the inherently lower SNR. It is possible that methods such as increasing the number of averages and/or increasing stimulus levels (but ensuring no MEMR activation) could improve measurement of MOCR in the presence of weak TEOAEs. It may also allow for measurement of MOCR in subjects with mild hearing loss, who often present with weak amplitude TEOAEs. However, this remains speculative and would require verification in subjects with hearing loss.

The presence of SSOAEs was anticipated to be a complication in the current analyses because it could interfere with measurements of phase and interfere with determination of peaks in the envelope response. Some studies have avoided analyzing OAE responses that were close in frequency to SSOAEs (e.g., Francis and Guinan 2010). However, up to 70% of normal-hearing individuals may have SSOAEs (Moleti et al. 2011), and experience in our lab has shown that subjects can often have numerous SSOAEs in the 1 – 2 kHz range. The effect of SSOAEs on MOCR measurement has not been studied previously, so its effects were unknown. Fig. 5.6 demonstrated that MOCR effects on both magnitude and phase could be reliably measured across time in a subject that had relatively strong SSOAEs. Given the high prevalence of SSOAEs in normal-hearing individuals, it was encouraging to see that it may not be a barrier to reliable measurement of MOCR effects. However, it may be possible that very robust SSOAEs would be detrimental to MOCR measurement, especially when analyzing short-latency and/or high-frequency responses that may be contaminated by SSOAEs. In a case such as this, use of a slower click rate may allow for the SSOAE to dissipate prior to the onset of

the next stimulus. Additionally, use of a 1/6-octave or narrower filter could allow for analysis of frequencies away from SSOAEs, but this may be unfeasible in the presence of many SSOAEs. The effect of SSOAEs on MOCR measurements warrants further investigation to determine if one must take steps to reduce or exclude them from analyses.

6.4 Implications of Group Results

Subjects exhibited a range of MOCR strength (see Fig. 5.7), consistent with previous reports (e.g., Backus and Guinan 2007; Goodman et al. 2013). Subjects also exhibited a range of response variability across time, as evidenced by the sizes of the box plots in Fig. 5.7. There was no apparent association between the strength of the MOCR and the variability across time (i.e., stronger effects were not necessarily less variable). Despite these differences across subjects, a large majority (approximately 92%) of the measured effects were statistically significant, consistent with a recent report (Goodman et al. 2013). This indicates that even small changes in TEOAEs invoked by the MOCR can be significant, and can be detected reliably using the current methods.

Nearly all changes in magnitude ($|\delta|$) and changes in phase ($\angle\delta$) were in the expected direction. Although the baseline measurements were constrained to fall within the expected direction, subsequent measurements could fall anywhere. The fact that subsequent changes were in the expected direction was qualitative evidence that the MOCR responses were reliable over time. In addition, the high values of Cronbach's alpha (α_C) were quantitative evidence of the high repeatability of responses across time. Although α_C tended to decrease slightly over time between the first measurement and the final measurement (comprising a span of approximately 5 weeks), the reliability was still high (0.85), suggesting that measurements were quite stable across time, on average.

6.5 Comparisons to Previous Literature

As discussed in Chapter 3.5.3, three previous studies have specifically focused on the repeatability of the MOCR. Graham and Hazell (1994) reported small MOCR effects

(0.3 – 0.6 dB) with low variability (*SD*s from 0.1 – 0.3 dB) in six subjects, but the statistical significance of the effects was unknown and limited conclusions could be drawn from such a small sample size. Kumar et al. (2013) reported poor repeatability (intraclass correlation coefficient values ranging from 0.1 – 0.3 across measurements) for MOCR effects on DPOAEs in a larger group of subjects. This may have been because many of the changes in DPOAEs appeared to be less than the smallest detectable difference, suggesting a lack of statistical significance. Relatively low CAS levels were used (40 dB SPL), which may not have been sufficient to elicit measurable MOCR effects in a number of subjects. Finally, Mishra and Lutman (2013) reported more favorable repeatability outcomes (α_C ranging from 0.7 – 0.8) using TEOAEs to assess MOCR. However, the statistical significance of their effects was not reported, and only test-retest reliability across several days was reported.

The current study found α_C values that exceeded those reported by previous studies. Due to numerous differences in methodology (e.g., stimulus levels, control of confounds, analysis methods), it is difficult to pinpoint the specific reasons for the improved reliability results in the current study. However, it was apparent that in the current study, the stimuli were able to elicit the MOCR and that the analysis methods were able to detect changes in TEOAEs. The fact that a large majority of these changes were statistically significant, and that careful control of confounds was exercised, further suggests that the MOCR was the effect that was primarily measured. It is recommended that future studies implement similar methods as in the current study in order to reliably assess the variability in the MOCR and to validate the current methodology.

6.6 MOCR Strength and Speech Perception in Noise

Based on previous studies (e.g., Giraud et al. 1997; Kumar and Vanaja 2004), it was hypothesized that stronger MOCR effects would be associated with better speech perception in noise. The rationale was that stronger MOCR should provide greater unmasking of signals in continuous noise (e.g., Kawase and Liberman 1993), and should

therefore be associated with better performance. However, the results of the current study revealed a trend that was in the opposite direction (i.e., better performance was associated with weaker MOCR effects), though this trend was not statistically significant after removing an outlier from the analysis. Results should be interpreted cautiously, given the relatively small sample size. It is possible that statistical significance would be achieved with greater statistical power.

Despite the lack of statistical significance, the trend in the data appeared to be contradictory to the assumption that greater unmasking would improve performance. De Boer et al. (2012) found that stronger MOCR effects were associated with poorer discrimination of vowel contrasts (/da/ vs. /ga/) in noise, whereas their group found the opposite effect in an earlier study that examined a different set of vowel contrasts (/bi/ vs. /di/) (de Boer and Thornton 2008). They discussed that the benefit from the MOCR may be highly dependent on the spectral and temporal properties of the stimuli, which could explain the discrepancies in findings. The current study used sentence materials drawn from a pool of 250 sentences, making it difficult to compare precise spectral and temporal properties between sentences. Moreover, the sentences included linguistic and contextual cues, which may have been more relevant to a subject's performance rather than their MOCR strength.

6.7 Limitations

Although the current study represents an improvement upon previous studies of MOCR variability, there were several limitations. Although most subjects showed consistent patterns of MOCR effects that had the expected magnitude and phase changes, it is unclear how to interpret the results of the subjects shown in Fig. 5.2, who exhibited variability within and across sessions except at the baseline. These cases may be the most worrisome because the baseline sessions were stable, but unusual effects were exhibited at all other sessions. In these cases, other frequencies were less well-behaved at baseline, making it difficult to determine if there was a decrement in MOCR or if the changes were

the result of some other source of error. Measurement of MOCR effects in the left ears at all sessions may provide complementary information when attempting to determine if a true change in MOCR occurred.

Although inclusion criteria were chosen to include young subjects with good hearing, it is not known how these results would generalize to other populations, such as older adults or individuals with some level of hearing loss. If reliable measurement of MOCR is limited to young adults with normal hearing, the clinical applications may be limited. Few studies have assessed MOCR effects in subjects with hearing loss, so it remains to be seen if these measurements hold promise for these populations.

The speech perception in noise tasks may not have been sensitive enough to probe the role of the MOCR. SDTs and SRTs resulted in a very narrow range (4 dB) of performance, making a correlational analysis unfeasible. This was likely due to the homogeneity of the subject population. Although the HINT allowed for more variability in performance across subjects, it was possible that the inclusion of linguistic and contextual cues in the materials had a larger influence on subject performance rather than an unmasking effect from the MOCR. Future studies are needed to reconcile the disparate results regarding the relationship between MOCR and speech perception in noise.

6.8 Conclusions

MOCR effects on TEOAEs were found to be highly repeatable across a 5-week time span in a large majority of young normal-hearing subjects. Methods were implemented to minimize the variability in responses not due to the MOCR and to detect statistically significant changes in both magnitude and phase simultaneously. Despite the reliability of the MOCR measurements, there were no statistically significant linear relationships between MOCR strength and speech perception in noise. Future studies should incorporate the measurement and analysis methods described in the current study, especially studies that are focused on detecting changes in MOCR across time.

REFERENCES

Abdala C, Ma E, Sininger YS (1999) Maturation of medial efferent system function in humans. J Acoust Soc Am 105:2392-2402

Abdala C, Mishra S, Garinis A (2013) Maturation of the human medial efferent reflex revisited. J Acoust Soc Am 133:938-950

Aibara R, Welsh JT, Puria S, Goode RL (2001) Human middle-ear sound transfer function and cochlear input impedance. Hear Res 152:100-109

Anderson SD, Kemp DT (1979) The evoked cochlear mechanical response in laboratory primates: A preliminary report. Arch Otorhinolaryngol 224:47-54

Arnesen AR (1984) Fibre population of the vestibulocochlear anastomosis in humans. Acta Otolaryngol 98:5-6

Backus BC (2006) Bias due to noise in otoacoustic emission measurements. J Acoust Soc Am 121:1588-1603

Backus BC, Guinan JJ Jr (2006) Time-course of the human medial olivocochlear reflex. J Acoust Soc Am 119:2889-2904

Backus BC, Guinan JJ Jr (2007) Measurement of the distribution of medial olivocochlear acoustic reflex strengths across normal-hearing individuals via otoacoustic emissions. J Assoc Res Otolaryngol 8:484-496

Berlin CI, Hood LJ, Hurley AE, Wen H, Kemp DT (1995) Binaural noise suppresses linear click-evoked otoacoustic emissions more than ipsilateral or contralateral noise. Hear Res 87:96-103

Berlin CI, Hood L, Morlet T, Rose K, Brashears S (2003) Auditory neuropathy/dys-synchrony: Diagnosis and management. Ment Retard Dev Disabil Res Rev 9:225-231

Berlin CI, Hood LJ, Morlet T, Wilensky D, John PS, Montgomery E, Thibodaux M (2005) Absent or elevated middle ear muscle reflexes in the presence of normal otoacoustic emissions: A universal finding in 136 cases of auditory neuropathy/dys-synchrony. J Am Acad Audiol 16:546-553

Berlin CI, Hood LJ, Wen H, Szabo P, Cecola RP, Rigby P, Jackson DF (1993) Contralateral suppression of non-linear click-evoked otoacoustic emissions. Hear Res 71:1-11

Bland JM, Altman DG (1997) Statistics notes: Cronbach's alpha. Brit Med J 314:572

Bland JM, Altman DG (1999) Measuring agreement in method comparison studies. Stat Methods Med Res 8:135-160

Boothalingam S, Lineton B (2012) Effect of contralateral acoustic stimulation on cochlear tuning measured using stimulus frequency and distortion product OAEs. Int J Audiol 51:892-899

Boyev KP, Liberman MC, Brown MC (2002) Effects of anesthesia on efferent-mediated adaptation of the DPOAE. J Assoc Res Otolaryngol 3:362-373

Brass D, Kemp DT (1986) Suppression of stimulus frequency otoacoustic emissions. J Acoust Soc Am 93:920-939

Bray P, Kemp D (1987) An advanced cochlear echo technique suitable for infant screening. Br J Audiol 21:191-204

Brown MC, Nuttall AL (1984) Efferent control of cochlear inner hair cell responses in the guinea-pig. J Physiol 354:625-646

Brownell WE (1990) Outer hair cell electromotility and otoacoustic emissions. Ear Hear 11:82-92

Brownell WE, Bader CR, Bertrand D, de Ribaupierre Y (1985) Evoked mechanical responses of isolated cochlear outer hair cells. Science 227:194-196

Büki B, Wit HP, Avan P (2000) Olivocochlear efferent vs. middle-ear contributions to the alteration of otoacoustic emissions by contralateral noise. Brain Res 852:140-150

Bũno W Jr, Velluti R, Handler P, Austt EG (1966) Neural control of the cochlear input in the wakeful free guinea-pig. Physiol Behav 1:23-35

Chambers AR, Hancock KE, Maison SF, Liberman MC, Polley DB (2012) Sound-evoked olivocochlear activation in unanesthetized mice. J Assoc Res Otolaryngol 13:209-217

Chéry-Croze S, Moulin A, Collet L (1993) Effect of contralateral sound stimulation on the distortion product $2f_1$-f_2 in humans: Evidence of a frequency specificity. Hear Res 68:53-58

Chew V (1966) Confidence, prediction, and tolerance regions for the multivariate normal distribution. J Am Statist Assoc 61:605-617

Choi Y-S, Lee S-Y, Parham K, Neely ST, Kim DO (2008) Stimulus-frequency otoacoustic emission: Measurements in humans and simulations with an active cochlear model. J Acoust Soc Am 123:2651-2669

Clarke EM, Ahmmed A, Parker D, Adams C (2006) Contralateral suppression of otoacoustic emissions in children with specific language impairment. Ear Hear 27:153-160

Collet L, Gartner M, Moulin A, Kauffmann I, Disant F, Morgon A (1989) Evoked otoacoustic emissions and sensorineural hearing loss. Arch Otolaryngol Head Neck Surg 115:1060-1062

Collet L, Kemp DT, Veuillet E, Duclaux R, Moulin A, Morgon A (1990) Effect of contralateral auditory stimuli on active cochlear micro-mechanical properties in human subjects. Hear Res 43:251-262

Collet L, Veuillet E, Chanal JM, Morgon A (1991) Evoked otoacoustic emissions: Correlates between spectrum analysis and audiogram. Audiol 30:164-172

Cooper NP, Guinan JJ Jr (2003) Separate mechanical processes underlie fast and slow effects of medial olivocochlear efferent activity. J Physiol 548:307-312

Cronbach LJ (1951) Coefficient alpha and the internal structure of tests. Psychometrika 16:297-334

Dallos P (1992) The active cochlea. J Neurosci 12:4575-4585

Dallos P (1996) Overview: Cochlear neurobiology. In: Dallos PJ, Popper AN, Fay RR (eds) The cochlea. Springer, New York, pp 1-43

Dallos P, Cheatham MA (1976) Production of cochlear potentials by inner and outer hair cells. J Acoust Soc Am 60:510-512

Darrow KN, Maison SF, Liberman MC (2007) Selective removal of lateral olivocochlear efferents increases vulnerability to acute acoustic injury. J Neurophysiol 97:1775-1785

Davis H (1983) An active process in cochlear mechanics. Hear Res 9:79-90

de Boer E (1996) Mechanics of the cochlea: Modeling efforts. In: Dallos PJ, Popper AN, Fay RR (eds) The cochlea. Springer, New York, pp 258-317

de Boer J, Thornton ARD (2007) Effect of subject task on contralateral suppression of click evoked otoacoustic emissions. Hear Res 233:117-123

de Boer J, Thornton ARD (2008) Neural correlates of perceptual learning in the auditory brainstem: Efferent activity predicts and reflects improvement at a speech-in-noise discrimination task. J Neurosci 28:4929-4937

de Boer J, Thornton ARD, Krumbholz K (2012) What is the role of the medial olivocochlear system in speech-in-noise processing? J Neurophysiol 107:1301-1312

de Ceulaer G, Yperman M, Daemers K, van Driessche K, Somers T, Offeciers FE, Govaerts PJ (2001) Contralateral suppression of transient evoked otoacoustic emissions: Normative data for a clinical test set-up. Otol Neurotol 22:350-355

Deeter R, Abel R, Calandruccio L, Dhar S (2009) Contralateral acoustic stimulation alters the magnitude and phase of distortion product otoacoustic emissions. J Acoust Soc Am 126:2413-2424

Delano PH, Elgueda D, Hamame CM, Robles L (2007) Selective attention to visual stimuli reduces cochlear sensitivity in chinchillas. J Neurosci 27:4146-4153

de Venecia RK, Liberman MC, Guinan JJ, Brown MC (2005) Medial olivocochlear reflex interneurons are located in the posteroventral cochlear nucleus: A kainic acid lesion study in guinea pigs. J Comp Neurol 487:345-360

Dolan DF, Guo MH, Nuttall AL (1997) Frequency-dependent enhancement of basilar membrane velocity during olivocochlear bundle stimulation. J Acoust Soc Am 102:3587-3596

Duifhuis H (1976) Cochlear nonlinearity and second filter: Possible mechanism and implications. J Acoust Soc Am 59:408-423

Efron B, Tibshirani RJ (1993) An introduction to the bootstrap. Champ and Hall, New York

Engdahl B, Arnesen AR, Mair IWS (1994) Reproducibility and short-term variability of transient evoked otoacoustic emissions. Scand Audiol 23:99-104

Evans EF (1972) The frequency response and other properties of single fibres in the guinea-pig cochlear nerve. J Physiol 226:263-287

Feeney MP, Keefe DH (2001) Estimating the acoustic reflex threshold from wideband measures of reflectance, admittance, and power. Ear Hear 22:316-332

Feliciano M, Saldaña E, Mugnaini E (1995) Direct projects from the rat primary auditory neocortex to nucleus sagulum, paralemniscal regions, superior olivary complex and cochlear nuclei. Aud Neurosci 1:287-308

Ferber-Viart C, Duclaux R, Collet L, Guyonnard F (1995) Influence of auditory stimulation and visual attention on otoacoustic emissions. Physiol Behav 57:1075-1079

Fex J (1959) Preliminary report: Augmentation of cochlear microphonic by stimulation of efferent fibres to the cochlea. Acta Otolaryngol 50:540-541

Fletcher H (1940) Auditory patterns. Rev Mod Phys 12:47-65

Francis NA, Guinan JJ Jr (2010) Acoustic stimulation of human medial olivocochlear efferents reduces stimulus-frequency and click-evoked otoacoustic emission delays: Implications for cochlear filter bandwidths. Hear Res 267:36-45

Franklin DJ, McCoy MJ, Martin GK, Lonsbury-Martin BL (1992) Test/retest reliability of distortion-product and transiently evoked otoacoustic emissions. Ear Hear 13:417-429

Froehlich P, Collet L, Chanal J-M, Morgon A (1990) Variability of the influence of a visual task on the active micromechanical properties of the cochlea. Brain Res 508:286-288

Froehlich P, Collet L, Morgon A (1993a) Transiently evoked otoacoustic emission amplitudes change with changes of directed attention. Physiol Behav 53:679-682

Froehlich P, Collet L, Valatx JL, Morgon A (1993b) Sleep and active cochlear micromechanical properties in human subjects. Hear Res 66:1-7

Galambos R (1956) Suppression of auditory activity by stimulation of efferent fibers to the cochlea. J Neurophysiol 19:424-437

Garinis AC, Glattke T, Cone-Wesson BK (2008) TEOAE suppression in adults with learning disabilities. Int J Audiol 47:607-614

Garinis A, Werner L, Abdala C (2011) The relationship between MOC reflex and masked threshold. Hear Res 282:128-137

Geisler CD (1998) From sound to synapse: Physiology of the mammalian ear. Oxford University Press, New York

George D, Mallery P (2003) SPSS for Windows step by step: A simple guide and reference. 11.0 update. Allyn and Bacon, Boston

Giard M-H, Collet L, Bouchet P, Pernier J (1994) Auditory selective attention in the human cochlea. Brain Res 633:353-356

Gifford ML, Guinan JJ Jr (1983) Effects of crossed-olivocochlear-bundle stimulation on cat auditory nerve fiber responses to tones. J Acoust Soc Am 74:115-123

Gilman S, Dirks DD (1986) Acoustics of ear canal measurement of eardrum SPL in simulators. J Acoust Soc Am 80:783-793

Giraud AL, Collet L, Chéry-Croze S, Magnan J, Chays A (1995) Evidence of a medial olivocochlear involvement in contralateral suppression of otoacoustic emissions in humans. Brain Res 705:15-23

Giraud AL, Perrin E, Chéry-Croze S, Chays A, Collet L (1996) Contralateral acoustic stimulation induces a phase advance in evoked otoacoustic emissions in humans. Hear Res 94:54-62

Giraud AL, Wable J, Chays A, Collet L, Chéry-Croze S (1997) Influence of contralateral noise on distortion product latency in humans: Is the medial olivocochlear efferent system involved? J Acoust Soc Am 102:2219-2227

Gold T (1948) Hearing. II. The physical basis of the action of the cochlea. Proc R Soc Lond B 135:492-498

Goodman SS, Fitzpatrick DF, Ellison JC, Jesteadt W, Keefe DH (2009) High-frequency click-evoked otoacoustic emissions and behavioral thresholds in humans. J Acoust Soc Am 125:1014-1032

Goodman SS, Keefe DH (2006) Simultaneous measurement of noise-activated middle-ear muscle reflex and stimulus frequency otoacoustic emissions. J Assoc Res Otolaryngol 7:125-139

Goodman SS, Mertes IB, Lewis JD, Weissbeck DK (2013) Medial olivocochlear-induced transient-evoked otoacoustic emission amplitude shifts in individual subjects. J Assoc Res Otolaryngol 14:829-842

Goodman SS, Mertes IB, Scheperle RS (2011) Delays and growth rates of multiple TEOAE components. AIP Conf Proc 1403:279-285

Gorga MP, Lilly DJ, Lenth RV (1980) Effect of signal bandwidth upon threshold of the acoustic reflex and upon loudness. Audiol 19:277-292

Gorga MP, Neely ST, Bergman BM, Beauchaine KL, Kaminski JR, Peters J, Schulte L, Jesteadt W (1993) A comparison of transient-evoked and distortion product otoacoustic emissions in normal-hearing and hearing-impaired subjects. J Acoust Soc Am 94:2639-2648

Gorga MP, Neely ST, Dorn PA, Hoover BM (2003) Further efforts to predict pure-tone thresholds from distortion product otoacoustic emission input/output functions. J Acoust Soc Am 113:3275-3284

Gorga MP, Neely ST, Ohlrich B, Hoover B, Redner J, Peters J (1997) From laboratory to clinic: A large scale study of distortion product otoacoustic emissions in ears with normal hearing and ears with hearing loss. Ear Hear 18:440-455

Graham RL, Hazell JWP (1994) Contralateral suppression of transient evoked otoacoustic emissions: Intra-individual variability in tinnitus and normal subjects. Br J Audiol 28:235-245

Guinan JJ Jr (1996) The physiology of olivocochlear efferents. In: Dallos PJ, Popper AN, Fay RR (eds) The cochlea. Springer, New York, pp 435-502

Guinan JJ Jr (2006) Olivocochlear efferents: Anatomy, physiology, function and the measurements of efferent effects in humans. Ear Hear 27:589-607

Guinan JJ (2011) Physiology of the medial and lateral olivocochlear systems. In: Ryugo DK, Fay RR, Popper AN (eds) Auditory and vestibular efferents. Springer, New York, pp 39-81

Guinan JJ Jr, Backus BC, Lilaonitkul W, Aharonson V (2003) Medial olivocochlear efferent reflex in humans: Otoacoustic emission (OAE) measurement issues and the advantages of stimulus frequency OAEs. J Assoc Res Otolaryngol 4:521-540

Guinan JJ Jr, Gifford ML (1988) Effects of electrical stimulation of efferent olivocochlear neurons on cat auditory-nerve fibers. III. Tuning curves and thresholds at CF. Hear Res 37:29-45

Hall JL (1977) Spatial differentiation as an auditory “second filter”: Assessment on a nonlinear model of the basilar membrane. J Acoust Soc Am 61:520-524

Harkrider AW, Bowers CD (2009) Evidence for a cortically mediated release from inhibition in the human cochlea. J Am Acad Audiol 20:208-215

Harris FP (1990) Distortion-product otoacoustic emissions in humans with high frequency sensorineural hearing loss. J Speech Hear Res 33:594-600

Harris FP, Probst R, Wenger R (1991) Repeatability of transiently evoked otoacoustic emissions in normally hearing humans. Audiol 30:135-141

Harrison WA, Burns EM (1993) Effects of contralateral acoustic stimulation on spontaneous otoacoustic emissions. J Acoust Soc Am 94:2649-2658

Heitmann J, Waldmann B, Schnitzler H-U (1998) Suppression of distortion product otoacoustic emissions (DPOAE) near $2f_1$-f_2 removes DP-gram fine structure—Evidence for a secondary generator. J Acoust Soc Am 103:1527-1531

Henin S, Thompson S, Abdelrazeq S, Long GR (2011) Changes in amplitude and phase of distortion-product otoacoustic emission fine-structure and separated components during efferent activation. J Acoust Soc Am 129:2068-2079

Hood LJ, Berlin CI, Bordelon J, Rose K (2003) Patients with auditory neuropathy/dys-syncrhony lack efferent suppression of transient evoked otoacoustic emissions. J Am Acad Audiol 14:302-313

Hood LJ, Berlin CI, Hurley A, Cecola RP, Bell B (1996) Contralateral suppression of transient-evoked otoacoustic emissions in humans: Intensity effects. Hear Res 101:113-118

Humphrey R (2008) Playrec (Version 2.1.0) [software], retrieved from http://www.playrec.co.uk (Last viewed July 3, 2014)

Hurley RM, Musiek FE (1994) Effectiveness of transient-evoked otoacoustic emissions (TEOAEs) in predicting hearing level. J Am Acad Audiol 5:195-203

Hussain DM, Gorga MP, Neely ST, Keefe DH, Peters J (1998) Transient evoked otoacoustic emissions in patients with normal hearing and in patients with hearing loss. Ear Hear 19:434-449

Jacobson M, Kim S, Romney J, Zhu X, Frisina RD (2003) Contralateral suppression of distortion-product otoacoustic emissions declines with age: A comparison of findings in CBA mice with human listeners. Laryngoscope 113:1707-1713

Johnsen NJ, Elberling C (1982) Evoked acoustic emissions from the human ear II. Normative data in young adults and influence of posture. Scan Audiol 11:69-77

Johnson TA, Neely ST, Kopun JG, Dierking DM, Tan H, Converse C, Kennedy E, Gorga MP (2007) Distortion product otoacoustic emissions: Cochlear-source contributions and clinical test performance. J Acoust Soc Am 122:3539-3553

Kaf WA, Danesh AA (2013) Distortion-product otoacoustic emissions and contralateral suppression findings in children with Asperger's Syndrome. Int J Ped Otorhinolaryngol 77:947-954

Kalluri R, Shera CA (2001) Distortion-product source unmixing: A test of the two-mechanism model for DPOAE generation. J Acoust Soc Am 109:622-637

Kalluri R, Shera CA (2007) Near equivalence of human click-evoked and stimulus-frequency otoacoustic emissions. J Acoust Soc Am 121:2097-2110

Kawase T, Delgutte B, Liberman MC (1993) Antimasking effects of the olivocochlear reflex. II. Enhancement of auditory-nerve response to masked tones. J Neurophysiol 70:2533-2549

Kawase T, Liberman MC (1993) Antimasking effects of the olivocochlear reflex. I. Enhancement of compound action potentials to masked tones. J Neurophysiol 70:2519-2532

Keefe DH (1998) Double-evoked otoacoustic emissions. I. Measurement theory and nonlinear coherence. J Acoust Soc Am 103:3489-3498

Keefe DH, Goodman SS, Ellison JC, Fitzpatrick DF, Gorga MP (2011) Detecting high-frequency hearing loss with click-evoked otoacoustic emissions. J Acoust Soc Am 129:245-261

Keefe DH, Gorga MP, Jesteadt W, Smith LM (2008) Ear asymmetries in middle-ear, cochlear, and brainstem responses in human infants. J Acoust Soc Am 123:1504-1512

Kemp DT (1978) Stimulated acoustic emissions from within the human auditory system. J Acoust Soc Am 64:1386-1391

Kemp DT (1979) Evidence of mechanical nonlinearity and frequency selective wave amplification in the cochlea. Arch Otorhinolaryngol 224:37-45

Kemp DT, Chum R (1979) Properties of the generator of stimulated acoustic emissions. Hear Res 2:213-232

Kemp DT, Ryan S, Bray P (1990) A guide to the effective use of otoacoustic emissions. Ear Hear 11:93-105

Keppler H, Dhooge I, Corthals P, Maes L, D'haenens W, Bockstael A, Philips B, Swinnen F, Vinck B (2010a) The effects of aging on evoked otoacoustic emissions and efferent suppression of transient evoked otoacoustic emissions. Clin Neurophysiol 121:359-365

Keppler H, Dhooge I, Maes L, D'haenens W, Bockstael A, Philips B, Swinnen F, Vinck B (2010b) Transient-evoked and distortion product otoacoustic emissions: A short-term test-retest reliability study. Int J Audiol 49:99-109

Khalfa S, Bougeard R, Morand N, Veuillet E, Isnard J, Guenot M, Ryvlin P, Fischer C, Collet L (2001) Evidence of peripheral auditory activity modulation by the auditory cortex in humans. Neurosci 104:347-358

Khalfa S, Morlet T, Micheyl C, Morgon A, Collet L (1997) Evidence of peripheral hearing asymmetry in humans: Clinical implications. Acta Otolaryngol 117:192-196

Khalfa S, Veuillet E, Collet L (1998) Peripheral auditory lateralization assessment using TEOAEs. Hear Res 121:29-34

Kiang NYS, Sachs MB, Peake WT (1967) Shapes of tuning curves for single auditory-nerve fibers. J Acoust Soc Am 42:1341-1342

Kim DO (1980) Cochlear mechanics: Implications of electrophysiological and acoustical observations. Hear Res 2:297-317

Kim SH, Frisina DR, Frisina RD (2002) Effects of age on contralateral suppression of distortion product otoacoustic emissions in human listeners with normal hearing. Audiol Neurotol 7:348-357

Kirk EC, Smith DW (2003) Protection from acoustic trauma is not a primary function of the medial olivocochlear efferent system. J Assoc Res Otolaryngol 4:445-465

Kline PK (1999) Handbook of psychological testing. Routledge, New York

Konrad-Martin D, Neely ST, Keefe DH, Dorn PA, Gorga MP (2001) Sources of distortion product otoacoustic emissions revealed by suppression experiments and inverse fast Fourier transforms in normal ears. J Acoust Soc Am 109:2862-2879

Kumar UA, Methi R, Avinash MC (2013) Test/retest repeatability of effect contralateral acoustic stimulation on the magnitudes of distortion product otoacoustic emissions. Laryngoscope 123:463-471

Kumar UA, Vanaja CS (2004) Functioning of olivocochlear bundle and speech perception in noise. Ear Hear 25:142-146

Lapsley Miller JA, Marshall L, Heller LM (2004) A longitudinal study of changes in evoked otoacoustic emissions and pure-tone thresholds as measured in a hearing conservation program. Int J Audiol 43:307-322

Liberman MC (1980) Efferent synapses in the inner hair cell area of the cat cochlea: An electron microscopic study of serial section. Hear Res 3:189-204

Liberman MC, Dodds LW, Pierece S (1990) Afferent and efferent innervation of the cat cochlea: Quantitative analysis with light and electron microscopy. J Comp Neurol 301:443-460

Liberman MC, Gao J, He DZZ, Wu X, Jia S, Zuo J (2002) Prestin is required for electromotility of the outer hair cell and for the cochlear amplifier. Nature 419:300-304

Liberman MC, Guinan JJ Jr (1998) Feedback control of the auditory periphery: Anti-masking effects of middle ear muscles vs. olivocochlear efferents. J Commun Disord 31:471-483

Liberman MC, O'Grady DF, Dodds LW, McGee J, Walsh EJ (2000) Afferent innervation of outer and inner hair cells is normal in neonatally de-efferented cats. J Comp Neurol 423:132-139

Liberman MC, Puria S, Guinan JJ Jr (1996) The ipsilaterally evoked olivocochlear reflex causes rapid adaptation of the $2f_1$-f_2 distortion product otoacoustic emission. J Acoust Soc Am 99:3572-3584

Lilaonitkul W, Guinan JJ Jr (2009) Human medial olivocochlear reflex: Effects as functions of contralateral, ipsilateral, and bilateral elicitor bandwidths. J Assoc Res Otolaryngol 10:459-470

Lim DJ (1986) Functional structure of the organ of Corti: a review. Hear Res 22:117-146

Little MA, Jones NS (2010) Sparse Bayesian step-filtering for high-throughput analysis of molecular machine dynamics. Proc IEEE Int Conf Acoust Speech Signal Process, pp 4162-4165

Long GR, Tubis A (1988) Modification of spontaneous and evoked otoacoustic emissions and associated psychoacoustic microstructure by aspirin consumption. J Acoust Soc Am 84:1343-1353

Lonsbury-Martin BL, Cutler WM, Martin GK (1991) Evidence for the influence of aging on distortion-product otoacoustic emissions in humans 89:1749-1759

Lonsbury-Martin BL, Martin GK, Probst R, Coats AC (1988) Spontaneous otoacoustic emissions in a nonhuman primate. II. Cochlear anatomy. Hear Res 33:69-94

Lukas JH (1980) Human auditory attention: The olivocochlear bundle may function as a peripheral filter. Psychophysiol 17:444-452

Maison SF, Liberman MC (2000) Predicting vulnerability to acoustic injury with a noninvasive assay of olivocochlear reflex strength. J Neurosci 20:4701-4707

Maison S, Micheyl C, Andéol, Gallégo S, Collet L (2000) Activation of medial olivocochlear efferent system in humans: Influence of stimulus bandwidth. Hear Res 140:111-125

Maison S, Micheyl C, Collet L (2001) Influence of focused auditory attention on cochlear activity in humans. Psychophysiol 38:35-40

Maison SF, Usubuchi H, Liberman MC (2013) Efferent feedback minimizes cochlear neuropathy from moderate noise exposure. J Neurosci 33:5542-5552

Margolis RH, Dubno JR, Wilson RH (1980) Acoustic-reflex thresholds for noise stimuli. J Acoust Soc Am 68:892-895

Marshall L, Heller LM (1996) Reliability of transient-evoked otoacoustic emissions. Ear Hear 17:237-254

Martin GK, Ohlms LA, Franklin DJ, Harris FP, Lonsbury-Martin BL (1990) Distortion product emissions in humans. III. Influence of sensorineural hearing loss. Ann Otol Rhinol Laryngol Suppl 147:30-42

Masterton RB, Imig TJ (1984) Neural mechanisms for sound localization. Ann Rev Physiol 46:275-287

Mauermann M, Uppenkamp S, van Hengel PWJ, Kollmeier B (1999) Evidence for the distortion product frequency place as a source of distortion product otoacoustic emission (DPOAE) fine structure in humans. I. Fine structure and higher-order DPOAE as a function of the frequency ratio *f*2/*f*1. J Acoust Soc Am 106:3473-3483

Mehl AL, Thomson V (2002) The Colorado newborn hearing screening project, 1992-1999: On the threshold of effective population-based universal newborn hearing screening. Pediatrics 109:E7

Meric C, Collet L (1992) Visual attention and evoked otoacoustic emissions: A slight but real effect. Int J Psychophysiol 12:233-235

Mertes IB, Goodman SS (2013) Short-latency transient-evoked otoacoustic emissions as predictors of hearing status and thresholds. J Acoust Soc Am 134:2127-2135

Micheyl C, Collet L (1996) Involvement of the olivocochlear bundle in the detection of tones in noise. J Acoust Soc Am 99:1604-1610

Micheyl C, Khalfa S, Perrot X, Collet L (1997) Difference in cochlear efferent activity between musicians and non-musicians. NeuroReport 8:1047-1050

Mishra SK, Lutman ME (2013) Repeatability of click-evoked otoacoustic emission-based medial olivocochlear efferent assay. Ear Hear 34:789-798

Mishra SK, Lutman ME (2014) Top-down influences of the medial olivocochlear efferent system in speech perception in noise. PLoS ONE 9:e85756

Moleti A, Al-Maaury AM, Bertaccini D, Botti T, Sisto R (2013) Generation place of the long- and short-latency components of transient-evoked otoacoustic emissions in a nonlinear cochlear model. J Acoust Soc Am 133:4098-4108

Moleti A, Botti T, Sisto R (2012) Transient-evoked otoacoustic emission generators in a nonlinear cochlea. J Acoust Soc Am 131:2891-2903

Møller AR (1962) Acoustic reflex in man. J Acoust Soc Am 34:1524-1534

Møller AR (1963) Transfer function of the middle ear. J Acoust Soc Am 35:1526-1534

Morand-Villeneuve N, Veuillet E, Perrot X, Lemoine P, Gagnieu MC, Sebert P, Durrant JD, Collet L (2005) Lateralization of the effects of the benzodiazepine drug oxazepam on medial olivocochlear system activity in humans. Hear Res 208:101-106

Morlet T, Goforth L, Hood LJ, Ferber C, Duclaux R, Berlin CI (1999) Development of human cochlear active mechanism asymmetry: Involvement of the medial olivocochlear system? Hear Res 134:153-162

Mott JB, Norton SJ, Neely ST, Warr WB (1989) Changes in spontaneous otoacoustic emissions produced by acoustic stimulation of the contralateral ear. Hear Res 38:229-242

Mountain DC (1980) Changes in endolymphatic potential and crossed olivocochlear bundle stimulation alter cochlear mechanics. Science 210:71-72

Mountain DC, Geisler CD, Hubbard AE (1980) Stimulation of efferents alters the cochlear microphonic and the sound-induced resistance changes measured in scala media of the guinea pig. Hear Res 3:231-240

Muchnik C, Ari-Even Roth DA-E, Othman-Jebara R, Putter-Katz H, Shabtai EL, Hildesheimer M (2004) Reduced medial olivocochlear bundle system function in children with auditory processing disorders. Audiol Neurotol 13:357-364

Mulders WHAM, Robertson D (2000) Evidence for direct cortical innervation of medial olivocochlear neurones in rats. Hear Res 144:65-72

Müller J, Janssen T, Heppelmann G, Wagner W (2005) Evidence for a bipolar change in distortion product otoacoustic emissions during contralateral acoustic stimulation in humans. J Acoust Soc Am 118:3747-3756

Murugasu E, Russell IJ (1996) The effect of efferent stimulation on basilar membrane displacement in the basal turn of the guinea pig cochlea. J Neurosci 16:325-332

Neely ST (1993) A model of cochlear mechanics with outer hair cell motility. J Acoust Soc Am 94:137-146

Neely ST, Kim DO (1983) An active cochlear model showing sharp tuning and high sensitivity. Hear Res 9:123-130

Neely ST, Kim DO (1986) A model for active elements in cochlear biomechanics. J Acoust Soc Am 79:1472-1480

Nilsson M, Soli SD, Sullivan JA (1994) Development of the Hearing in Noise Test for the measurement of speech reception thresholds in quiet and in noise. J Acoust Soc Am 95:1085-1099

Norman M, Thornton ARD (1993) Frequency analysis of the contralateral suppression of evoked otoacoustic emissions by narrow-band noise. Br J Audiol 27:281-289

Norton SJ, Gorga MP, Widen JE, Folsom RC, Sininger Y, Cone-Wesson B, Vohr BR, Mascher K, Fletcher K (2000) Identification of neonatal hearing impairment: Evaluation of transient evoked otoacoustic emission, distortion product otoacoustic emission, and auditory brain stem response test performance. Ear Hear 21:508-528

Oatman LC (1976) Effects of visual attention on the intensity of auditory evoked potentials. Exp Neurol 51:41-53

Parthasarathy TK (2001) Aging and contralateral suppression effects on transient evoked otoacoustic emissions. J Am Acad Audiol 12:80-85

Patuzzi R, Johnstone BM, Sellick PM (1984) The alteration of the vibration of the basilar membrane produced by loud sound. Hear Res 13:99-100

Patuzzi R, Robertson D (1988) Tuning in the mammalian cochlea. Physiol Rev 68:1009-1082

Patuzzi RB, Yates GK, Johnston BM (1989) Outer hair cell receptor current and sensorineural hearing loss. Hear Res 42:47-72

Penner MJ, Zhang T (1997) Prevalence of spontaneous otoacoustic emissions in adults revisited. Hear Res 103:28-34

Perrot X, Micheyl C, Khalfa S, Collet L (1999) Stronger bilateral efferent influences on cochlear biomechanical activity in musicians than in non-musicians. Neurosci Lett 262:167-170

Perrot X, Ryvlin P, Isnard J, Guénot M, Catenoix H, Fischer C, Mauguiére F, Collet L (2006) Evidence for corticofugal modulation of peripheral auditory activity in humans. Cereb Cortex 16:941-948

Philibert B, Veuillet E, Collet L (1998) Functional asymmetries of crossed and uncrossed medial olivocochlear efferent pathways in humans. Neurosci Lett 253:99-102

Pickles JO (2012) Introduction to the physiology of hearing. Emerald Insight, Bingley, England

Popelka GR, Karlovich RS, Wiley TL (1974) Acoustic reflex and critical bandwidth. J Acoust Soc Am 55:883-885

Prieve BA, Falter SR (1995) COAEs and SSOAEs in adults with increased age. Ear Hear 16:521-528

Prieve BA, Gorga MP, Schmidt A, Neely S, Peters J, Schultes L, Jesteadt W (1993) Analysis of transient-evoked otoacoustic emissions in normal-hearing and hearing-impaired ears. J Acoust Soc Am 93:3308-3319

Probst R, Hauser R (1990) Distortion product otoacoustic emissions in normal and hearing-impaired ears. Am J Otolaryngol 11:236-243

Probst R, Lonsbury-Martin BL, Martin GK, Coats AC (1987) Otoacoustic emissions in ears with hearing loss. Am J Otolaryngol 8:73-81

Puel J-L, Bonfils P, Pujol R (1988) Selective attention modifies the active micromechanical properties of the cochlea. Brain Res 447:380-383

Rajan R (2000) Centrifugal pathways protect hearing sensitivity at the cochlea in noisy environments that exacerbate the damage induced by loud sound. J Neurosci 20:6684-6693

Raphael Y, Altschuler RA (2003) Structure and innervation of the cochlea. Brain Res Bull 60:397-422

Rasmussen GL (1946) The olivary peduncle and other fiber projections of the superior olivary complex. J Comp Neurol 84:141-219

Rawool VW (1995) Ipsilateral acoustic reflex thresholds at varying click rates in humans. Scand Audiol 24:199-205

Ren T, He W, Porsov E (2011) Localization of the cochlear amplifier in living sensitive ears. PLoS One 6:e20149

Reuter K, Hammershøi D (2006) Distortion product otoacoustic emission fine structure analysis of 50 normal-hearing humans. J Acoust Soc Am 120:270-279

Rhode WS (1971) Observations of the vibration of the basilar membrane in squirrel monkeys using the Mössbauer technique. J Acoust Soc Am 49:1218-1231

Robertson D, Anderson C-J, Cole KS (1987) Segregation of efferent projections to different turns of the guinea pig cochlea. Hear Res 25:69-76

Robles L, Ruggero MA (2001) Mechanics of the mammalian cochlea. Physiol Rev 81:1305-1352

Robles L, Ruggero MA, Rich NC (1986) Basilar membrane mechanics at the base of the chinchilla cochlea. I. Input-output functions, tuning curves, and response phases. J Acoust Soc Am 80:1364-1374

Ruggero MA, Rich NC (1991) Furosemide alters organ of Corti mechanics: Evidence for feedback of outer hair cells upon the basilar membrane. J Neurosci 11:1057-1067

Russell IJ, Cody AR, Richardson GP (1986) The responses of inner and outer hair cells in the basal turn of the guinea-pig cochlea and in the mouse cochlea grown in vitro. Hear Res 22:199-216

Russell IJ, Nilsen KE (1997) The location of the cochlear amplifier: Spatial responses of a single tone on the guinea pig basilar membrane. Proc Acad Nat Sci USA 94:2660-2664

Rutten WLC (1980) Evoked acoustic emissions from within normal and abnormal human ears: Comparison with audiometric and electrocochleographic findings. Hear Res 2:263-271

Ryan S, Kemp DT, Hinchcliffe R (1991) The influence of contralateral acoustic stimulation on click-evoked otoacoustic emissions in humans. Br J Audiol 25:391-397

Sanches SGG, Carvallo RM (2006) Contralateral suppression of transient evoked otoacoustic emissions in children with auditory processing disorder. Audiol Neurotol 11:366-372

Schairer KS, Ellison JC, Fitzpatrick D, Keefe DH (2006) Use of stimulus-frequency otoacoustic emission latency and level to investigate cochlear mechanics in human ears. J Acoust Soc Am 120:901-914

Sellick PM, Patuzzi R, Johnstone BM (1982) Measurement of basilar membrane motion in the guinea pig using the Mössbauer technique. J Acoust Soc Am 72:131-141

Sewell WF (2011) Pharmacology and neurochemistry of olivocochlear efferents. In: Ryugo DK, Fay RR, Popper AN (eds) Auditory and vestibular efferents. Springer, New York, pp 83-101

Shaw EAG, Teranishi R (1968) Sound pressure generated in an external-ear replica and real human ears by a nearby point source. J Acoust Soc Am 44:240-249

Shera CA (2004) Mechanisms of mammalian otoacoustic emission and their implications for the clinical utility of otoacoustic emissions. Ear Hear 25:86-97

Shera CA (2007) Laser amplification with a twist: Traveling-wave propagation functions from throughout the cochlea. J Acoust Soc Am 122:2738-2758

Shera CA, Guinan JJ Jr (1999) Evoked otoacoustic emissions arise by two fundamentally different mechanisms: A taxonomy for mammalian OAEs. J Acoust Soc Am 105:782-798

Shera CA, Guinan JJ Jr (2008) Mechanisms of mammalian otoacoustic emission. In: Manley GA, Fay RR, Popper AN (eds) Active processes and otoacoustic emissions. Springer, New York, pp 305-342

Shera CA, Guinan JJ Jr, Oxenham AJ (2002) Revised estimates of human cochlear tuning from otoacoustic and behavioral measurements. Proc Acad Nat Sci USA 99:3318-3323

Shera CA, Tubis A, Talmadge CL (2008) Testing coherent reflection in chinchilla: Auditory-nerve responses predict stimulus-frequency emissions. J Acoust Soc Am 124:381-395

Shera CA, Zweig G (1991) A symmetry suppresses the cochlear catastrophe. J Acoust Soc Am 89:1276-1289

Shrout PE, Fleiss JL (1979) Intraclass correlations: Uses in assessing rater reliability. Psych Bull 86:420-428

Siegel JH, Cerka AJ, Recio-Spinoso A, Temchin AN, van Dijk P, Ruggero MA (2005) Delays of stimulus-frequency otoacoustic emissions and cochlear vibrations contradict the theory of coherent reflection filtering. J Acoust Soc Am 118:2434-2443

Sininger YS, Cone-Wesson B (2004) Asymmetric cochlear processing mimics hemispheric specialization. Science 305:1581

Sisto R, Moleti A, Lucertini M (2001) Spontaneous otoacoustic emissions and relaxation dynamics of long decay time OAEs in audiometrically normal and impaired subjects. J Acoust Soc Am 109:638-647

Slepecky NB (1996) Structure of the mammalian cochlea. In: Dallos PJ, Popper AN, Fay RR (eds) The cochlea. Springer, New York, pp 44-129

Souter M (1995) Suppression of stimulus frequency otoacoustic emissions by contralateral noise. Hear Res 91:167-177

Sridhar TS, Liberman MC, Brown MC, Sewell WF (1995) A novel cholinergic "slow effect" of efferent stimulation on cochlear potentials in the guinea pig. J Neursoci 15:3667-3678

Starr A, Picton TW, Sininger Y, Hood LJ, Berlin CI (1996) Auditory neuropathy. Brain 119:741-753

Steinberg J, Montgomery H, Gardner M (1940) Results of the world's fair hearing tests. J Acoust Soc Am 12:291-301

Stinson MR, Shaw EAG, Lawton BW (1982) Estimation of acoustical energy reflectance at the eardrum from measurements of pressure distribution in the human ear canal. J Acoust Soc Am 72:766-773

Sückfull M, Schneeweiβ S, Dreher A, Schorn K (1996) Evaluation of TEOAE and DPOAE measurements for the assessment of auditory thresholds in sensorineural hearing loss. Acta Otolaryngol 116:528-533

Sun X-M (2008) Distortion product otoacoustic emission fine structure is responsible for variability of distortion product otoacoustic emission contralateral suppression. J Acoust Soc Am 123:4310-4320

Talmadge CL, Long GR, Tubis A, Dhar S (1999) Experimental confirmation of the two-source interference model for the fine structure of distortion product otoacoustic emissions. J Acoust Soc Am 105:275-292

Thompson AM, Thompson GC (1993) Relationship of descending inferior colliculus projections to olivocochlear neurons. J Comp Neurol 335:402-412

Thompson GC, Thompson AM (1986) Olivocochlear neurons in the squirrel monkey brainstem. J Comp Neurol 254:246-258

Tognola G, Grandori F, Ravazzani P (1997) Time-frequency distributions of click-evoked otoacoustic emissions. Hear Res 106:112-122

Tokgoz-Yilmaz S, Kose, SK, Turkyilmaz MD, Atay G (2013) The role of the medial olivocochlear system in the complaints of understanding speech in noisy environments by individuals with normal hearing. Aurus Nasus Larynx 40:521-524

Tonndorf J, Khanna SM (1967) Some properties of sound transmission in the middle and outer ears of cats. J Acoust Soc Am 41:513-521

Velenovsky DS, Glattke TJ (2002) The effect of noise bandwidth on the contralateral suppression of transient evoked otoacoustic emissions. Hear Res 164:39-48

Vetter DE, Saldaña E, Mugnaini E (1993) Input from the inferior colliculus to medial olivocochlear neurons in the rat: A double label study with PHA-L and cholera toxin. Hear Res 70:173-186

Veuillet E, Collet L, Duclaux R (1991) Effect of contralateral acoustic stimulation on active cochlear micromechanical properties in human subjects: Dependence on stimulus variables. J Neurophysiol 65:724-735

Veuillet E, Magnan A, Ecalle J, Tha-Van H, Collet L (2007) Auditory processing disorder in children with reading disabilities: Effect of audiovisual training. Brain 130:2915-2928

Veuillet E, Martin V, Suc B, Vesson JF, Morgon A, Collet L (2001) Otoacoustic emissions and medial olivocochlear suppression during auditory recovery from acoustic trauma in humans. Acta Otolaryngol 121:278-283

von Békésy G (1960) Experiments in hearing. McGraw-Hill, New York

Wagner W, Frey K, Heppelmann G, Plontke SK, Zenner H-P (2008) Speech-in-noise intelligibility does not correlate with efferent olivocochlear reflex in humans with normal hearing. Acta Otolaryngol 128:53-60

Wagner W, Heppelmann G, Kuehn M, Tisch M, Vonthein R, Zenner H-P (2005) Olivocochlear activity and temporary threshold shift-susceptibility in humans. Laryngoscope 115:2021-2028

Wagner W, Heppelmann G, Müller J, Janssen T, Zenner H-P (2007) Olivocochlear reflex effect on human distortion product otoacoustic emissions is largest at frequencies with distinct fine structure dips. Hear Res 223:83-92

Wagner W, Heppelmann G, Vonthein R, Zenner HP (2008) Test-retest repeatability of distortion product otoacoustic emissions. Ear Hear 29:378-391

Wagner W, Plinkert PK (1999) The relationship between auditory threshold and evoked otoacoustic emissions. Eur Arch Otorhinolaryngol 256:177-188

Walsh EJ, McGee J, McFadden SL, Liberman MC (1998) Long-term effects of sectioning the olivocochlear bundle in neonatal cats. J Neurosci 18:3859-3869

Warr WB (1992) Organization of olivocochlear efferent systems in mammals. In: Webster DB, Popper AN, Fay RR (eds) Mammalian auditory pathway: Neuroanatomy. Springer, New York, pp 410-448

Warr WB, Guinan JJ Jr (1979) Efferent innervation of the organ of Corti: Two separate systems. Brain Res 173:152-155

Whitehead ML, Martin GK, Lonsbury-Martin BL (1991) Effects of the crossed acoustic reflex on distortion-product otoacoustic emissions in awake rabbits. Hear Res 51:55-72

Wiederhold ML, Kiang NYS (1970) Effects of electric stimulation of the crossed olivocochlear bundle on single auditory-nerve fibers in the cat. J Acoust Soc Am 48:950-965

Williams DM, Brown AM (1997) The effect of contralateral broad-band noise on acoustic distortion products from the human ear. Hear Res 104:127-146

Wilson JP (1980) Evidence for a cochlear origin for acoustic re-emissions, threshold fine-structure and tonal tinnitus. Hear Res 2:233-252

Wilson JP, Evans EF (1983) Effects of furosemide, flaxedil, noise and tone over-stimulation on the evoked otoacoustic emission in cat. Proc Cong Int Union Phys Sci 15:100

Winslow RL, Sachs MB (1987). Effect of electrical stimulation of the crossed olivocochlear bundle on auditory nerve response to tones in noise. J Neurophysiol 57:1002-1021

Winslow RL, Sachs MB (1988) Single-tone intensity discrimination based on auditory-nerve rate responses in backgrounds of quiet, noise, and with stimulation of the crossed olivocochlear bundle. Hear Res 35:165-189

Wit HP, Ritsma RJ (1980) Evoked acoustical responses from the human ear: Some experimental results. Hear Res 2:253-261

Withnell RH, Shaffer LA, Lilly DJ (2002) What drives mechanical amplification in the mammalian cochlea? Ear Hear 23:49-57

Wolpert S, Heyd A, Wagner W (2014) Assessment of the noise-protective action of the olivocochlear efferent in humans. Audiol Neurotol 9:31-40

Wu X, Gao J, Guo Y, Zuo J (2004) Hearing threshold elevation precedes hair-cell loss in prestin knockout mice. Mol Brain Res 126:30-37

Yates GK, Withnell RH (1999) The role of intermodulation distortion in transient-evoked otoacoustic emissions. Hear Res 136:49-64

Zhao W, Dhar S (2010) The effect of contralateral acoustic stimulation on spontaneous otoacoustic emissions. J Assoc Res Otolaryngol 11:53-67

Zheng J, Shen W, He DZZ, Long KB, Madison LD, Dallos P (2000) Prestin is the motor protein of cochlear outer hair cells. Nature 405:149-155

Zheng X-Y, Henderson D, McFadden SL, Hu B-H (1997) The role of the cochlear efferent system in acquired resistance to noise-induced hearing loss. Hear Res 104:191-203

Zhu X, Vasilyeva ON, Kim S, Jacobson M, Romney J, Waterman MS, Tuttle D, Frisina RD (2007) Auditory efferent feedback system deficits precede age-related hearing loss: Contralateral suppression of otoacoustic emissions in mice. J Comp Neurol 503:593-604

Zurek PM (1980) Spontaneous narrowband acoustic signals emitted by human ears. J Acoust Soc Am 69:514-523

Zweig G, Shera CA (1995) The origin of periodicity in the spectrum of evoked otoacoustic emissions. J Acoust Soc Am 98:2018-2047

Zwicker E (1983) Delayed evoked oto-acoustic emissions and their suppression by Gaussian-shaped pressure impulses. Hear Res 11:359-371